

**LAND USE AND VEGETATION CHANGES IMPACT
ON THERMAL COMFORT IN URBAN OPEN SPACES
OF NAIROBI CITY, KENYA**

SHARON ANYANGO ONYANGO

**MASTER OF SCIENCE
(Landscape Planning and Conservation)**

**JOMO KENYATTA UNIVERSITY
OF
AGRICULTURE AND TECHNOLOGY**

2024

**Land Use and Vegetation Changes Impact on Thermal Comfort in
Urban Open Spaces of Nairobi City, Kenya**

Sharon Anyango Onyango

**A Thesis Submitted in Partial Fulfillment of the Requirements for
the Degree of Master of Science in Landscape Planning and
Conservation of the Jomo Kenyatta University of Agriculture and
Technology**

2024

DECLARATION

This thesis is my original work and has not been presented for a degree in any other University.

Signature.....Date.....

Sharon Anyango Onyango

This thesis has been submitted for examination with our approval as University Supervisors

Signature.....Date.....

Prof. John Bosco Njoroge, PhD

JKUAT, Kenya

Signature.....Date.....

Dr. Aggrey Ochieng Adimo, PhD

JKUAT, Kenya

DEDICATION

I dedicate this work, with entirety, to my beloved parents, Mr. George Onyango and Mrs. Valeria Onyango, my siblings Hildah, Edwin, Tom and Brian Dan for their colossal support through this complete stretch.

ACKNOWLEDGMENT

I would like to convey my earnest appreciation for all efforts made by various distinctive persons, in different capacities, for having enabled me to develop this thesis so far.

With regard to expertise and professionalism, I am particularly indebted to my supervisors Prof. John Bosco Njoroge and Dr. Ochieng' Adimo for their consistent and constant urge, support and availability throughout, and in the supervision of this work. I would also like to thank our research project coordinator, Prof. John Wesonga for ensuring timely funding and smooth running of the research under "*Local Climate Adaptation in Three Cities: Cairo, Nairobi and Istanbul*" (LOCLIM-3) project. May the Almighty bless you all.

A special mention of my sincere gratitude to the Freie University Berlin team, led by Prof. Dr. Sahar Sodoudi, for the extensive cross-disciplinary training on microclimate measurement and modeling. To all my colleagues from JKUAT and the staff from the Department of Landscape and Environmental Sciences, thank you so much for your support, be abundantly blessed.

Above and beyond, I am grateful to my family for the great love and support. Most importantly, I am grateful to God for these milestones reached.

TABLE OF CONTENTS

DECLARATION.....	ii
DEDICATION.....	iii
ACKNOWLEDGMENT	iv
TABLE OF CONTENTS.....	v
LIST OF TABLES	x
LIST OF FIGURES	xii
ACRONYMS AND ABBREVIATIONS.....	xiv
ABSTRACT	xvi
CHAPTER ONE	1
INTRODUCTION.....	1
1.1 Background Information	1
1.2 Problem Statement	4
1.3 Justification	5
1.4 Objectives.....	6
1.4.1 General Objective	6
1.4.2 Specific Objectives	6
1.5 Research Hypotheses.....	7

1.5.1 Null Hypothesis (Ho).....	7
1.6 Scope of Study.....	7
1.7 Study Limitations	7
CHAPTER TWO	9
LITERATURE REVIEW.....	9
2.1 Introduction	9
2.2 Theoretical Review.....	9
2.2.1. Urban Morphology and Climate	9
2.2.2 Urban Environments and Microclimate.....	14
2.2.3 Plants and Microclimate Control for Urban Environments	17
2.3 Conceptual Framework	21
2.4 The Critiques of Existing Literature and Case studies	22
2.4.1 Spatiotemporal Vegetation Changes Monitoring Using LULC within LCZs	22
2.4.2 Land Surface Temperature (LST) and Surface Urban Heat Island (SUHI) Nexus along the Urban-Rural Gradient	25
2.4.3 Prediction of Land Use/Cover, Vegetation and Land Surface Temperatures.....	27
2.4.4. Urban Trees Species’ Microclimate Modification and UHI Mitigation Nexus to Improve Human Thermal Comfort.....	28

2.5 Summary	30
2.6 Research Gap.....	31
CHAPTER THREE	33
RESEARCH METHODOLOGY	33
3.1 Introduction	33
3.1.1 Methodological Overview	33
3.2 Study Area.....	34
3.3 Data Collection.....	36
3.3.1 Evaluation of Spatial and Temporal Changes of Vegetation Cover Based on Local Climate Zones of Nairobi	36
3.3.2 Determining Land Surface Temperature (LST) Changes in Nairobi along an Urban Gradient.....	40
3.3.3 Determining the Effects of Plant Species on Microclimatic Parameters in an Urban Environment.....	44
3.4 Data Analysis	50
3.4.1 Evaluation of the Spatial and Temporal Changes of Vegetation Cover in LCZ of Nairobi from 1988 to 2018.....	50
3.4.2 Determining LST Changes in Nairobi along an Urban Gradient	55
3.4.3 Determining the Effects of Plant Species on Thermal Comfort in an Urban Environment.....	56

CHAPTER FOUR.....	58
RESULTS AND DISCUSSION	58
4.1 Introduction	58
4.2 Spatial and Temporal Changes of Vegetation Cover in Local Climate Zones of Nairobi from 1988 - 2018.....	58
4.2.1 LULC Images' Accuracy.....	58
4.2.2 Changes in LULC within LCZs of Nairobi (1988-2018)	59
4.2.3 Conversions of LULC and within LCZs of Nairobi (1988-2018).....	65
4.2.4 Predicted Land Use/Cover for 2033	71
4.2.5 Discussion.....	73
4.3 Determining LST Changes in Nairobi along an Urban Gradient.....	74
4.3.1 NDVI Maps of Nairobi 1988 - 2018.....	74
4.3.2 LST Maps of Nairobi 1988 - 2018.....	75
4.3.3 LST Gradient Trends	77
4.3.4 Predicted Vegetation and Land Surface Temperature for 2033	78
4.3.5 Discussion.....	78
4.4 The Effects of Plant Species on Microclimatic Parameters in the Sampled Sites	80
4.4.1 Plant Canopy Density and the Tree Allometric Properties.....	80

4.4.2 Mean Microclimatic Variables Distribution at the Trunk, at 5 m and Control	81
4.4.3 Inter-Site / Inter-Species Effects on Microclimatic Parameters	83
4.4.4 Human Thermal Comfort (TC) Evaluation	86
4.4.5 Discussion.....	88
CHAPTER FIVE.....	91
SUMMARY, CONCLUSION AND RECOMMENDATION	91
5.1 Summary	91
5.2 Conclusion.....	92
5.2.1 Spatial and Temporal Changes of Vegetation Cover in LCZ of Nairobi from 1988 to 2018	92
5.2.2 LST Changes in Nairobi along an Urban Gradient.....	92
5.2.3 Effects of Plant Species on Microclimatic Parameters in the Study Area.	93
5.3 Recommendations	94
REFERENCES.....	96

LIST OF TABLES

Table 3.1: General Landsat Image Characteristics for Landsat 8, 7 and 4	37
Table 3.2: Source and Properties of the Images and Auxiliary Data Used in LULC Assessment	38
Table 3.3: The Radiance Value Equation's Symbols and Their Meaning	41
Table 3.4: Values and Constants for Thermal Bands of Landsat 4, 7 and 8	41
Table 3.5: Wavelengths of the Landsat Imagery Bands Used to Calculate NDVI and Their Spatial Resolution	42
Table 3.6: Selected Plants General Description, Canopy Forms and Their Uses	46
Table 3.7: Attributes of the Study Sites; Plant (P), site (S) and Control (C)	48
Table 3.8: Land Use Land Cover Classification Schema.....	52
Table 4.1: The LULC Accuracy Assessment Report for 1988, 2002 and 2018	58
Table 4.2: Areal Extent of the LULC Types of Nairobi County (1988, 2002 and 2018)	59
Table 4.3: Transition of LULC Composition within the Built-type LCZs 1-10 in 1988, 2002 and 2018	62
Table 4.4: Transition of LULC composition within the Land Cover-Type LCZs A-G in 1988, 2002 and 2018)	63
Table 4.5: LULC Conversion and Area of Change from 1988 to 2018.....	67
Table 4.6: LULC Conversion and Area of Change in Each LCZ from 1988 to 2002 (15 Yrs).....	68

Table 4.7: LULC Conversion and Area of Change in Each LCZ from 2002 to 2018 (15 Yrs).....	69
Table 4.8: LULC Conversion and Area of Change in Each LCZ from 1988 to 2018 (30 Yrs).....	70
Table 4.10: LST and NDVI Mean, Range and Standard Deviations (1988 – 2018)	76
Table 4.11: Selected Plants’ Allometric Properties; Site 1: CP - Central Park, Site 2:TR - Taifa Rd	80
Table 4.12: Mean Microclimatic Variable Measurements under the Tree for the Study Sites	85
Table 4.13: The Comfort Index of PET Formulated for Specific Thermal Conditions	86
Table 4.14: Computed PET and SVF Values for Each Tree Species and the Control Points in Central Park (CP) and Taifa Road (TR).....	87

LIST OF FIGURES

Figure 2.1: Graphical Representaton of the UHI Profile.	11
Figure 2.2: The Causes, Facilitators, Impacts and Consequences of UHI.....	11
Figure 2.3: Outlined Descriptions for LCZs	16
Figure 2.4: Benefits of Urban Greenery.....	21
Figure 2.5: The study’s Conceptual Framework.....	22
Figure 3.1: Overview of the Study’s Methodological Flowchart	33
Figure 3.2: The Maps Kenya, Nairobi County and the Selected Study Sites: Central Park (CP) and Taifa Road (TR) within the Central Business District (CBD).....	35
Figure 3.3: Spatial Distribution of the LCZs in Nairobi for 2018 Retrieved from World Urban Database and Access Portal Tools (WUDAPT).....	39
Figure 3.4: Overview of the LULC Prediction Methodological Process.....	40
Figure 3.5: The Four Different Plant Species Sampled from the Two Study Sites and the Control Points (Open Areas with No Trees).	45
Figure 3.6: (a) The below and above Canopy Points Where LAI was Measured around the Isolated Trees (Cater <i>et al.</i> , 2009), (b) Microclimatic Variables’ Measurement Points Illustration.....	47
Figure 3.7: Pinned Locations for the Sample Plants in Central Park (Site 1) and Taifa Road (Site 2) Sites.....	48
Figure 3.8: Summary of Image Sub-Setting, Enhancement and Classification.....	51
Figure 3.9: Flowchart of the LULC Transition Analysis within LCZs of Nairobi ...	54

Figure 3.10: Overview of the PET Analysis Process.....	57
Figure 4.1: Land Use Land Cover (LULC) Distribution Maps of Nairobi for the Years 1988, 2002, and 2018	60
Figure 4.2: LULC Change Trends (A) and Percentage Change (B) between 1988 and 2018.....	61
Figure 4.3: Spatial Changes of LULC within LCZs of Nairobi for 1988 to 2018....	64
Figure 4.4: Spatial Variables Used in the Study	71
Figure 4.5: (a) Predicted LULC for 2033 and (b) the Rate of Change Maps (2018-2033).....	72
Figure 4.6: NDVI Distribution Maps of Nairobi for the Year 1988 - 2018.....	75
Figure 4.7: LST (°C) Distribution Maps of Nairobi for 1988, 2002 and 2018.....	76
Figure 4.8: LST Profile Trends for Nairobi (North-South, West-East) in 1988, 2002 & 2018.....	77
Figure 4.9: (a) Predicted NDVI Map and (b) LST Map for 2033.....	78
Figure 4.10: The Mean Values of Climatic Variables for Continuous 10-Hour Measurement for Site 1 (Central Park) (Trunk, 5 m).....	81
Figure 4.11: The Mean Values of Climatic Variables for Continuous 10-Hour Measurement for Site 2 (Taifa Road) (Trunk, 5 m)	82
Figure 4.12: Derived PET (A) and SVF (B) for the Sampled Tree Species for the Two Study Sites (Central Park and Taifa Road)	88

ACRONYMS AND ABBREVIATIONS

ANOVA	Analysis of Variance
ArcGIS	Geographic Information System (Environment System Research Institute Software)
CBD	Central Business District
CORINE	Coordination of Information on the Environment
DBH	Diameter at Breast Height
ERDAS	Earth Resource Data Analysis System
GCM	General Circulation Models
GPS	Geographical Positioning System
IPCC	Intergovernmental Panel on Climate Change
LAI	Leaf Area Index
LCZ	Local Climate Zone(s)
LST	Land Surface Temperature
LULC	Land Use, Land Cover
NDVI	Normalized Difference Vegetation Index
PM	Particulate Matter
PET	Physiological Equivalent Temperature
RCP	Representative Concentration Pathways
SPSS	Statistical Package for Social Sciences

SSA	Sub-Saharan Africa
SVF	Sky View Factor
TC	Thermal Comfort
UGS	Urban Green Space(s)
UHI	Urban Heat Island
UNDP	United Nations Development Program
UN-DESA	United Nations Department of Economic and Social Affairs
USEPA	United States Environmental Protection Agency
USGS	United States Geological Survey
VOC	Volatile Organic Compounds

ABSTRACT

Urban heat islands (UHI) emanates from the difference in temperature between urban climatic conditions and the surrounding peri-urban and rural zones. Kenya's capital, Nairobi city, is amongst the cities in Sub-Saharan African (SSA) that are rapidly urbanizing and is directly associated with the UHI co-occurrence. Anthropogenic activities such as rural-urban migration, land cover transformation, and industrial operations have intensified the effects of UHI within the city. Contemporary studies have demonstrated that vegetation within urban areas can regulate urban microclimate, thereby reducing the UHI effects. To support informed decision making on climate resilience planning for Nairobi, there is a need to establish UHI's spatial distribution and quantify the degree to which mature plant species can improve human thermal comfort and urban livability. This study focused on assessment of land use change and effect of vegetation impact on thermal comfort in urban open spaces of Nairobi City. The objectives of the study were; (i) to investigate the spatiotemporal changes of vegetation cover in local climate zones (LCZs) of Nairobi, (ii) to determine the changes in land surface temperatures (LST) of Nairobi in the period between 1988 and 2018 and (iii) to determine the effects of *in-situ* plant species on microclimatic parameters within two distinct LCZs in Nairobi's CBD. Changes in land use/cover (LULC) types were evaluated using three Landsat satellite images; Landsat 4 (1988), Landsat 7 (2002) and Landsat 8 (2018). In the LCZs of Nairobi, forests and rangelands declined in area by 80 Km² and 127 Km², about 47% and 24%, sequentially. Built-up areas, urban agriculture and water showed an increase by 195 Km², 9 Km² and 3 Km², an approximation of 71%, 4% and 40%, respectively, between 1988 and 2018. The Normalized Difference Vegetation Index (NDVI) and Land Surface Temperatures (LST) were calculated from the same Landsat images. Results showed an increase in mean LST by 4.15°C and a reduction in highest NDVI values by 0.38. A statistical correlation analysis of LST and NDVI showed a significant negative coefficient (r) value of -0.94, -0.87, -0.90 in the years 1988, 2002 and 2018 respectively. A prediction of the LULC, NDVI and LST to 2033 were simulated to establish the future development possibilities for the next 15 years. The LST gradient trends showed higher surface temperatures on the central and eastern sides of Nairobi. Similarly, predictions (2033) indicate a similar trend for LULC, NDVI and LST. The differences in tree species' effect on microclimatic variables were established in a park (Central park) and a street (Taifa rd) within Nairobi CBD. In both sites, *Terminalia mantaly* species provided the best cooling effect with a Physiological Equivalent Temperature (PET) reduction of 9.6°C and 9.3°C in Central Park (Site 1, LCZ B) and Taifa Road (Site 2, LCZ 4), respectively. *Tipuana tipu* was the second best with 9.2°C and 8.2°C, followed by *Cassia spectabilis* with 8.5°C and 7.6°C, respectively. Air temperatures in Site 1 (Park) were 2.3°C, 1.3°C and 1.0°C reduced compared to those in Site 2 (Street) at 1pm, 6pm and 8am, respectively. The study highlighted the need for monitoring LULC and LST changes with respect to vegetation cover, to improve thermal comfort for the urban dwellers. Further, it recommended advanced urban climate studies to be conducted involving direct human physiological measurements, and to establish a guide for urban practitioners, with planting plans suitable for green infrastructure developments towards sustainable urban cooling of the wider Nairobi and other SSA cities.

CHAPTER ONE

INTRODUCTION

1.1 Background Information

Climate change is a key global concern today, particularly in urban areas. Urban climates contrast from those of rural regions and the degree of the differences may be quite huge. Oftentimes, the differences occur with respect to geometrical and urban thermo-physical attributes, weather conditions and anthropogenic moisture existent in the area. Local climate change in urban areas is primarily linked to the emission of greenhouse gasses from alterations in albedo and natural or human sources. This causes an occurrence known as Urban Heat Islands (UHI) (Santamouris *et al.*, 2017; Voogt, 2020), where urban areas tend to be warmer than the surrounding peri-urban areas.

The heat islands cause major threats to the environment, biodiversity, ecosystem functions and the city dwellers (Bellard, 2012; Soltani & Sharifi, 2017). Additionally, UHI from urban development contributes to an increase in urban ambient temperatures, among other implications, including elevated urban thermal discomfort and retrogression of the city dwellers' health and wellbeing (Heaviside *et al.*, 2017; Soltani & Sharifi, 2017; Voogt, 2020). As the greenhouse gas (GHGs) intensifies in Kenya, GIZ, (2018) has projected a temperature increase of 1.2 to 3.2°C between the 2080 to 2100, based on global climate models (GCM) with low and high emission scenarios of representative concentration pathways (RCP) 2.6 and 6.0 respectively. Correspondingly, a study by University of Cape Town, (2017) projects an average temperature increase in Nairobi by 2.5°C in 2100, considering GCM simulation of RCP8.5.

Local Climate Zones (LCZs) approach, a climate-based classification of both city and countryside regions, established by Stewart & Oke, (2012), has been considered effective in UHI and thermal environment investigation. It divides the urban LULC into the built and natural surface categories, based on their spatial distribution. LCZs

can be utilized for possible mitigation of the overall UHI effects through informed urban planning and management practices. There are 17 LCZs, classified as 10 classes (1-10) built-up and 7 (A-G) natural zones (Demuzere *et al.*, 2021). This urban landscape classification system's universality is essential, allowing comparison and modeling between and within specific climate zones at a local scale, especially for developing cities with minimal data infrastructure (Stewart & Oke, 2012; Demuzere *et al.*, 2021). Equally, using thermal indices like Physiologically Equivalent Temperature (PET) (Matzarakis & Amelung, 2008; Teshnehdel *et al.*, 2022), is necessary in quantifying the thermal comfort rate within these LCZs.

Earlier studies have revealed that Urban Green Spaces (UGS), such as urban gardens and communal parks can potentially moderate UHI effects (Chiesura, 2004; Feyisa, 2014). Urban vegetation, particularly mature trees are crucial in improving out-of-door thermal comfort and promoting urban cooling, while offering numerous services to urban dwellers and the environment (Ren, 2011; Bellard, 2012). Depending on the varied architecture, form and species, these trees improve outdoor and human thermal comfort (HTC) (Van Hoof *et al.*, 2010; Elnabawi & Hamza, 2019), providing several environmental benefits, like carbon sequestration, improved air quality and a habitat provision for urban biodiversity (Saxe *et al.*, 2001; Georgi & Zafiriadis, 2006; Bellard, 2012).

In 2020, Nairobi City had about 820 public open and green spaces covering approximately 3,100 hectares spatially, (UN-Habitat, 2020), which included forests, natural reserves, gardens, parks, sports fields among others. At a scale, block and city level, spaces constituted 64% and 25%, while linear and neighborhood spaces covered 6% and 5%, respectively. Out of these, about 80% had unrestricted access with multi-functional activities. These spaces provide important benefits for city residents and are often used for events, recreational and cultural activities, while contributing to biodiversity habitation and enhancing the aesthetic value of Nairobi city and its environment.

The WHO, (2017) recommends an UGS per capita of 9m², which is yet to be attained by most SSA cities. Since the 1980s, Nairobi's UGS have undergone significant

positive and negative advances. While some new parks, such as the John Michuki Memorial Park were established during this period, others like Ngong and Karura Forests have experienced degradation and loss due to urban developments and encroachment. The presently experienced rapid urbanization rate, increased population and the projected increase in temperatures indicate that Nairobi's open spaces are likely to suffer gradual dilapidation from overcrowding, and conversion from natural to built surfaces, lowering their value and decreasing quality of life (Makworo & Mireri, 2011). Comparably, Makokha & Shisanya, (2010) established that Nairobi City has experienced significant warming trends with higher temperatures present around the CBD, towards its peri-urban outskirts.

Similarly, LULC prediction is crucial with an array of substantial benefits, particularly in urban planning and environmental management. Accurate LULC data helps in identifying areas of urban growth, green spaces, and impervious surfaces, which are crucial for urban planning (Abbas *et al.*, 2021; Halmy *et al.*, 2015). By understanding how different land uses affect heat distribution, city planners can design interventions such as increasing vegetation cover and optimizing building materials to mitigate UHI. Additionally, the integration of LST predictions provides insights into temperature variations across different parts of Nairobi. This information is essential for developing localized cooling strategies, such as implementing reflective surfaces and shading in hot spots. It also supports the creation of climate-resilient infrastructure, ensuring that new developments are better adapted to withstand temperature extremes (Nagendra *et al.*, 2013).

This study, therefore, assessed the vegetation and UHI effect mitigation nexus within Nairobi City's open spaces to improve human thermal comfort. At a macro-scale, it examined alterations in vegetation cover and land surface temperatures over the last thirty-years within the LCZs. At a micro-scale, the study explored how plant architecture influences the extent of microclimate amelioration in immediate urban environments. Furthermore, it sought to pinpoint the specific timing and locations where the most significant changes occurred among various urban surfaces.

Knowledge generated from the study will be useful to urban green managers, landscape designers, arborists and nursery plant suppliers when making decisions regarding plant selection, planting design, installation, and overall maintenance. Additionally, the findings will provide valuable insights for shaping appropriate policies regarding the management of urban open spaces in Nairobi, specifically focusing on plant selection to achieve sustainable cooling and regulate microclimates through the implementation of green infrastructure projects.

1.2 Problem Statement

Presently, Kenya's urbanization rate is 29% (Statista, 2021), with a similar trend projected in the next thirty years. Due to the low albedo of most construction materials used in urban development, they store enormous quantities of radiation energy, releasing it at night, while compromising the general thermal comfort. Pollalis *et al.*, (2013) highlighted that, urban planners tend to pick construction supplies based on several specialized necessities like strength, longevity, and expenditures, but ordinarily focus less attention to their environmental aspects. Since the 1960's, Kenya's mean temperature per decade rose by 0.3°C, highlighted by (CCN, 2007; Tibaijuka, 2007). A cumulative increase of 2-3°C temperature is projected between 2060 to 2100, leading to scarcity in precipitation by approximately twenty percent (Tibaijuka, 2007).

Nairobi City, in the past, was once recognized as the '*Green City in the Sun*' (CCN, 2007), characterized by lush greenery, safe and healthy residences, flowing riverine ecosystems among others. Despite that, urban development has contributed to urban sprawl, vastly accounting for tree cover reduction and degradation of natural areas, including shrublands and rangelands (Tibaijuka, 2007). Comparatively, Nairobi city's land cover alterations, where most of the vegetative cover are transformed to non-heat absorbents, such as concrete paving, has also led to a rise in UHI and flooding. These adversely affect both Nairobi residents and its environment, from poor air and water quality.

In addition, increased anthropogenic activities, particularly the use of automobiles, poor inorganic waste disposal, and deforestation are significant contributors to local

climate change in Nairobi city. If not monitored and managed, UHI will exacerbate the thermal environments, affecting the quality of life with increased heat-related mortalities, air pollution, energy costs and underlying human health conditions (Heaviside *et al.*, 2017; Singh *et al.*, 2020). There is, therefore, a need to develop nature-based solutions to reduce UHI effects and make Nairobi City adaptive to the changing climate.

1.3 Justification

Urban forests and tree cover are progressively becoming crucial in sustaining the quality of a habitable urban setting. Common studies on urban trees' modification of microclimate to improve thermal comfort in urban areas have been mostly studied within the humid temperate oceanic climates (Park *et al.*, 2012; Teshnehdel *et al.*, 2022). Even so, there is a dire scarcity of information regarding the effectiveness of diverse mature tree species in microclimate variation within heterogeneous urban environments, particularly in tropical climate areas. Incorporation of UGS, predominantly matured tree species in urban domains, presents a significant temperature reduction impact to the city dwellers (Chiesura, 2004; Park *et al.*, 2012; Feyisa, 2014).

Plants, particularly mature trees in the urban areas, play varied roles (Chiesura, 2004; Loughner *et al.*, 2012; Feyisa, 2014), including cooling the environment through evapotranspiration, thus moderating the air temperatures and saving energy required for cooling. As air pollution is becoming rampant in urban areas, the urban vegetation acts as pollutant sinks (Jim, 2013; Shahidan, 2015), filtering out particulate matter (PM) and the toxic gasses such as CO₂. However, the quality of urban forests and tree ecosystems' interaction with the present climate inconsistency remains complex (Georgi & Zafiriadis, 2006; Soltani & Sharifi, 2017). Cities in the Global North have been leading large-scale tree planting campaigns, with their positive impact on urban resilience and attractiveness inspiring global adoption, including in Nairobi, Kenya's capital.

Nairobi's tree cover comprises various urban forest categories, such as expansive natural forested regions like Karura Forest, alongside city parks, informal pocket

parks, yard trees, vacant lots, and street trees (Oloo *et al.*, 2020). Recent research investigated people's perspectives on the city's natural vegetated spaces, the trees' medicinal uses, disparities in their accessibility, and the factors affecting their survival (Binyanya *et al.*, 2022; Furukawa *et al.*, 2016; Okech & Nyadera, 2022). However, limited research exists on Nairobi's urban trees, with a specific focus on the effects of individual mature trees, their tree architecture, canopy form, and other allometric properties on microclimate regulation. Although there is no readily accessible greening strategy, recent endeavors have been made to establish and rejuvenate green areas by planting trees both within these spaces and along roadways. Therefore, developing a comprehensive guide for both urban practitioners and policy makers is critical. This will make it easier to screen and select suitable plants for different LCZs of Nairobi, while maximizing their potential in making the city adaptive to climate change and improving livability.

1.4 Objectives

1.4.1 General Objective

To assess the land use and vegetation changes impact on thermal comfort in urban open spaces of Nairobi City, Kenya.

1.4.2 Specific Objectives

1. To investigate the spatial and temporal changes of vegetation cover in local climate zones (LCZ) of Nairobi in the period between 1988 and 2018
2. To determine Land Surface Temperature (LST) changes in Nairobi along the urban gradient
3. To determine the effect of *in-situ* plant species on microclimatic parameters within distinct LCZs of Nairobi's central business district (CBD)

1.5 Research Hypotheses

1.5.1 Null Hypothesis (Ho)

1. Vegetation cover and other land use and land cover (LULC) within the local climate zones (LCZ) of Nairobi City have not significantly changed over the past three decades (1988-2018)
2. Land surface temperatures of Nairobi City along the urban gradient have not significantly changed over the past three decades (1988-2018)
3. Different plant species do not have the same effect on microclimatic parameters irrespective of location within urban environments.

1.6 Scope of Study

This study was set out in Nairobi, which serves as the capital city of Kenya located in East Africa. It was limited to the urban environment, covering areas with similar features across the horizontal scale based on surface porosity; porous surface (park) and impervious surface (street). Primary data collection was executed in two different local climate zones (LCZ) within Nairobi CBD (LCZ B: Scattered trees and LCZ 4: Open high rise). The two locations were selected to compare the degree of microclimate regulation by different tree species in an urban park and an urban street, represented by Central Park and Taifa Road in Nairobi. The factor of time was considered to determine the duration taken for the changes in vegetation cover and temperature of Nairobi to occur. This was a constant difference of ten years for three decades from 1988 to 2018. Plant measurements were limited to tree morphology and architecture. This study applied both local climate spatial scale (entire Nairobi County) and microclimate spatial scale (involving the immediate environment of the plants).

1.7 Study Limitations

Despite the study's promising findings considering the immediate environment of the isolated urban trees while comparing their effectiveness in microclimate modification in Nairobi's open spaces during the warm season, it did consider clustered trees through possible scenarios within similar settings and during the cold season. Further,

it did not incorporate direct human physiological and psychological measurements under these same urban open spaces. For instance, measurements of the heart rate variability, and mental stress, based on different demographics such as age and gender of the city dwellers who commonly use these spaces.

CHAPTER TWO

LITERATURE REVIEW

2.1 Introduction

A comprehensive overview of the existing research on the urban vegetation and UHI mitigation nexus using LCZs in cities were discussed in this chapter, to localize the context for Nairobi and develop urban climate adaptive measures for future planning of the city. Sub-section 2.2 highlights theoretical literature review, and sub-section 2.3 outlines the study's conceptual framework. A critical review of the global, regional and local case studies is illustrated in 2.4, the overall summary in 2.5 and the research gap under 2.6.

2.2 Theoretical Review

Comprehending the connection between urban climate and urban greenery is important in quantifying green spaces' impact on improving urban microclimate. The section presents the theoretical review on the significance of urban greenery, particularly isolated *in-situ* plants, as a potential solution to counteract the adverse effects of urban heat and urbanization on local climate conditions for Nairobi.

2.2.1. Urban Morphology and Climate

Universally, cities continue to grow and expand, and this sprawl directly influences the urban morphology and form (Yin *et al.*, 2018), where they experience changes in land use patterns, building heights, and the distribution of urban features, influencing the overall spatial arrangement and character of the urban environment. Consequently, these morphological changes pose significant impacts on the local and microclimate by creating an Urban Heat Island (UHI) effect, with compact urban forms exacerbating heat retention and limited vegetation hindering cooling processes (Tesfamariam *et al.*, 2023; Yin *et al.*, 2018). Understanding these impacts is crucial for sustainable urban planning and implementing strategies to manage the urban climate and mitigate adverse effects on human well-being and the environment.

Sub-Saharan African (SSA) cities typically exhibit unique and closely interrelated morphology and climatic characteristics (Amegah *et al.*, 2016; Li *et al.*, 2023), with an average of approximately 6% urbanization rate annually over the past three decades (Mundia & Murayama, 2013). Often, this encompasses a blend of modern infrastructure and traditional architecture that reflect cultural diversity. These cities experience tropical climates, characterized by high temperatures and distinct wet and dry seasons, with UHI effects from rapid urbanization and increased heat absorption from the common use of concrete and asphalt materials in construction (Simwanda *et al.*, 2019; Li *et al.*, 2021). This prevalence of impervious surfaces and inadequate urban planning intensify heat-related challenges for urban dwellers in SSA.

Nairobi, like many other SSA cities, exhibits a diverse urban morphology comprising a mix of high-rise buildings, commercial centers, residential areas, and sprawling informal settlements, with increasingly impervious surfaces that contribute to the UHI effect. (KMD, 2020; Li *et al.*, 2021) the city experiences a subtropical highland climate with distinct wet and dry seasons, where its highest annual temperatures occur in February, reaching an average of 29°C (84°F), while the coldest month is July, with an average temperature of 17°C (63°F). Temperature variations and precipitation patterns play a crucial role in shaping Nairobi's urban climate and require sustainable urban planning to address heat-related challenges and promote resilience. Additionally, innovative urban design and planning strategies, such as incorporating green infrastructure (Soudoudi *et al.*, 2018; Soltani & Sharifi, 2017; Onyango *et al.*, 2021; Zafiriadis, 2014) and passive cooling techniques can help mitigate these challenges to enhance the livability of the city.

2.2.1.1 Urban Heat Island (UHI)

UHI is an occurrence that refers to the perceived temperature variation in the urban environments and the neighboring peri-urban areas. Observational evidence has indicated that temperatures in urban centers can be higher with up to twelve degrees Celsius compared to the adjacent regions (Anjos & Lopes, 2017; Voogt, 2020) (Figure 2.1).

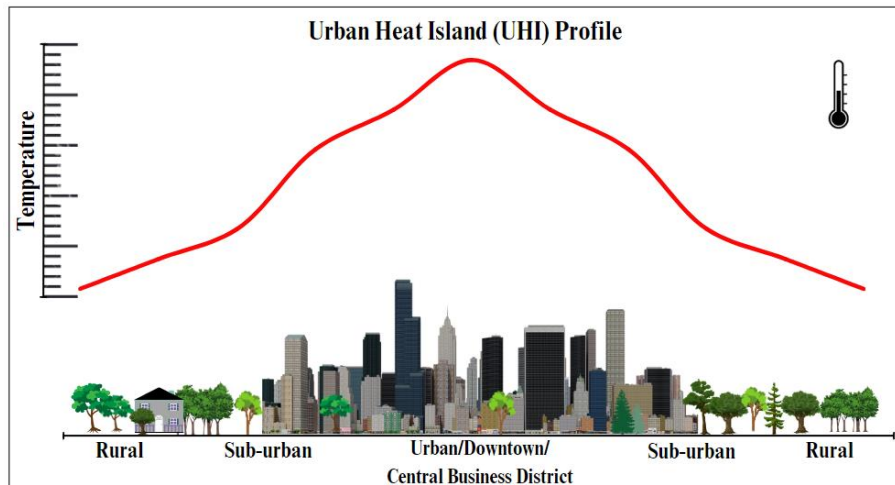


Figure 2.1: Graphical Representation of the UHI Profile

Source: (Author, 2023)

i) Drivers of UHI and Impacts

The local climate is affected by several meteorological parameters like relative humidity, temperature, and wind. Several anthropogenic factors foster the development and surge of urban heat islands (UHI). Among them are greenhouse gas effusion, impermeability and low albedo materials, urban forest cover loss and the materials' thermal properties (Figure 2.2). Additionally, the urban morphology and city extent also largely contribute to UHI development.

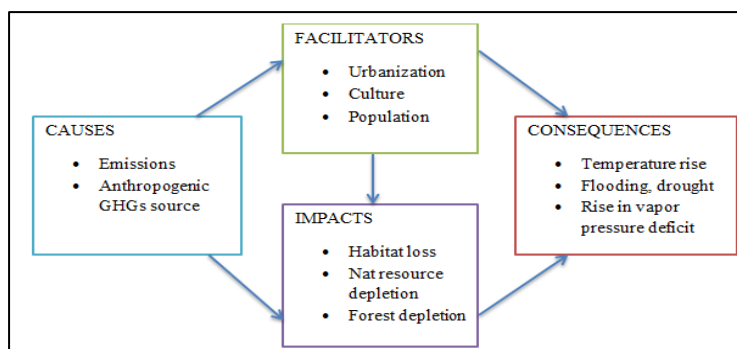


Figure 2.2: The Causes, Facilitators, Impacts and Consequences of Urban Heat Island

The generation of human-induced heat such as ones radiated by vehicles, and manufacturing operations also adds to the formation of UHI. Predominantly, this

happens in compact urban areas where events and activities are centralized (USEPA, 2015). In urban environments, greenhouse gas sources primarily are the industrial processes, vehicles and fossil fuel heating of buildings. Greenhouse gasses entrap solar power in the environment which contributes to the atmospheric heat up (Rossi *et al.*, 2015).

Similarly, urban development has equally led to alterations in ground cover types, where impermeable materials such as asphalt and various construction materials replace natural surfaces. These materials have low albedo (Ouyang *et al.*, 2022), contributing to urban warming, and they equally do not allow water infiltration or absorption (Brudler *et al.*, 2016), hence changing the natural route of storm water. The impermeable surfaces cause increased runoff that conveys chemical pollutants like pesticides and hydrocarbons to water bodies (Müller *et al.*, 2020). They also cause sewer overflows as a result of heavy rains.

According to (Forman, 2013; Pollalis *et al.*, 2013), urban planners and architects select the paving and building supplies based on several specialized necessities such as durability, security and the cost. Ordinarily, they always pay little attention to environmental considerations while making their selections. Even so, as explained by (Park *et al.*, 2012; Teshnehdel *et al.*, 2022), vegetation has a vital function in the prevention of heat build-up. Vegetation achieves this through processes such as casting shade over buildings and the ground, as well as evapotranspiration. Additionally, a significant role played by vegetation is in enhancing efficient stormwater management and quality of air in urban environments (Georgi & Zafiriadis, 2006; Park *et al.*, 2012).

ii) Impacts of UHI

Air Quality

Air quality in urban areas is a concerning issue, often compromised by high levels of pollutants and emissions that can pose significant health risks to the city residents. Geddes & Murphy, (2012) assert that smog formation is highly heightened by UHI, and is made of tropospheric ozone and fine particulate matter (PM), with the common contaminants being nitrogen oxides and explosive volatiles organic compounds

(VOCs) (Ulpiani, 2021). Likewise, indoor air cooling, besides refrigeration requirements, normally escalates energy demands, causing greenhouse gas emissions that negatively affect the urban environments and directly contribute to global warming (Voogt, 2020).

Wellbeing

Human wellbeing encompasses the holistic state of individuals (Ryff, 2014; Stoewen, 2017), including their physical, mental, and social prosperity, involving aspects such as happiness, fulfillment, and the capacity to live a purposeful and gratifying life. However, as a result of intensified UHI, cities experience phases of elevated temperatures (Ulpiani, 2021). Oftentimes, these temperature changes may lead to human heat stresses, worsening both respiratory and chronic diseases (Heaviside *et al.*, 2017; Singh *et al.*, 2020), which eventually deteriorate the health and wellbeing of urban dwellers. Ordinarily, the most vulnerable populations get affected, including persons with long-standing diseases and underlying conditions, very tender aged children, and the elderly (Leal *et al.*, 2018; Onyango, 2022). Urban planning strategies to improve mitigate UHI can enhance wellbeing by promoting cooler and healthier urban environments

2.2.1.2 Human Thermal Comfort

Human thermal comfort (HTC) is a psychological situation that tends to express contentment with the thermic atmosphere (Van Hoof *et al.*, 2010; Elnabawi & Hamza, 2019). Dissimilarities in urban microclimate may result in diverse thermal impressions varying from severe to moderate and mild degrees of physiological stress. TC evaluation is realizable by using various thermal climate indices (Matzarakis & Amelung, 2008), in particular, the Physiological Equivalent Temperature (PET).

As elaborated by Van Hoof *et al.*, (2010), PET is a human bio-meteorological scale that outlines the thermal perception of individuals. It sets out the precise climatic feeling encountered by humans regardless of their dressing and metabolism (Matzarakis & Amelung, 2008; Elnabawi & Hamza, 2019), and is quantified in °C.

PET is suitable for all climates (Abdel-Ghany *et al.*, 2013), both interior and out-of-door and is computed using the RayMan software.

As a tool used for predicting human TC, RayMan software evaluates outdoor thermal environments. It is based on the principles of the PET index, considering different environmental variables, such as, air temperature, humidity, wind speed, and solar radiation, as well as personal factors such as clothing and activity level (Fang *et al.*, 2018; Ji *et al.*, 2022). Additionally, the software uses climate measurement input data from weather stations to create spatial TC maps of specific outdoor environments. It is commonly used in urban planning and design, outdoor event planning (Abdel-Ghany *et al.*, 2013), and in assessing the thermal comfort of city dwellers in outdoor environments while identifying the necessary mitigation measures.

2.2.2 Urban Environments and Microclimate

Urban climate varies from those in the city outskirts and the rural areas. The levels of the differences could occasionally be reliant on weather status, urban geometrical and thermo-physical properties, and warm stations existent in the area. Ordinarily (Hang *et al.*, 2012), urban contaminants densities may be ten times greater compared to those of rural areas, with air temperatures normally higher with an average two degrees Celsius (USEPA, 2015). The distinction between rural and urban climates is commonly heightened by human-induced heat and contaminants getting into the atmosphere (Voogt, 2020). These result in negative effects for both the urban dwellers and the environment at large. Urban greenery, thus, considerably changes the microclimate within these open spaces making them livable.

A heat island may occur at a variety of measures (Giguère, 2012; Santamouris *et al.*, 2017). It could exhibit itself around a small vegetative canopy, a single building, or a large percentage of a city. Reliant on prevailing weather conditions and geographic location, heat islands could be beneficial or harmful to the urban occupant and energy consumer. Incorporating high albedo materials lessens the magnitude of solar radiation being absorbed in urban structures and building envelopes (Ouyang *et al.*, 2022). In the end, it keeps their surfaces cooler.

In Nairobi, Bosco *et al.*, (2011) underscores that over the past three decades, the capital city's urban environment has undergone significant transformation, characterized by rapid urbanization, population growth, and infrastructural developments. It has experienced the growth of built-up areas, resulting in reduced green spaces and increased urban density, which have had a notable impact on the city's microclimate (Sanusi & Bidin, 2020). Notably, Nairobi has shown signs of increasing temperatures, particularly in the built-up regions around the city center (Li *et al.*, 2021), leading to an increase in urban heat islands. Reduced vegetation coverage and increased impervious surfaces have contributed to altered wind patterns, heightened air pollution, and changes in precipitation patterns, exacerbating the urban heat island effect (Simwanda *et al.*, 2019; Sanusi & Bidin, 2020) and posing challenges for urban planning and environmental sustainability for the city.

2.2.2.1 Local Climate Zones (LCZ) Classification

The ratio and dispersion of land cover classes comprising constructed, vegetated and bare lands and surface water are drivers of heat interchange within the urban fringe and adjacent countryside areas (Karatasou *et al.*, 2006; Soltani & Sharifi, 2017). The resulting occurrence is UHI, which has detrimental implications especially during warm seasons, such as, outdoor distress from heatstroke, increased energy cost among others. Therefore (Giguère, 2012; Santamouris *et al.*, 2017), various urban studies relating to quantification of UHI effects have been performed to comprehensively understand the phenomenon, and devise possible mitigation and adaptation strategies.

Stewart & Oke, (2012) describe Local Climate Zones (LCZ) as sections of homogenous surface cover, structures and human activities that stretch over several meters on horizontal scale. The LCZs were each independently designated names and systematically arranged applying a single or multiple distinctive surface characteristics. In particular, the objects' height, building materials or predominant land cover. Moreover, their physical properties are quantifiable and nonspecific to locality or time and are a representation at the local scale, which is suitable for urban climate studies in any city (Stewart & Oke, 2012), applying their existing local

characteristics. The standard set of LCZs existing within any landscape consist of 17 zones in total (Figure 2.3), categorized into two:

- i) **Built Types (LCZ 1 to 10):** these zones constitute constructed features as the primary land cover. They have both compact zones that are paved and built, together with open zones that may have scattered trees.
- ii) **Land Cover Types (LCZ A to G):** they constitute the existing natural vegetation, pervious surfaces and open to sparsely distributed trees, for instance the urban green spaces (UGS).






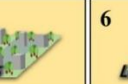


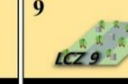









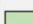


 LCZ 1 Compact Highrise Dense mix of tall, highrise buildings to tens of stories. Few or no trees. Land cover mostly paved. Concrete, steel, stone, and glass construction materials.	 LCZ 2 Compact Midrise Dense mix of midrise buildings (3-9 stories). Few or no trees. Land cover mostly paved. Stone, brick, tile, and concrete construction materials.	 LCZ 3 Compact Lowrise Dense mix of lowrise buildings (1-3 stories). Few or no trees. Land cover mostly paved. Stone, brick, tile, and concrete construction materials.	 LCZ 4 Open Highrise Open arrangement of tall, highrise buildings to tens of stories. Abundance of pervious land cover (low plants, scattered trees). Concrete, steel, stone, and glass construction materials.	 LCZ 5 Open Midrise Open arrangement of midrise buildings (3-9 stories). Abundance of pervious land cover (low plants, scattered trees). Concrete, steel, stone, and glass construction materials.	 LCZ 6 Open Lowrise Open arrangement of lowrise buildings (1-3 stories). Abundance of pervious land cover (low plants, scattered trees). Concrete, steel, stone, and glass construction materials.
 LCZ 7 Lightweight Lowrise Dense mix of single-story buildings. Few or no trees. Land cover mostly hard-packed. Lightweight construction materials (wood, thatch, etc.).	 LCZ 8 Large Lowrise Open arrangement of large lowrise buildings (1-3 stories). Few or no trees. Land cover mostly paved. Steel, concrete, metal, and stone construction materials.	 LCZ 9 Sparsely Built Sparse arrangement of small or medium-sized buildings in a natural setting. Abundance of pervious cover (low-plants, scattered trees).	 LCZ 10 Heavy Industry Lowrise and midrise industrial structures (towers, tanks, stacks). Few or no trees. Land cover mostly paved or hard-packed. Metal, steel, concrete construction materials.	 LCZ A Dense Trees Heavily wooded landscape of deciduous and/or evergreen trees. Land cover mostly pervious (low-plants). Zone function is natural forest, tree cultivation, or urban park.	 LCZ B Scattered Trees Lightly wooded landscape of deciduous and/or evergreen trees. Land cover mostly pervious (low-plants). Zone function is natural forest, tree cultivation, or urban park.
 LCZ C Bush, Scrub Open arrangement of bushes, shrubs, and short, woody trees. Land cover mostly pervious (bare soil or sand). Zone function is natural scrubland or agriculture.	 LCZ D Low Plants Featureless landscape of grass or herbaceous plants/crops. Few or no trees. Zone function is natural grassland, agriculture, or urban park.	 LCZ E Bare Rock/Paved Featureless landscape of rock or paved cover. Few or no trees or plants. Zone function is natural desert (rock) or urban transportation.	 LCZ F Bare Soil/Sand Featureless landscape of soil or sand cover. Few or no trees or plants. Zone function is natural desert or agriculture.	 LCZ G Water Large open water bodies such as seas and lakes, or small bodies such as rivers, reservoirs, and lagoons.	LEGEND  Built-Up LCZ 1 – LCZ 10  Natural LCZ A – LCZ G  

Figure 2.3: Outlined Descriptions for LCZs

Source: (Stewart & Oke, 2012; Kim *et al.*, 2021)

2.2.2.2 Land Surface Temperatures (LST)

Surface temperature itself is a universal, unspecified word denoting the amassed temperatures of the total features (Billah & Haque, 2021), existing in a location. LST reserves the inbound longwave and solar radiation (Anbazhagan & Paramasivam, 2016), outgoing physical infrared radiation, ground flux, and the sensible and potential

heat flux. Jiang & Lin, (2021) confirmed that it is a dependable pointer of the energy counterbalance on the ground's surface, along with the existing UHI and its effects in urban areas.

Conventionally, LST were primarily acquired using estimated data from weather stations. Though dependable and long lasting (Jiang & Lin, 2021), these LST data have a scattered distribution while providing minimal precise coverage for larger spatial extents. They also have thermal infrared detector bands, strengthening their practicability in LST valuation using multiple algorithms. For these reasons, quantifying higher resolutions and correct LST for bigger scales, such as Nairobi city, is only feasible through remotely sensed satellite imagery (Kumar & Shekhar, 2016; Jiang & Lin, 2021).

2.2.3 Plants and Microclimate Control for Urban Environments

2.2.3.1 Plant Ecophysiology

Affirmed by Armson, (2012), plant physiological ecology has advanced over the past hundred years. Since the 1980s (Armson, 2012; Lin *et al.*, 2017), the advancement of new technology has enabled creation of models that define the fundamental physiological mechanisms of plant reactions to changing urban environments at greater spatial and temporal scale. Plant ecophysiology plays a vital role in microclimate control within urban areas, while providing different degrees of environmental advantages. Loughner *et al.*, (2012) through the process of transpiration, plants release water vapor, which cools the surrounding air, thereby reducing temperatures.

As plants provide shade to mitigate heat stress, their stomatal conductance regulates gas exchange, influencing the relative humidity (Klingberg *et al.*, 2015). Transpiration rate is intensely affected by stomatal conductance and leaf temperature that fluctuate during the day. Photosynthesis contributes to carbon sequestration (Lorenz & Lal, 2010; Klingberg *et al.*, 2015; Gayathri *et al.*, 2021), reducing greenhouse gasses, and improving urban air quality. Moreover, tree leaves are very much efficient in

entrapping atmospheric particles and pollutants, and this is especially vital in urban areas.

Anjos & Lopes, (2017) asserts that urban settings tend to experience windstorms and other adverse effects resulting from the urban canyon delineated by existent constructions. The urban trees, therefore, act as windbreakers by modifying the wind patterns, eventually reducing wind speed and enhancing wind direction within these spaces. By fostering urban biodiversity through optimizing plant species selection and urban green infrastructure, plant ecophysiology can sustain ecological balance, ensuring more resilient and habitable environments in cities. This natural approach to microclimate control offers sustainable solutions to combat both rising urban temperatures and the environmental challenges.

2.2.3.2 Urban Trees Performance

Urban greening plays a pivotal role in enhancing human well-being and environmental quality as highlighted in Figure 2.4. Selecting appropriate tree species for urban areas necessitates an understanding of their performance under diverse disturbances. (Tesfamariam *et al.*, 2023; Yin *et al.*, 2018) in tropical climate cities, urban tree performance is crucial for mitigating the adverse effects of urbanization. Recent studies indicate that certain tree species demonstrate remarkable adaptability and exhibit superior resilience to urban stressors, such as air pollution, soil salinity and compaction, pests and temperature fluctuations. Countless numbers of used species, particularly the native ones, are prone to these rough urban environmental settings. (Loughner *et al.*, 2012; Anjos & Lopes, 2017) to counter these effects and other related disturbances, water accessibility is critical for recently planted urban trees, ensuring they achieve maximum functionality and performance within these areas.

As demonstrated by (FONA, 2020; Maundu *et al.*, 2005) in Nairobi, certain tree species possess promising attributes for its environments. For instance, *Jacaranda mimosifolia* and *Tipuana tipu* have demonstrated a high survival rate and rapid growth in the city's urban settings with high average annual carbon sequestration rates (FONA, 2020; Maundu *et al.*, 2005). Additionally, indigenous species like meru oak (*Vitex kinensis*) and yellow acacia (*Vachellia xanthophloea*) (Maundu *et al.*, 2005) have been

found to enhance ecosystem services including nitrogen fixation to promote soil fertility. Such findings highlight the potential of specific tree species to contribute to urban greening efforts and ecological services in SSA cities. However, despite the importance of this knowledge, there is still a lack of comprehensive data on the performance of numerous tree species under these urban disturbances (Pauleit *et al.*, 2017), necessitating further research to inform sustainable urban greening practices for Nairobi City.

2.2.3.3 Plant Responses to Climate Change

Shifts in temperature, precipitation patterns, and atmospheric CO₂ concentrations profoundly affect plant physiology and ecology, leading to altered growth and fruiting. (Grime *et al.*, 2007; Rossi *et al.*, 2015) many plant species are shifting their geographical ranges in response to changing climate conditions, as phenotypic plasticity enables diverse plant species to adapt and maintain their dominance in spatiotemporally variable environments. Furthermore, elevated CO₂ levels can stimulate photosynthesis and growth in some plants (Grime *et al.*, 2007; Rossi *et al.*, 2015), but prolonged drought conditions may counteract these benefits. Climate change can also influence plant interactions with other organisms, such as pests, pathogens, and pollinators (Poorter *et al.*, 2009), further affecting plant health and population dynamics. Understanding these complex responses is vital for predicting future vegetation distribution, biodiversity changes, and ecosystem functioning, aiding in the formulation of effective conservation and adaptation strategies.

i) Urban forests Response Climate Change

Urban forests worldwide are experiencing notable impacts in response to climate change. Increasing temperatures and altered precipitation patterns influence urban forest dynamics, where these trees face stress from heat, drought, and increased occurrence of extreme weather events. As global climate changes, forest biomes also experience transformations due to potential surpassing of species' physiological limits and alterations in the degrees of biophysical woodland processes (Robinson, 2004; Loughner *et al.*, 2012). Urban forests provide essential ecosystem services, such as temperature modification and carbon sequestration, but climate stressors can

compromise their resilience. Klingberg *et al.*, (2015) assert that in situations where water availability becomes limiting, the heights and densities of forest canopies may be reduced from eco-physiological constraints.

Several changes may occur in forests when climate varies (Ouyang *et al.*, 2022), which are often caused by variation in albedo, altered carbon cycle dynamics (Pauleit, 2003; Pauleit *et al.*, 2017) energy fluxes and moisture exchange. A rise in ambient CO₂ concentrations could moderate the aperture of stomata necessary to allow a certain quantity of CO₂ to go into the plant, decreasing its transpiration. Saxe *et al.*, (2001) trees possess the ability to adjust to warm climates, though the reaction anticipated from species vary, and the influence on photo-inhibition and respiration are further hard to hypothesize.

In Nairobi, urban forests encounter additional challenges due to rapid urbanization, leading to deforestation that has led to the reduction of green spaces over time (Oloo *et al.*, 2020). Climate-induced disturbances, such as heatwaves and water scarcity, often affect tree health and urban biodiversity. Nairobi's urban forests such as Karura, Ngong and the National Park, are vital for urban cooling and air quality improvement, even so, they face risks of fragmentation (CCN, 2007; Oloo *et al.*, 2020) and degradation from urban expansion and climate stressors, necessitating climate-resilient urban planning and management.

ii) Isolated Urban Trees Response Climate Change

Isolated trees are the trees that stand-alone and have quite some distance to the next nearby trees, unlike clustered trees (Shahidan, 2015), which are close, like in the case of forests. Often, they are planted following certain landscape designs for urban setups (Robinson, 2004; Georgi & Zafiriadis, 2006), or randomly grow within a green space. Individual tree species have various responses to variations in urban climate based on their diverse allometric properties.

Some of these attributes largely regulate microclimate (Klingberg *et al.*, 2015; Shahidan, 2015), in particular, their canopy sizes and foliage densities, which highly determine the trees' shade efficiency, thermal abilities along with their

evapotranspiration frequency. As demonstrated by Soltani & Sharifi, (2017), during warm seasons, these trees' microclimate modification abilities are at their peak around midday and late afternoons. Tapping into the potential of native evergreen isolated trees is therefore (Jim, 2013), essential in advancing human thermal comfort.

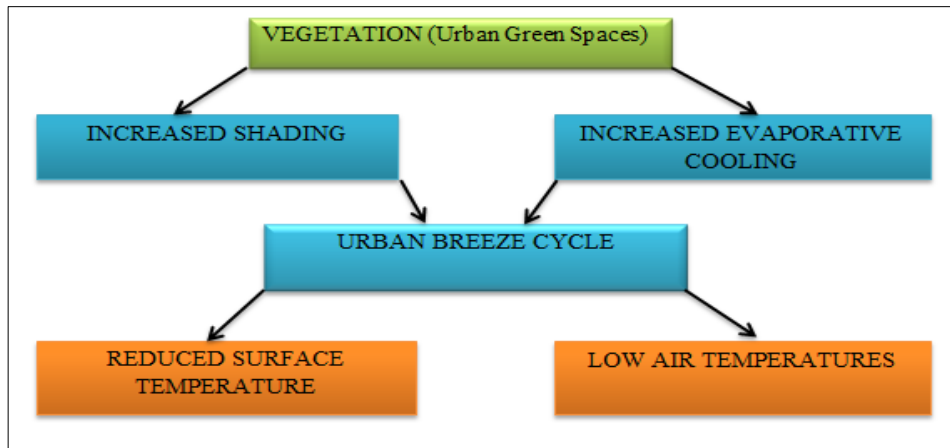


Figure 2.4: Benefits of Urban Greenery

2.3 Conceptual Framework

This subsection summarizes the study's conceptual framework interlinking the independent, dependent, mediating and moderating variables, showing the cause-effect relationship between these variables, as well as the expected outcomes of the study, as highlighted in figure 2.5.

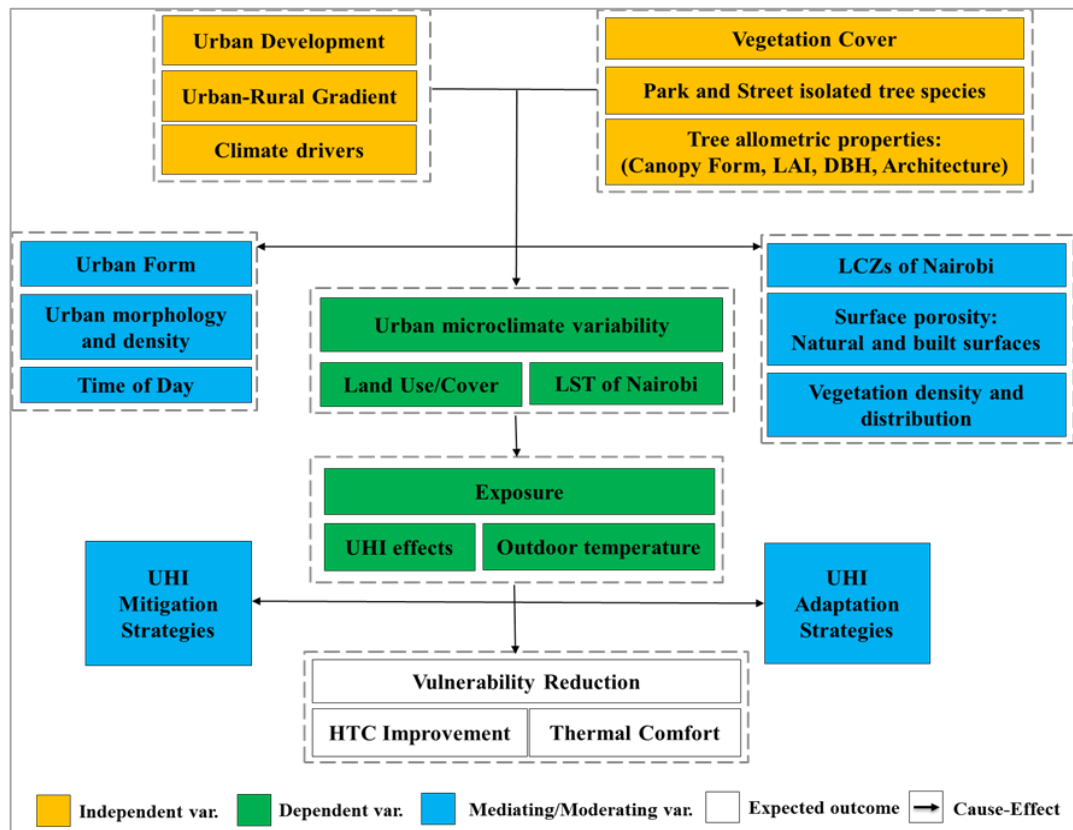


Figure 2.5: The Study's Conceptual Framework

2.4 The Critiques of Existing Literature and Case Studies

This section presents an extensive global, regional and local context critical review, as well as case studies of the concepts of spatiotemporal vegetation changes monitoring in LCZs under 2.4.1, LST and SUHI nexus along the urban gradient under 2.4.2, and the linkage between urban trees species' microclimate modification and UHI mitigation to improve human thermal comfort under 2.4.3.

2.4.1 Spatiotemporal Vegetation Changes Monitoring Using LULC within LCZs

The spatiotemporal monitoring of vegetation and LULC in cities provides valuable data for assessing urban growth patterns, identifying changes in green spaces, and informing sustainable urban planning and management strategies (Aabeyir *et al.*, 2022; Amiri *et al.*, 2009; Liu *et al.*, 2013; Silva *et al.*, 2018). Recent studies have demonstrated the possibilities of using local climate zones (LCZs) to monitor and manage urban vegetation cover at different spatial scales. LCZ-based approach enables

vegetation-tracking dynamics over time (Aslam *et al.*, 2021; Bechtel *et al.*, 2015; Brousse *et al.*, 2019; F. Huang *et al.*, 2023; Zhao *et al.*, 2022), providing valuable insights into ecosystem health, climate change impacts, and urbanization effects.

Further, the monitoring allows for the identification of critical vegetation shifts, aiding in conservation strategies and land management decisions. It equally facilitates the assessment of ecological responses to natural and anthropogenic disturbances (Bigsby *et al.*, 2014; Ferreira & Duarte, 2019), aiding in understanding biodiversity patterns and ecological resilience. However, there is a need for more research on the application of this approach in different urban contexts and climates to determine its effectiveness in promoting sustainable urban development.

Globally, in Austin, Texas, USA, (Zhao *et al.*, 2022) effectively analyzed the relationship between the local climate and vegetation patterns using LCZ, revealing significant spatiotemporal variations in vegetation phenology within the city from 2008-2018. It showed an increase of about 70% in the built-up LCZ and decline of about 33% in the natural LCZ types, exhibiting significant phenological differences. In addition, these spatial variations were found to be greatly impacted by changes in surface temperatures that are influenced by factors such as altitude, topography, and soil conditions. As urban morphology gradually changes, in Baltimore, MD, and Raleigh, NC, (Bigsby *et al.*, 2014) revealed it to play a substantial part in driving the homogenization of tree cover. In Paço do Lumiar (Brazil), assessing its thermal characteristics and evaluating the influence of greenery cover and disintegration on the city's urban environment using LULC, indicated extensive urban growth from 2000 to 2015 (Silva *et al.*, 2018).

In southern Asia's Islamabad (Pakistan), the spatiotemporal dynamics of LULC, LST, and LCZ using spectral indices (Aslam *et al.*, 2021). It showed a noteworthy >95% increase in the city's built-up area from 2013 to 2019, with a positive correlation between LST and NDBI, and a negative correlation between LST and NDVI, indicating the effect of urbanization and reduced vegetation cover on local temperatures. While in north-eastern Asia (Liu *et al.*, 2013), based on LCZs, NDVI changes were highly attributed to the LULC dynamics between 1982 and 2009.

Similarly, employing a temperature-vegetation-index space to determine the interrelation between LULC and LST in Tabriz (Iran) (Amiri *et al.*, 2009) revealed that urbanization led to shifts in pixels from low-temperature-dense greenery to high-temperature-sparse greenery conditions from 1989-2001. Riyadh city's (Saudi Arabia) vegetation conversion to built-up areas was 35% between 1985-2014, while Delhi city's (India) vegetation cover reduced by 38% as built-up areas increased by >90% from 1990-2018 (Alqurashi & Kumar, 2019; Naikoo *et al.*, 2020).

In Africa's Mekelle City (Ethiopia) (Tesfamariam *et al.*, 2023), comparing the dry and wet seasons from 1990-2020, vegetation cover declined by 20% to 18% respectively, with pervious surfaces increasing by 77%. (Aabeyir *et al.*, 2022) Wa Municipality's (Ghana) urban tree density reduced from 85% to 55% between 2014-2020, attributed to the high demand for commercial spaces, creating strong competition and leading to conflicts between physical infrastructure development and the preservation of existing green areas. In East London (South Africa) from 1986-2016, there was a decline of nearly 360 Km² in vegetation cover, whereas the built-up area expanded by 180 Km² (Orimoloye *et al.*, 2018), resulting in changes in thermal features that pose risks of heat stroke occurrences and cardiovascular-related diseases to city residents.

Kenya's capital, Nairobi has equally experienced drastic changes in land cover, particularly its urban vegetation consisting of forests and parks among others. Spatiotemporal LULC monitoring between 1976 to 2015 have shown a substantial upsurge in built-up areas by around 50 Km² (Mundia & Aniya, 2006; Oyugi *et al.*, 2017). In contrast, nearly 15% of forested land in Nairobi was lost between 2000-2015 in six of the urban forests, with a positive trend observed, indicating an ongoing disturbance of urban forests in the city (Oloo *et al.*, 2020). The primary factors leading to forest loss were identified as growing residential development and agricultural activities, construction of large infrastructure projects cutting through forests, timber harvesting, and other resources to facilitate urban development. However, there is limited use of LCZs in monitoring vegetation changes in Nairobi for the past three decades for effective and sustainable urban management.

2.4.2 Land Surface Temperature (LST) and Surface Urban Heat Island (SUHI) Nexus along the Urban-Rural Gradient

In cities, the LST and SUHI nexus along the urban-rural gradient is significant in understanding the complex interactions between urbanization and local climate (Dissanayake *et al.*, 2019; Estoque *et al.*, 2017). LST data, obtained through remote sensing, allows for precise monitoring of surface temperatures across urban areas, providing crucial insights into SUHI patterns and their temporal variations. Additionally (Pal & Ziaul, 2017; Yin *et al.*, 2018), it is possible to identify the drivers and impacts of urban heating, to aid in the formulation of effective urban planning and mitigation strategies.

It offers valuable information for urban climate modeling, as it contributes to the understanding of heat-related health risks, energy consumption patterns, and overall urban sustainability. (Cilek & Cilek, 2021; Peng *et al.*, 2018) investigating the LST-SUHI nexus using LCZ facilitates informed decision-making for enhancing urban resilience and promoting sustainable urban development in the face of ongoing climate change. It holds great potential for advancing general comprehension of urban climatology and guiding policymakers in fostering more livable and climate-resilient cities.

Increased rate of urbanization in most cities poses a great risk of increasing LST and UHI, eventually deteriorating both the urban dwellers and the urban environment. (Cheng & Su, 2010; Onyango, 2022) extreme heat can potentially trigger cardiovascular events from heat stress, representing climate-induced effects on human health. Likewise, UHI intensify the impact of air pollution by elevating pollutant levels through increased air turbulence, consequently exacerbating respiratory infections and diseases that disproportionately affect vulnerable urban populations (Cheng & Su, 2010; Onyango, 2022), such as those with pre-existing conditions, children, and the elderly, resulting in higher rates of premature mortalities.

In Guangzhou (China) during heatwaves, the UHI effect exhibited notable amplification in built-type LCZs (Chen *et al.*, 2023). Throughout the day, the UHI intensity increased by 0.4°C, whereas during the night, it rose by 0.6°C. In contrast,

land-cover-type LCZs showed a significant reduction in UHI intensity when compared to built-type LCZs. (Peng *et al.*, 2018) correspondingly, during summertime across >280 china's cities, 95% of the cities observed SUHI with over 3.5°C (2001-2010), compared to rural areas, leading to a growing urban-rural LST difference.

Southeast Asia's Bangkok (Thailand), Jakarta (Indonesia), and Manila (Philippines) (Estoque *et al.*, 2017), observed a distinct UHI profile, revealing a significant and strong correlation between mean LST and the compactness of impermeable surfaces (positive) and green spaces (negative) across the urban-rural gradients of these cities. The impervious surfaces' LST was nearly 2.5°C greater than that of the green spaces, underscoring the significant role of green spaces as an essential urban ecosystem service in mitigating UHI effects. In Sydney (Australia) (Sidiqui *et al.*, 2016), during summer, the daytime UHI effect was observed to reach a magnitude of >5°C. (Geletič *et al.*, 2019) in Prague, Brno and Novi Sad (Europe), the most significant SUHI effects were observed in densely developed and industrial areas, while the coolest LCZs during summer were dense tree cover and water areas from 2013-2018.

In Addis Ababa (Ethiopia) between 1986–2016 (Dissanayake *et al.*, 2019), nearly 35% of the entire land area was covered by impervious surfaces with mean LST increase of about 4°C. (Dissanayake *et al.*, 2019) a shift in the distribution of LST between 2002 and 2013 in Lagos (Nigeria) was due to changes in urban surface characteristics and socio-economic activities, with LST showing a significant positive correlation with NDBI and a notable negative correlation with NDVI. Similarly, between 1998 and 2015 in Sierra Leon, Freetown's average surface temperature rose by 1.5°C, while Bo Town experienced an increase 3.5°C. Despite Freetown's larger population, greater urban development, and faster expansion rate, it consistently remained 2°C cooler than Bo Town, from its proximity to the sea and the significant vegetation cover surrounding the city. (Tarawally *et al.*, 2018)

Nairobi has undergone noticeable changes in surface temperatures, indicating shifts in average temperature patterns. (Makokha & Shisanya, 2010) minimum surface temperature experienced a greater increase than the maximum surface temperature (1966-1999), with more pronounced warming trends observed at urban stations,

pointing towards the expansion of the city from CBD to the sub-urban zones. Between 2015 and 2017, the Upper-Hill area experienced a substantial temperature rise, reaching up to 4°C (Karanja & Kamau, 2018). The informal settlements (Mathare, Kibera and Mukuru) experienced higher temperatures during hot seasons of 2015 and 2016, similar to the temperatures at the CBD from lack of enough greenery (Scott *et al.*, 2017). Enhancing urban design and increasing green spaces in Nairobi could potentially alleviate some of the urban heating, but further data is required for a comprehensive assessment.

2.4.3 Prediction of Land Use/Cover, Vegetation and Land Surface Temperatures

LULC greatly affects both environmental and socio-economic conditions. Accurately predicting these changes is essential for effective urban planning, resource management, and environmental conservation. Beyond tracking current changes over time, simulating future scenarios provides a comprehensive understanding of current trends and potential future developments (Muhammad *et al.*, 2022). In addition, predictive models are key in assessing the potential impacts of urbanization on natural resources, thereby facilitating more efficient and sustainable land use practices for the city. Advancements in techniques for studying LULC mechanisms have rapidly progressed, particularly in spatial analysis, simulation, and understanding changing transition potentials (Abbas *et al.*, 2021; Halmy *et al.*, 2015).

Simulation models, which are effective and reproducible, play a crucial role in examining the determinants of past, present, and future LULC projections across various contexts. Several spatially distributed models, such as Markov-FLUS, and Cellular Automata-Artificial Neural Networks (CA-ANN), have been proposed by researchers for analyzing and projecting LULC dynamics (Abbas *et al.*, 2021; Halmy *et al.*, 2015; Mondal *et al.*, 2016). Each model offers a unique approach to address the complexities of LULC dynamics, with neural network models being particularly considered for their ability to accurately capture nonlinear spatially probabilistic land-use transformations. Cellular Automata (CA) models are also highly effective in understanding land-use systems and their underlying dynamics, especially when

combined with tools like artificial neural networks, making CA-ANN suitable for development and land change simulation studies (Abbas *et al.*, 2021; Muhammad *et al.*, 2022).

Predicting future land changes necessitates considering past, present, and future scenarios, with predictions dating back to the early 1930s (Akın *et al.*, 2015; El-Tantawi *et al.*, 2019; Perović *et al.*, 2018). Prior studies have highlighted the recent emergence of the Module for Land Use Change Evaluation (MOLUSCE) tool, which became prominent after 2010 (Abbas *et al.*, 2021; Perović *et al.*, 2018). Initially, the SLEUTH model was utilized, followed by the adoption of CA-Markov in 1980 to forecast land changes post-2010 (Liu *et al.*, 2012). In 2015, the MOLUSCE plugin (CA-ANN) in QGIS 2.18 to forecast LULC for 2025 and 2030, examining transitions in the Bhavani basin (Huang *et al.*, 2019). Likewise, a study in China applied a similar methodology to forecast future changes in LULC and LST (Nagendra *et al.*, 2013).

2.4.4. Urban Trees Species' Microclimate Modification and UHI Mitigation Nexus to Improve Human Thermal Comfort

Urban vegetation is essential in cities as it provides several significant advantages in enhancing human thermal comfort and improving the urban environment. (Morakinyo *et al.*, 2020; Rahman *et al.*, 2019; Wang *et al.*, 2018) by accurately quantifying the microclimate modification potential of individual tree species, urban planners and policymakers can make informed decisions about tree selection and placement. Different tree species possess varying capacities to alter local microclimates by providing shade, reducing wind speed, and transpiring water vapor, which can significantly impact human thermal perception in urban environments (Boukhabla & Alkama, 2012; Priya & Senthil, 2021; Turner-Skoff & Cavender, 2019).

Comparably, understanding the collective impact of forested areas on UHI mitigation allows for the strategic design of urban green spaces, reducing the overall temperature of urban areas and mitigating the adverse health consequences associated with extreme heat events. Furthermore, incorporating tree allometric properties, such as canopy size, leaf area, and biomass, into microclimate and UHI models enables accurate predictions of thermal benefits (Kwong, 2022; Morakinyo *et al.*, 2020; Rahman *et al.*, 2019). This

data-driven approach facilitates evidence-based urban planning, ensuring that tree planting initiatives are optimally tailored to improve human thermal comfort while considering factors like species resilience and ecological compatibility.

The PET thermal index has been considered suitable in assessing the outdoor thermal comfort ranges in urban open spaces. In Xi'an city (China) (Xu *et al.*, 2018), the neutral PET was established to range between 12-22°C in the city's urban park. Similarly, in Wuhan's residential area, the influence of vegetation on the thermal surroundings was demonstrated to rely on factors such as tree organization, LAI, crown girth, tree height, and aspect ratio of trees (ART) (Zhang *et al.*, 2018). It highlighted that prioritizing trees with an ART of less than 2, particularly tall evergreen species with a large LAI and canopy diameter, can effectively mitigate warm environments in summer towards improving the outdoor comfort.

In SSA's Addis Ababa, the park's cool intensity reached 7°C, where the *Eucalyptus spp.* displayed the most substantial cooling effect, whereas *Grevillea spp.* and *Cupressus spp.* had the least impact on temperature (Feyisa, 2014). The cooling influence of parks on their environs was positively associated with park size and NDVI on a larger scale, primarily influenced by species group, canopy cover, and park size and shape. In Bobo-Dioulasso (Burkina Faso), vegetated areas had lower temperatures compared to nearby impervious urbanized regions (Di-Leo *et al.*, 2016), highlighting that enhancing temperature reduction benefits from urban greenery requires consideration of seasonal phenological disparities influenced by rainfall patterns, existing planting space, and location restraints. (Yahia *et al.*, 2018) dense trees improved thermal comfort in Dar es Salaam (Tanzania), by efficiently reducing the average PET to 23°C in vegetated areas and 35°C in non-vegetated areas through effective shading.

Nairobi's rapid urbanization since the 1960s has negatively affected both its public green and open spaces, as initially designed for a population of three-hundred thousand people, are currently serving over four million residents (Makworo & Mireri, 2011; Oloo *et al.*, 2020; UN-Habitat, 2020). This has led to their decline from overcrowding, ultimately depriving city residents of essential recreational and leisure opportunities.

The decline in vegetation and tree cover in Nairobi, particularly the forested areas that are lost to urbanization, pose greater risk to the city population with the current rising temperatures. (Binyanya *et al.*, 2022; Furukawa *et al.*, 2016; Okech & Nyadera, 2022) contemporary studies have investigated people's perspectives on the city's natural vegetated spaces, the trees' medicinal uses, disparities in their accessibility, and the factors affecting their survival. Even so, there is minimal evidence on the impacts of isolated tree species on microclimate regulation in the city. By promoting greener urban landscapes, decision-makers can foster more comfortable and sustainable living environments, contributing to the overall well-being and health of Nairobi's urban residents.

2.5 Summary

Numerous factors influence vegetation changes in urban open spaces over time. These include rapid urban sprawl and development evident in all these cities, industrialization, urban planning and land use policies, location and climate change extremes. They also include water scarcity, air pollution, growing informal settlements and demand for agricultural land, which have played a key role in urban biophysical features, particularly urban vegetation, affecting their influence on urban microclimate within the different LCZs. Nevertheless, cities' LULC cannot be transferable due to the unique urban variations and combination of factors, such as local planning regulations and policies, population growth rates, economic activities, cultural context, and geographical constraints, which influence land use decisions. Additionally, cities have distinct development patterns and histories, making direct transfer of LULC impractical without considering the specific context of each location/city.

Similarly, comprehensive assessment of urban trees' influence on microclimate and UHI can aid in designing greener and more sustainable urban environments. Quantifiable data on microclimate modification enables the integration of trees as effective components of climate adaptation strategies, while harnessing the scientific knowledge of tree allometric properties and their role in thermal comfort promotes greener cities and fosters a healthier urban lifestyle. However, species occurrence, distribution patterns and growth of urban vegetation, particularly roadside trees, are

significantly affected by their surrounding physical environment. To enhance urban tree selection and planning in Nairobi, more comprehensive assessments are necessary to understand the performance and ecological impact of tree species under diverse environmental disturbances. Additionally, city managers should promote species diversity, especially native species, and prioritize planting strategies based on relevant achievable site dimensions when greening their cities.

2.6 Research Gap

Current studies have employed contemporary methods of relating LULC within LCZs, and LST with the UHI phenomenon in different cities, commonly in the global north, unlike in the global south. Despite that, the adaptability of existing knowledge on these methods is intransferable owing to the unique characteristics of cities, such as their size, morphology, purpose, geography, and general climate among other conditions. Therefore, there is need for comprehensive studies that integrate spatiotemporal monitoring of vegetation changes using LULC data within LCZs in tropical climate global south cities such as Nairobi, to better understand the specific effects of urbanization on different urban vegetation types and their ecological dynamics over time, towards informed green strategies.

Acquiring a comprehensive knowledge of urban mature tree performance under various local climate zones is crucial for urban greening selection, yet presently, ample information on the performance of numerous species remains unavailable. In Nairobi, there exists a dire scarcity of research-based evidence regarding the efficacy of isolated trees in microclimate control within its urban settings. Therefore, this research sought to assess the vegetation status and the impact of isolated *in-situ* plant species on thermal comfort in Nairobi city.

The research predominantly contributed towards enhancing the knowledge and expertise in urban tree selection and tree planting, as a way of mitigating Urban Heat Island (UHI) in Nairobi City. Moreover, the findings will contribute to policymaking on urban open space management considering plant selection and microclimate modification. Further, the findings will influence the practice of various city management parties, from the planting designs to installation and overall maintenance.

Majority of the stakeholders include the landscape designers, urban planners, arborists and plant suppliers, streetscape and urban green space managers in Nairobi.

CHAPTER THREE

RESEARCH METHODOLOGY

3.1 Introduction

This chapter covers a comprehensive methodology of the study with the methodological overview summarized in 3.1.1. Sub-section 3.2 describes the study area, the selected study sites and their geographical scope. It equally presents a detailed explanation of the data collection methods and processing, data analysis techniques applied in sub-section 3.3 and 3.4 respectively.

3.1.1 Methodological Overview

The methodological overview applied in the study for each objective is as abridged in figure 3.1.

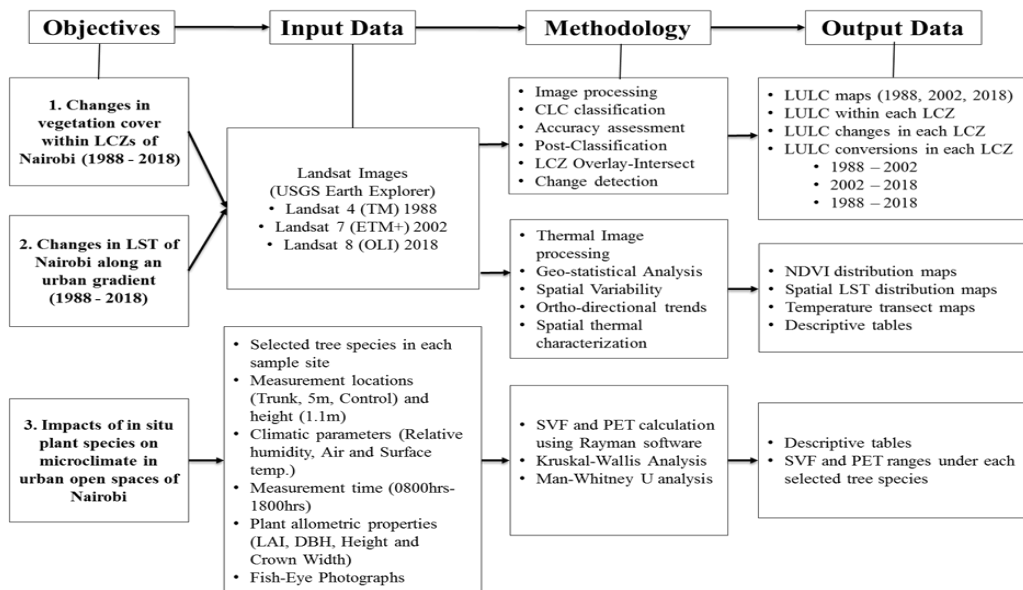


Figure 3.1: Overview of the Study’s Methodological Flowchart

3.2 Study Area

This research was carried out in Nairobi, the capital city of Kenya in East Africa. Nairobi is situated in the central uplands of Kenya within the latitudes 1°10' and 1°25'S and longitudes 36°34' and 37°00' E (Figure 3.2). The elevation ranges from 1400 meters to the southeast side to an elevation of approximately 2200 m to the northwest side.

Nairobi has a dual temperature period; the maximum monthly average recorded in the months of February at approximately 29°C in the day and 15°C in the nighttime. The minimum temperature is recorded in the months of July at approximately 21°C daytime and 12°C nighttime (KMD, 2020).

The average monthly precipitation limits vary between a maximum of 195 mm in April and a minimum of 15 mm in the months of July throughout the year. Nairobi has a population of approximately 4.5m people, making it the biggest and most populous city in Kenya (KNBS, 2019) and in East Africa.

The study is timely in this region as a result of rapid urbanization experienced through the past three decades leading to a significant landscape transformation with an elaborate mix of commercial centers, green open spaces, residential and industrialized sections (Bosco *et al.*, 2011).

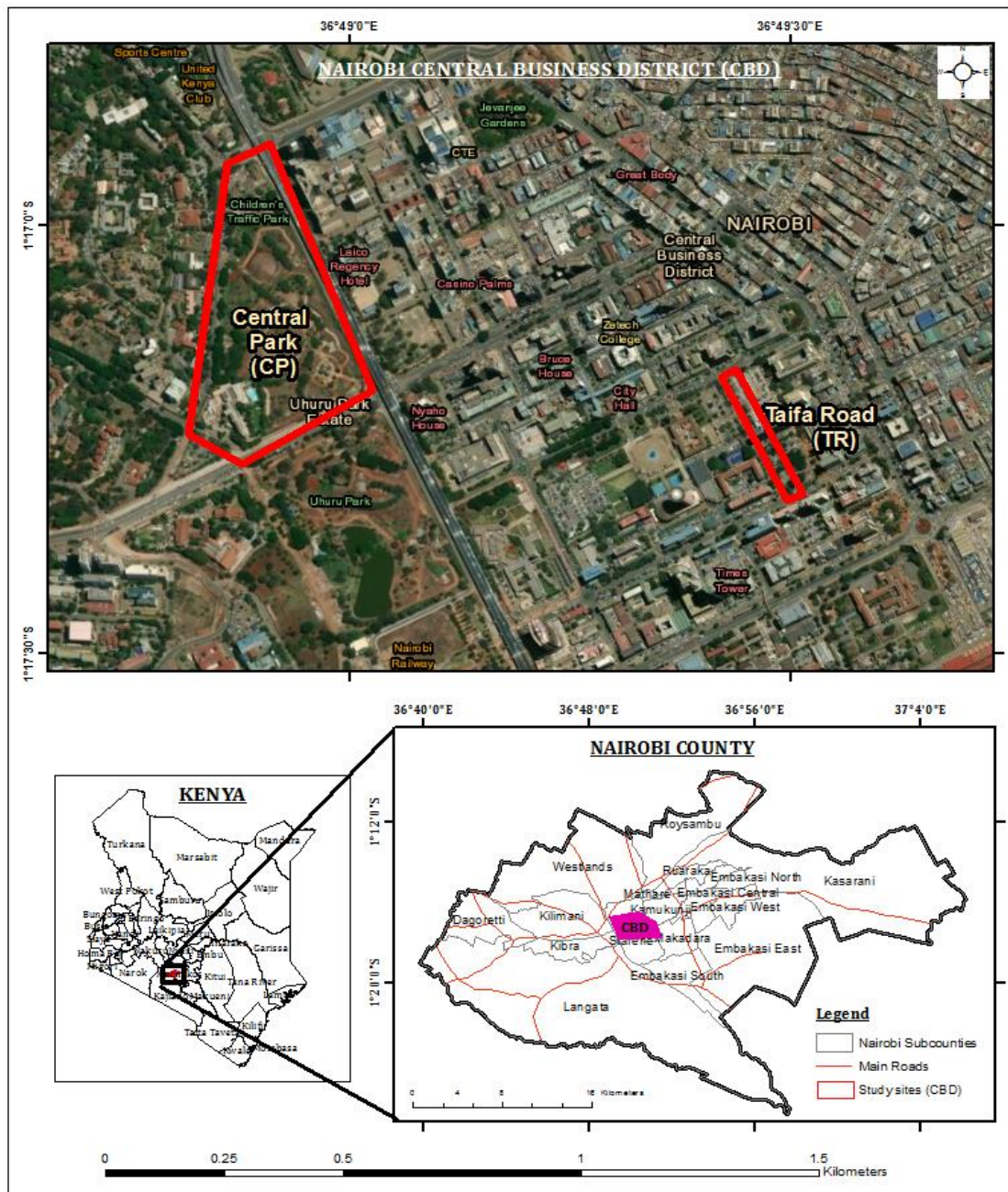


Figure 3.2: The Maps Kenya, Nairobi County and the Selected Study Sites: Central Park (CP) and Taifa Road (TR) within the Central Business District (CBD).

3.3 Data Collection

3.3.1 Evaluation of Spatial and Temporal Changes of Vegetation Cover Based on Local Climate Zones of Nairobi

3.3.1.1 Image Retrieval

Satellite images (Landsat) were used to create the LULC maps of three different years for 1988, 2002 and 2018 all acquired from USGS Earth Explorer. The specific multispectral satellite images downloaded were Landsat 4 (TM) for 1988, Landsat 7 (ETM+) for 2002 and Landsat 8 (OLI) for 2018. The band characteristics of the images are shown in Table 3.1. They were all retrieved on cloud free days during the warm seasons on path 168 and row 061 scenes for all the Landsat sensors (Table 3.2). Both ERDAS Imagine and ArcGIS software were used interchangeably for data processing of all the images.

The fifteen-years constant difference was to evaluate; the nature and rate of changes in spatial (area size) extent covered by vegetation and other LULCs; to quantify the trend (temporal); how much was lost or gained, LULC that had the highest gain or loss and where (location) it occurred most.

Table 3.1: General Landsat Image Characteristics for Landsat 8, 7 and 4

Bands	Landsat 8 (OLI)			Landsat 7 (ETM+)			Landsat 4 (TM)		
	Wavelength (micrometers)	Resolution (Meters)	Nominal Spectral Location	Wavelength (micrometers)	Resolution (Meters)	Nominal Spectral Location	Wavelength (micrometers)	Resolution (Meters)	Nominal Spectral Location
Band 1	0.43-0.45	30	Coastal aerosol	0.45-0.52	30	Blue	0.45-0.52	30	Blue
Band 2	0.45-0.51	30	Blue	0.52-0.60	30	Green	0.52-0.60	30	Green
Band 3	0.53-0.59	30	Green	0.63-0.69	30	Red	0.63-0.69	30	Red
Band 4	0.64-0.67	30	Red	0.77-0.90	30	Near Infrared (NIR)	0.76-0.90	30	Near Infrared (NIR)
Band 5	0.85-0.88	30	Near Infrared (NIR)	1.55-1.75	30	Shortwave Infrared (SWIR) 1	1.55-1.75	30	Shortwave Infrared (SWIR) 1
Band 6	1.57-1.65	30	Shortwave Infrared (SWIR) 1	10.40-12.50	60*(30)	Thermal	10.40-12.50	120*(30)	Thermal
Band 7	2.11-2.29	30	Shortwave Infrared (SWIR) 2	2.09-2.35	30	Shortwave Infrared (SWIR) 2	2.08-2.35	30	Shortwave Infrared (SWIR) 2
Band 8	0.50-0.68	15	Panchromatic	.52-.90	15	Panchromatic			
Band 9	1.36-1.38	30	Cirrus						
Band 10	10.6-11.19	100 * (30)	Thermal Infrared (TIRS) 1						
Band 11	11.50-12.51	100 * (30)	Thermal Infrared (TIRS) 1						

Source: (USGS)

Table 3.2: Source and Properties of the Images and Auxiliary Data Used in LULC Assessment

Satellite image	Spatial resolution	Date and year of acquisition	Path	Row	Band Combination (RGB)	Source
Landsat 4	30m	17/10/1988	168	061	432	USGS
Landsat 7	30m	10/02/2002	168	061	432	USGS
Landsat 8	30m	29/01/2018	168	061	543	USGS
Spatial variable data			Source			
Digital Elevation Model (DEM)			Africa Living Atlas - Powered by Esri			
Slope			Calculated from DEM			
Roads			World Resource Institute			
Distance from roads			Calculated from Road Network			

3.3.1.2 Local Climate Zones (LCZ) of Nairobi

To obtain the LCZs for Nairobi, high-resolution satellite imagery (Landsat 8-OLI) for 2018 and ancillary data for Nairobi, including LULC and climatic data were collected. (Bechtel *et al.*, 2015; Brousse *et al.*, 2016; Ching *et al.*, 2018). The WUDAPT protocol for LCZ classification was then applied to the collected data, involving systematic categorization of Nairobi's morphology and surface cover characteristics. Once the LCZ classification was completed (Bechtel & Daneke, 2012; Brousse *et al.*, 2016), the results were aggregated and integrated to create a comprehensive LCZ map for Nairobi, which was converted into the shapefile format presented in figure 3.3. The summary of the method employed for deriving LCZs of Nairobi is highlighted in figure 3.8.

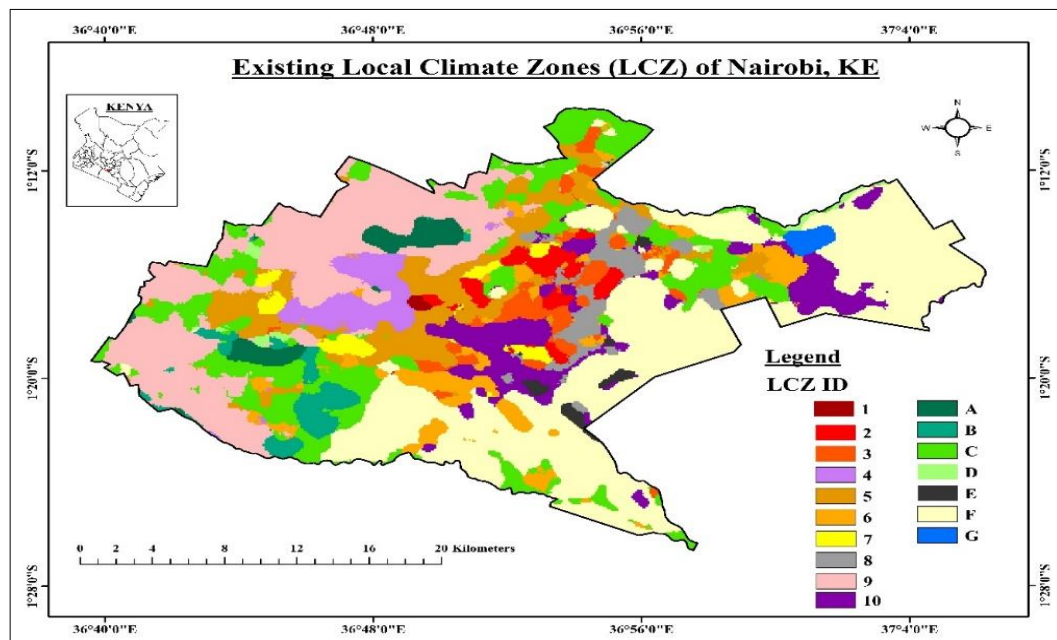


Figure 3.3: Spatial Distribution of the LCZs in Nairobi for 2018 Retrieved from World Urban Database and Access Portal Tools (WUDAPT)

3.3.1.3 Prediction of Land Use/Cover for Nairobi to 2033

To simulate the future spatiotemporal changes, the LULC maps generated for 2002 and 2018, with a 15-year interval were used to predict the LULC for 2033 (next 15 years). This study employed the MOLUSCE tool within the QGIS 2.18 software to forecast LULC changes (Abbas *et al.*, 2021; Muhammad *et al.*, 2022; Rahman *et al.*, 2017). MOLUSCE was calibrated using historical LULC data from 2002 and 2018, along with spatial variables such as DEM, slope, and road proximity within QGIS 2.18. The sources of these variables have been described in Table 3.2. The tool incorporates diverse modeling techniques, including machine learning algorithms, to analyze historical LULC data and forecast future changes. Specifically, the prediction model utilizes CA-ANN, a form of machine learning algorithm, to enhance accuracy and efficiency in predicting LULC changes over time (Muhammad *et al.*, 2022; Rahman *et al.*, 2017). In addition, the plugin offers a range of established techniques for assessing the relationship between LULC data and geographical factors, including Pearson's correlation coefficient. An overview of the methodological process is presented in figure 3.4.

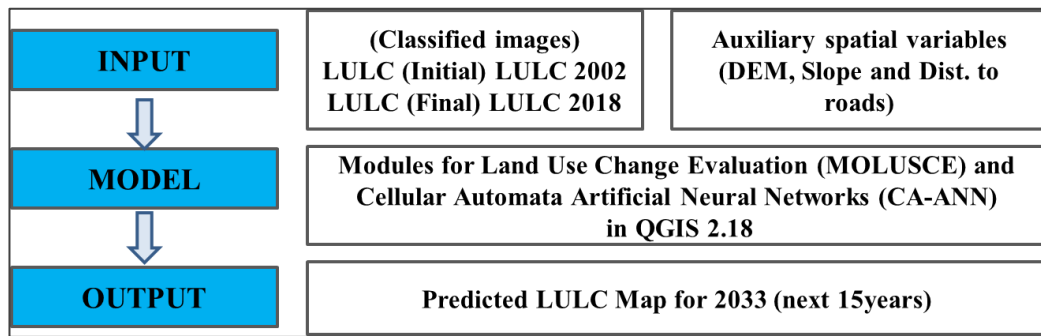


Figure 3.4: Overview of the LULC Prediction Methodological Process

3.3.2 Determining Land Surface Temperature (LST) changes in Nairobi along an Urban Gradient

This step employed the use of a mono-window algorithm (Jiang & Lin, 2021; Aabeyir *et al.*, 2022; Tesfamariam *et al.*, 2023) for the computation of LST of Nairobi from 1988 to 2018 using ArcMap 10.8.2. This algorithm uses a single narrow atmospheric window in the thermal spectrum where the atmosphere is nearly transparent to thermal radiation. The brightness temperature within this window is related to the LST using equations that account for emissivity and other factors. The detailed steps are highlighted in sub-section 3.3.2.1.

3.3.2.1 LST Map Generation Using Mono-Window Algorithm

The Landsat images of years 1988, 2002 and 2018 were used to estimate LST using ArcMap 10.8.2. (Jiang & Lin, 2021; Aabeyir *et al.*, 2022; Tesfamariam *et al.*, 2023) the procedure/steps were as follows:

Step 1: Conversion of Digital Numbers (DN) to Radiance Values

$$R = ((L_{MAX} - L_{MIN}) / (Q_{CALMAX} - Q_{CALMIN})) \times (Q_{CAL} - Q_{CALMIN}) + L_{MIN}$$

Table 3.3: The Radiance Value Equation's Symbols and Their Meaning

Symbol	Meaning
R	Spectral radiance at the sensor's aperture in watts/ (meter squared * ster * μm)
Q _{CAL}	Quantized calibrated pixel value in DN
L _{MIN}	Spectral radiance that is scaled to Q _{CALMIN} in watts/(meter squared * ster * μm)
L _{MAX}	Spectral radiance that is scaled to Q _{CALMAX} in watts/(meter squared * ster * μm)
Q _{CALMIN}	Minimum quantized calibrated pixel value (corresponding to L _{MIN}) in DN
Q _{CALMAX}	Maximum quantized calibrated pixel value (corresponding to L _{MAX}) in DN

The meaning of each symbol in the equation is presented in table 3.3, while the values and constants for thermal bands of Landsat 4, 7 and 8 used in the calculation for step one are presented on table 3.4.

Table 3.4: Values and Constants for Thermal Bands of Landsat 4, 7 and 8

Values and Constants	Landsat 4 (1988)	Landsat 7 (2002)	Landsat 8 (2018)
Thermal Band	Band 6 (11.45um)	Band 6 (11.45um)	Band 10 (10.895um)
L _{MAX}	15.303	15.303	22.00180
L _{MIN}	1.238	1.238	0.10033
Q _{CALMAX}	255	1	65535
Q _{CALMIN}	255	1	1
K1 constant	671.62	666.09	774.8853
K2 constant	1284.30	1282.71	1321.0789

Step 2: Conversion of Radiance Values to Brightness Temperature (Bt)

Calculating brightness temperature using Planck's Black Body Radiation Law

$$Bt = K_2 / \text{Log} \{(K_1 / R) + 1\}$$

(Where: *Bt* = Brightness temperature, *R* = Radiance values, *K₁* = Calibration constant 1 for the thermal band, *K₂* = Calibration constant 2 for the thermal band)

K₁ and *K₂* are the two calibration constants used to transform the measured at-sensor radiance into temperature values. *K₁* accounts for the spectral response of the sensor and the spectral radiance of the earth's surface (Jiang & Lin, 2021; Aabeyir *et al.*, 2022; Tesfamariam *et al.*, 2023), while *K₂* considers the sensor's sensitivity and the absolute temperature of the calibration target. *K₁* and *K₂* are critical factors in accurately

converting radiance to brightness temperature and are specific to the thermal bands of the satellite sensor.

Step 3: Calculation of NDVI

The normalized difference vegetation index (NDVI) was derived from red (R) and near-infrared (NIR) bands of satellite imagery, (Aslam *et al.*, 2021; Liu *et al.*, 2013) (Table 3.5). Computation was done in ArcMap, using the raster calculator function. NDVI ranges from -1 to 1 (vegetated to non-vegetated). The formula is;

$$NDVI = (NIR - R) / (NIR + R)$$

Table 3.5: Wavelengths of the Landsat Imagery Bands Used to Calculate NDVI and their Spatial Resolution

Satellite	Red Band [Wavelength (μm)]	NIR Band [Wavelength (μm)]	Spatial Resolution
Landsat 4	Band 3 (0.63-0.69μm)	Band 4 (0.76-0.90μm)	30m
Landsat 7	Band 3 (0.63-0.69μm)	Band 4 (0.76-0.90μm)	30m
Landsat 8	Band 4 (0.64–0.68μm)	Band 5 (0.85–0.88 μm)	30m

Step 4: Calculation of Land surface emissivity (LSE) ε

Emissivity (ε) is the surface property that describes how effectively an object emits thermal radiation (Jiang & Lin, 2021; Huang *et al.*, 2023), and it is estimated to correct for radiative energy emitted by the surface. In the same way, Pv represents the proportion of vegetation within a pixel, used to account for vegetation's cooling effect (Tarawally *et al.*, 2018; Yin *et al.*, 2018). Accurate emissivity and Pv values are crucial for precise LST calculations as they directly impact the accuracy of temperature estimates in thermal infrared satellite imagery. Emissivity is calculated using the formula:

$$NDVI = (NIR - IR) / (NIR + IR)$$

$$Pv = ((NDVI - NDVI_{min}) / (NDVI_{max} - NDVI_{min}))^2$$

For thermal Band of Landsat TM and ETM; (ε = 0.004 x Pv + 0.986)

Step 5: Retrieval of LST image

The final step involves calculating the brightness temperature (B_t), which represents the radiance-based brightness temperature by utilizing the equation:

$$B_t / \{1 + \lambda \times (B_t / \rho) \times \log \varepsilon\}$$

Where; λ = Wavelength of emitted radiance (11.5 μm),

$$\rho = h \times c / \sigma = 1.438 \times 10^{-2} \text{ Mk}; (\sigma = \text{Boltzmann constant} = 1.38 \times 10^{-23} \text{ J/K}, h = \text{Planck's constant} = 6.626 \times 10^{-34} \text{ Js}, c = \text{velocity of light} = 2.998 \times 10^8 \text{ m/s})$$

The term λ denotes the slope of the Planck function, which is dependent on the sensor characteristics and wavelength. The parameter ρ represents the reflectance of the surface at the thermal band wavelength (Jiang & Lin, 2021; Huang *et al.*, 2023). The logarithm of the emissivity (ε) of the land surface is also considered in the equation. This step takes into account sensor-specific factors, surface properties, and atmospheric conditions to accurately determine the B_t , which is a crucial measure for subsequent LST retrieval.

3.3.2.2 Urban-Rural Temperature Gradient

Variation of environmental conditions with respect to urban expansion severity from the city center to the outskirts, best describes an urban-rural gradient (Billah & Haque, 2021). Correspondingly, temperature gradients feasibly depict the occurrence frequency, along with the direction of temperature variations within a specified location. These gradients have been applied in the UHI related studies (Kumar & Shekhar, 2016; Jiang & Lin, 2021), in order to pinpoint the areas that need more attention to mitigate its effects. The urban temperature gradient is estimated per unit length applying the formula:

$$dT / dx = (T_2 - T_1) / (X_2 - X_1)$$

(Where d is the change, T is unit temperature and X is the unit distance)

The study involved selecting linear paths extending from the urban core towards the rural outskirts in both the north-south and east-west directions, with the expected resulting LST images for Nairobi (1988, 2002, and 2018) to be subjected to a profile analysis (Jiang & Lin, 2021; Aabeyir *et al.*, 2022; Zhao *et al.*, 2022).

3.3.2.3 Prediction of Vegetation and Land Surface Temperature for Nairobi to 2033

To predict NDVI and LST, a similar procedure to section 3.3.1.3 was followed. The already classified NDVI and LST maps for 2002 and 2018 were used for the prediction. MOLUSCE tool was employed to analyze the transition matrix and predict future land cover changes based on historical trends. Concurrently, the CA-ANN model was utilized to simulate the spatiotemporal dynamics of NDVI and LST, while incorporating the auxiliary spatial variables. These models were calibrated and validated using historical data, and the resulting predictions are extrapolated to forecast NDVI and LST trends up to 2033, providing valuable insights for long-term land use planning and environmental management strategies in Nairobi City.

3.3.3 Determining the Effects of Plant Species on Microclimatic Parameters in an Urban Environment

3.3.3.1 Study Sites

Local climates zones (LCZ), a climate-based categorization of both metropolitan and countryside regions developed by Stewart & Oke, (2012) was used to describe the selected study sites (Figure 3.2). Similar plant species in two different LCZ within Nairobi central business district (CBD) were compared. The two sites representing the two LCZs were namely:

1. LCZ B: *Scattered trees*; a landscape having grown trees with permeable and low thermal capacity surface, which is also one of the oldest parks in Nairobi, - Central Park (Site 1)
2. LCZ 4: *Open high-rise*; Open organization of tall buildings with scattered trees. The site is characterized with hard and high thermal capacity surfaces

such as concrete and glass construction materials. The street is called Taifa road (Site 2).

3.3.3.2 Plant Species Selection

In each of the two study sites, the most common isolated tree species (*in situ* plants) with spreading, round, pyramidal and vase tree canopy forms, which could easily be replicated in both sample sites were identified. Out of this criteria, four plant species were chosen which included; *Cassia spectabilis* (Cassia), *Terminalia mantaly* (Umbrella tree), *Podocarpus falcatus* (Podo/East African yellow wood), and *Tipuana tipu* (Tipu tree/Rosewood). The types and geometry of the sample *in situ* trees is shown in Figure 3.5. A general description of the selected tree species within the two sites, including their scientific names, common names, family and overall uses is shown in Table 3.6.

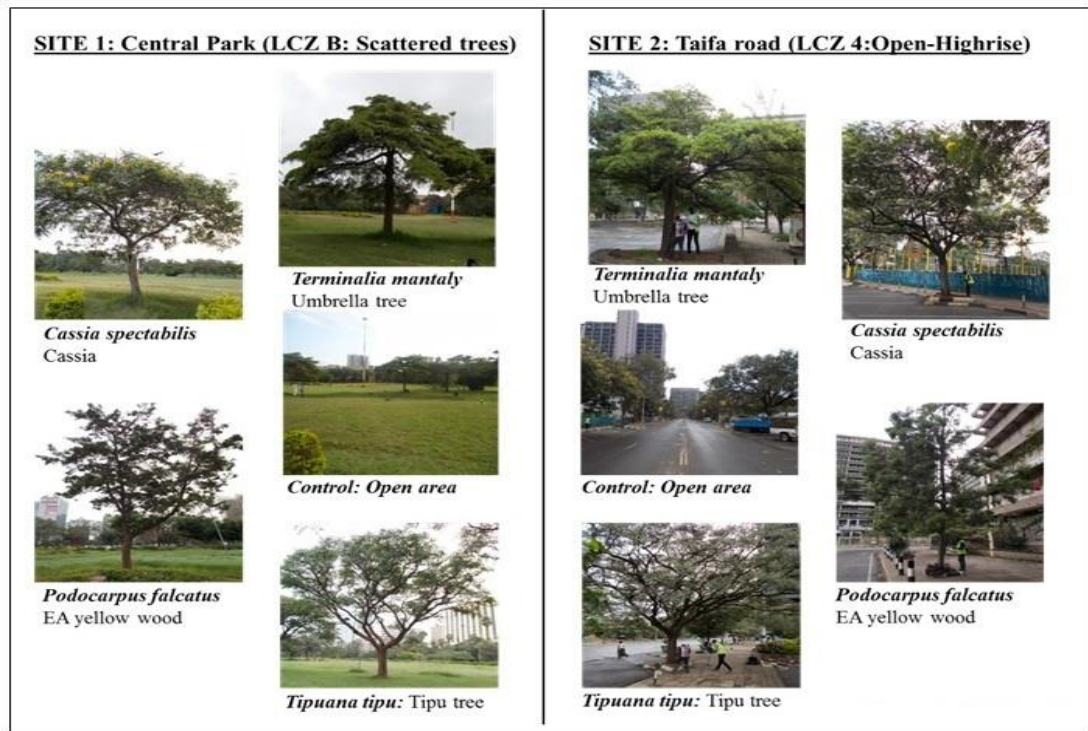


Figure 3.5: The Four Different Plant Species Sampled from the Two Study Sites and the Control Points (Open Areas With No Trees).

Table 3.6: Selected Plants General Description, Canopy Forms and their Uses

No.	Plant Scientific, Common Name and Family	General Description	Uses	Tree Canopy Form
1.	<i>Cassia spectabilis</i> (Cassia) Family: Fabaceae	It is a deciduous tree which is small with a spreading crown and grows to a height of 10m.	<ul style="list-style-type: none"> • Ornamental boundary plant. • Firewood 	Vase form
2.	<i>Podocarpus falcatus</i> (Podo/East African yellow wood) Family: Podocarpaceae	A tall evergreen tree with a trunk that is long and cylindrical and grows to 46m. It has less-crowded branches with a slender crown.	<ul style="list-style-type: none"> • Wood; furniture • Bark; tanning leather. • Sap; treat chest pains. 	Pyramidal form
3.	<i>Terminalia mantaly</i> (Umbrella tree) Family: Combretaceae	A 10-20m tall broad-leafed tree with a straight stem and very distinct amass branches	<ul style="list-style-type: none"> • Bark & wood; dyeing & treating dysentery (Madagascar) • Ornamental plant 	Spreading form
4.	<i>Tipuana tipu</i> (Tipu tree/Rosewood) Family: Fabaceae	A large semi-broadleaf tree that spreads and grows to 20 m and 30 m with a light outspread in both crown and branches.	<ul style="list-style-type: none"> • Timber • Soil stabilization in reforestation • Ornamental street/park plant for shade 	Round form

3.3.3.3 Measurement of Tree Canopy Density and Allometric Properties

Canopy density was estimated by measuring the leaf area index (LAI) using the LAI-2200C meter. The LAI meter (LAI-2200C) is non-destructive, fast, cost effective, eases on-site evaluation and it can also be used for a variety of plant canopies (Welles & Norman, 2001; Cater *et al.*, 2009; Fahmy, Sharples, & Yahiya, 2010; Klingberg *et al.*, 2015). The LAI data was recorded at four different points, at the edge of the tree canopy diameter for the above canopy, and also measured at four different points (Figure 3.6(a)), at the trunk below canopy using the 90⁰ cap (Cater *et al.*, 2009; Fahmy *et al.*, 2010).

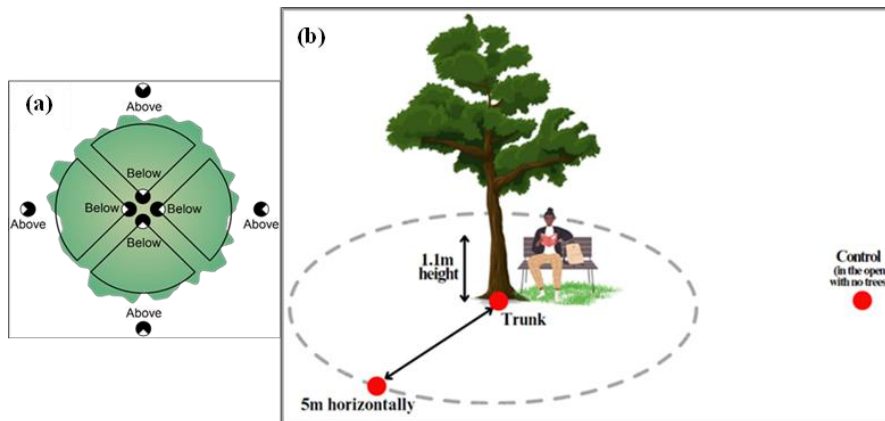


Figure 3.6: (a) The below and above Canopy Points Where LAI was Measured around the Isolated Trees (Cater *et al.*, 2009), (b) Microclimatic Variables' Measurement Points Illustration

The diameters at breast height (DBH) were measured 1.3 m from the ground using a measuring tape measure. To get the average crown diameters for each tree, two measurements were taken; the widest spread (longer axis) below the canopy and the widest cross-spread (shorter axis), and the mean ($n=2$) calculated. To measure the sample tree heights, a Suunto clinometer (PM-5/360PC) was used. By aligning the device with the horizon and then measuring the angle between the horizon and the line of sight, using the formula:

$$\text{Tree height} = ((\text{Distance from tree}) \times \tan(\theta)) + \text{Height above eye level}$$

3.3.3.4 Measurement of Microclimatic Variables

The microclimatic variables that were measured included air temperature, the wind speed, relative humidity, together with the surface temperatures. Measurement campaign was conducted in the month of May from day 135 up until day 138 of the year 2018. Climatic variables were measured from 0800hrs to 1800hrs at an interval of 20 minutes for three consecutive days at the same time for the two study sites. They were measured in 3 points; under the tree shades, at 5 m and away from the shade (in the open with no trees) as a control point, illustrated in figure 3.6(b). Attributes of the study sites and selected plants are shown in Table 3.7.

Table 3.7: Attributes of the Study Sites; Plant (P), site (S) and Control (C)

Code	Explanation	Feature	GPS location	
			Latitude	Longitude
S ₁	Site 1: (LCZ B; Scattered Trees)	Central Park	1°17'9.13"S	36°48'58.14"E
S ₂	Site 2: (LCZ 4; Open High-rise)	Taifa Road	1°17'14.88"S	36°49'27.51"E
P ₁ S ₁	Plant 1, Site 1	<i>Cassia spectabilis</i>	1°17'10.16"S	36°48'55.55"E
P ₂ S ₁	Plant 2, Site 1	<i>Podocarpus falcatus</i>	1°17'9.87"S	36°48'59.25"E
P ₃ S ₁	Plant 3, Site 1	<i>Terminalia mantaly</i>	1°17'8.80"S	36°48'58.45"E
P ₄ S ₁	Plant 4, Site 1	<i>Tipuana tipu</i>	1°17'7.81"S	36°48'57.14"E
C ₁	Control area for Site 1	Grass with no trees	1°17'9.05"S	36°48'55.84"E
P ₁ S ₂	Plant 1, Site 2	<i>Cassia spectabilis</i>	1°17'10.98"S	36°49'25.97"E
P ₂ S ₂	Plant 2, Site 2	<i>Podocarpus falcatus</i>	1°17'18.69"S	36°49'29.23"E
P ₃ S ₂	Plant 3, Site 2	<i>Terminalia mantaly</i>	1°17'17.44"S	36°49'29.27"E
P ₄ S ₂	Plant 4, Site 2	<i>Tipuana tipu</i>	1°17'16.52"S	36°49'27.91"E
C ₂	Control area for Site 2	Open road with no trees	1°17'12.72"S	36°49'26.38"E

Measurements were recorded at 1.1m above the ground (approximate mean human height) (Rossi *et al.*, 2015) (Figure 3.6(b)). Air temperature and the relative humidity measurements were conducted using digital pyrometers (PCE-889B). Surface temperatures were measured using infrared meters (Testo 830 – T1) and wind speed measurements were taken using wind meters (Testo 410 – 2). A geographical positioning system (GPS) receiver was used to authenticate the geographical locations of the sample sites and the specific trees used for the study (Figure 3.7).



Figure 3.7: Pinned Locations for the Sample Plants in Central Park (Site 1) and Taifa Road (Site 2) Sites

Image source: (Google Earth)

3.3.4.5 Evaluation of Human Thermal Comfort

To ascertain the temperature reduction impact of the trees in relation to human thermal comfort, Physiologically Equivalent Temperature (PET) was used as the thermal index. As a widely used thermal comfort index used in various environmental conditions, (Chen *et al.*, 2012; Middel *et al.*, 2018), PET plays an important role in designing and evaluating thermal environments for human well-being and productivity. Fish-eye photographs (FEP) were employed to assess thermal conditions, documenting the distribution of both sunlight and shadow beneath the tree canopies. At 1.1m height, a fisheye lens camera, positioned on the ground facing upwards, was employed to capture the photographs, offering a hemispherical view of each trees' canopy. The FEP were taken under the trees and away from the tree shades (control) at 1pm (Figure 3.6(b)), as at this time the maximum heat effect of the sun is mostly felt (Chen *et al.*, 2012; Middel *et al.*, 2018).

The FEP and the climate data were used to compute the sky view factor (SVF) and PET by the use of statistical algorithms within the Rayman software (Matzarakis *et al.*, 2009; Deb & Alur, 2010). The software calculates PET index based on various environmental factors such as humidity, air temperature and radiation, as well as physiological responses such as thermal sensation and clothing insulation, which helps in predicting and assessing thermal comfort levels for occupants in indoor and outdoor environments (Chen *et al.*, 2012; Middel *et al.*, 2018). SVF values range from 0 to 1 (Chapman & Thrones, 2004; Middel *et al.*, 2018) (SVF = 0; the sky is fully covered with an obstacle). PET and SVF were then used to determine the thermal reduction effect of the trees compared to their surroundings and determine the thermal comfort range at the measurement points (Figure 3.6(b)).

3.4 Data Analysis

3.4.1 Evaluation of the Spatial and Temporal Changes of Vegetation Cover in LCZ of Nairobi from 1988 to 2018

3.4.1.1 Digital Image Pre-Processing

Image pre-processing preceded the data analysis and was conducted with the purpose of improving the image data to suppress unsought distortions and function at the minimal level of abstraction (Alqurashi & Kumar, 2019). The downloaded Landsat images were georeferenced with correspondence to world geodetic system (WGS 84) datum, (Karanja & Kamau, 2018; Oloo *et al.*, 2020; Oyugi *et al.*, 2017) the projection system used was universal transverse Mercator (UTM – Zone 37) in ArcMap 10.8.2. All the images had a spatial resolution of 30m.

i) Image Sub-setting

An image sub-setting process was executed to discard the irrelevant areas of each of the satellite scenes, while retaining the focus Area of Interest (AOI). ERDAS Imagine software was used to define and clip out the AOI using a pre-existing shapefile of Nairobi in this study.

ii) Image Enhancement

Correspondingly (Cilek & Cilek, 2021; Sidiqi *et al.*, 2016), the satellite images usually vary in contrast resulting from various factors such as low detector sensitivities or objects having similar reflectivity. Variability in environmental conditions during the data recording by the sensors may also affect the image contrast. A digital image enhancement was performed to enhance visual interpretation by improving the imagery appearances. (Pal & Ziaul, 2017; Tarawally *et al.*, 2018; Naikoo *et al.*, 2020) given that the satellite imagery exhibit discrete spectral characteristics, false color composite bands; Red, Green, and Blue (RGB) combination for the selected images was performed using ArcMap 10.8.2 (Figure 3.8). Band 4, 3 and 2 were used for both Landsat 4 and Landsat 7, while bands 5, 4 and 3 were used for Landsat 8.

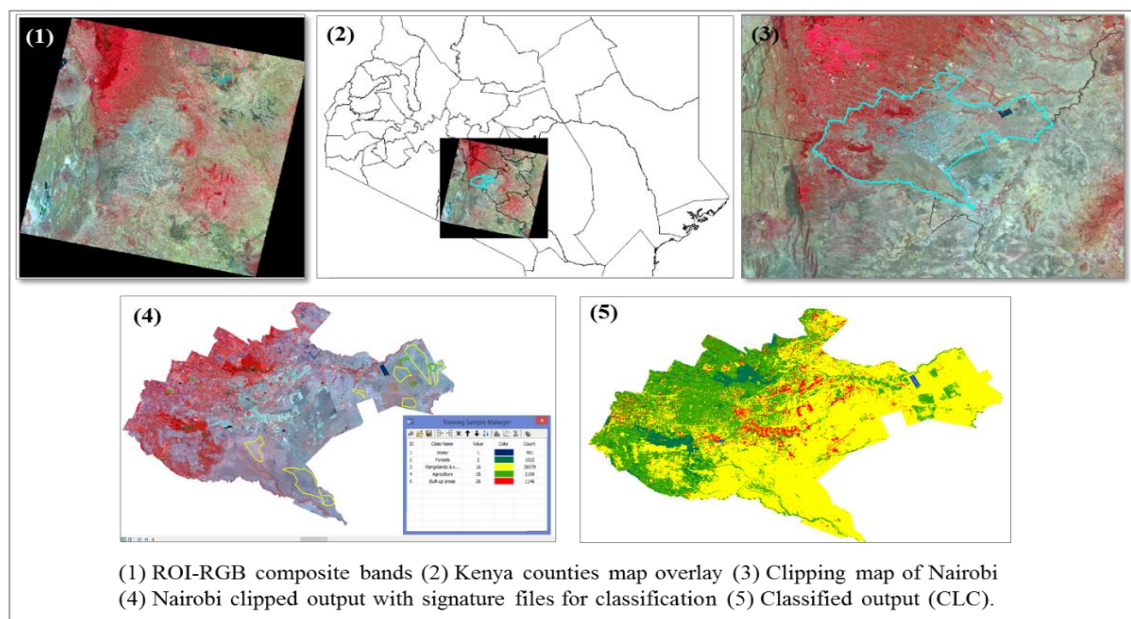


Figure 3.8: Summary of Image Sub-Setting, Enhancement and Classification

3.4.1.2 Image Classification

Feature and attribute extraction in remote sensing has been made possible through the application of image classification approach. The process separates the imagery pixels (Alqurashi & Kumar, 2019; Bechtel & Daneke, 2012; Liu *et al.*, 2013), grouping and placing them in specific land cover classes based on their spectral characteristics. To obtain a more accurate outcome, this study applied the supervised classification approach using the ArcGIS software (Figure 3.8). The process entailed the creation of training samples and signature files for the classification. Using the established training samples, the maximum likelihood classification algorithms were applied.

i) Classification System

In line with this study's objectives, the CORINE classification system was applied (Table 3.8). It is a vector map that sets out comparable scenery patterns (Corine & Cover, 2012), i.e. more than 75% of the patterns display the properties of a particular class from the terminology. The nomenclature is ideally a 3-level gradable classification system that has 44 distinct classes by the third and majorly

detailed levels (Corine & Cover, 2012). The research established five LULC classes for classification.

Table 3.8: Land Use Land Cover Classification Schema

LULC Classes		Description
i.	Forests and Semi-natural zones	Tall mature clusters of trees, botanical greenery including hedges, parks and green spaces with vegetation
ii.	Built-Up Areas/Artificial Surfaces	Commercial and office buildings, residencies, roads, constructions, city structure and non-agricultural areas
iii.	Urban Agriculture/Cropland	Tillable land, crops and graze lands, secondary growth, open transitional spaces
iv.	Rangelands and Shrubs	Dispersed short trees and shrubbery, bare ground or concealed by grass but scantily distributed
v.	Water Bodies and Wetlands	Both on land and marine waters

Source: (Corine & Cover, 2012).

A descriptive data analysis was applied to explain how the LULC dynamics had occurred in Nairobi between 1988 and 2018 from the output images; the vegetation class was majorly considered.

ii) Ancillary Data and Ground Truth

Any sourced data that is not from remote sensing but can be applied for classification purposes and digital image processing is ancillary data (Jiang & Lin, 2021). To ascertain that the entire attributes represented in the classified images matched with those existing on the actual surface, the ground truth procedure was executed. It involved the use of field observation, google earth imagery, GPS points in addition to individual experiences (Bechtel *et al.*, 2015; Ferreira & Duarte, 2019). These data were later used for precision evaluation of the classified LULC maps. Removal of the images' stray pixels was conducted to generate seamless and uniform LULC classes as part of the post-classification screening.

3.4.1.3 Accuracy Assessment

A precision evaluation of the classified images was performed through a comparison of the output and other accurate reference data. (Huang *et al.*, 2023; Tesfamariam *et al.*, 2023) The study integrated the use of ground truth data including google earth

imagery for referencing. Using ArcMap 10.8.2, sets of arbitrary points from the baseline data were established and used for comparability with the LULC maps. A confusion matrix table was applied to assess any possible omitted errors during the image classification process. The errors measured included the producer's accuracy, the user's accuracy, the overall accuracy and the Kappa index statistics (Tang *et al.*, 2015; Vang *et al.*, 2021).

- i) Producer's Accuracy = $\sum NCCP / \sum RP$ (column total) x 100
- ii) User's Accuracy = $\sum NCCP / \sum CP$ (row total) x 100
- iii) Overall Accuracy = $\sum NCCP$ (Diagonal) / $\sum RP$ x 100
- iv) Kappa index = (Observed accuracy - X) / (1 - X)

Where:

- $\sum NCCP$: - Total Number of Correctly Classified Pixels per category
- $\sum CP$: - Total Classified Pixels per category
- $\sum RP$: - Total Reference Pixel per category
- X: - Chance agreement

3.4.1.4 Change Detection

i) Classified LULC

This process involved the quantification of both the spatial and temporal changes that had occurred in Nairobi through the thirty-year period. This research incorporated the application of remote sensing approaches to detect the changes. Overlaying the raster data as well as combining the vector data was executed on ArcMap 10.8.2 using the image differencing approach (Alqurashi & Kumar, 2019; Fenta *et al.*, 2017; Naikoo *et al.*, 2020) (Figure 3.9). The post-classification technique was used to detect the percentage and the rate of change in addition to pinpointing the locations where they occurred using the formulae below:

$$\text{Absolute Difference} = (\text{Pixel Value in Image A} - \text{Pixel Value in Image B})$$

$$\text{Rate of Change} = ((\text{LULC in Year B} - \text{LULC in Year A}) / \text{LULC in Year A}) \times 100\%$$

ii) LULC extraction within LCZs of Nairobi

Using the LCZ shapefile (2018) derived from WUDAPT (Figure 3.3) for Nairobi, classified LULC maps were extracted within each of the 17 LCZs for the study period (Bechtel *et al.*, 2015; Bechtel & Daneke, 2012; Brousse *et al.*, 2016; Ching *et al.*, 2018). An overlay intersect geo-processing technique was employed, where the LCZ shapefile was overlaid on each of the classified LULC maps in ArcMap 10.8.2. The software identifies the spatial areas where the LCZ polygons and the LULC classifications intersected (Aabeyir *et al.*, 2022; Geletič *et al.*, 2019; Huang *et al.*, 2023), indicating the specific regions where each LCZ type coexisted with corresponding LULC categories. Since the LCZ shapefile was for 2018, the LULC 2002 and 1988 LULC images were overlaid to infer what LCZs were transformed. The expected result of this is a new dataset that shows the LULC composition within each of the 17 LCZs, focusing on the vegetated LCZs that were transformed to built-up type LCZs (Figure 3.9).

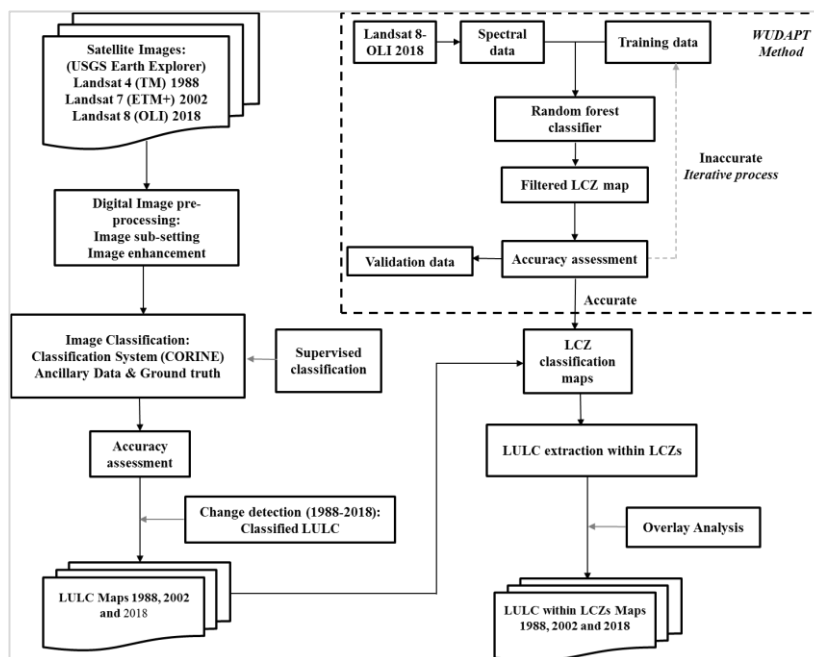


Figure 3.9: Flowchart of the LULC Transition Analysis within LCZs of Nairobi

3.4.1.5 Land Use/Cover Prediction for Nairobi to 2033

The research employed the MOLUSCE tool within the QGIS 2.18 software to analyze spatiotemporal changes and calculate the transitions and predict LULC for 2033. The CA-ANN technique within the MOLUSCE plugin was employed to model transition potentials and forecast future scenarios. This approach aligns with recent research demonstrating the efficacy of the CA-ANN method for accurate future predictions, as highlighted in previous studies (El-Tantawi *et al.*, 2019; Muhammad *et al.*, 2022; Perović *et al.*, 2018). To validate the model and prediction accuracy, the MOLUSCE plugin offers a kappa validation technique and comparison of actual and projected LULC images. Post-model validation, the LULC data for 2002 and 2018, the auxiliary variables, and the transition matrices, were used for predicting LULC for 2033.

3.4.2 Determining LST Changes in Nairobi along an Urban Gradient

Spatial LST distribution maps were developed from the estimated satellite derived LST geo-statistical analysis (Jiang & Lin, 2021; Aabeyir *et al.*, 2022; Tesfamariam *et al.*, 2023). The outputs were used to analyze and describe the spatial variability together with their thermal characteristics. NDVI distribution maps were also generated for the same period using ArcMap 10.8.2. In this research, two temperature transects were established in four cardinal directions of Nairobi at an interval of 400m for all the LST images in ArcMap 10.8.2.

These were ordinary transects and they passed through the urban-rural areas to represent the overall LST trends within Nairobi using ArcMap 10.8.2 platform. (Kumar & Shekhar, 2016; Jiang & Lin, 2021) the transect lines were centered on Nairobi's CBD area and extensive through the West – East and the North – South directions. A profile analysis of the images was applied using the two established transects and the temperature profiles obtained for each LST map. A statistical correlation analysis of LST and NDVI was executed using the SPSS statistical software. Descriptive tables, graphs and figures were obtained for interpretation.

3.4.2.1 Vegetation and Land Surface Temperature Prediction for Nairobi to 2033

To predict the NDVI and LST for Nairobi in 2033, a similar approach to section 3.4.1.5 were followed. To ensure the model's accuracy and validity, the MOLUSCE plugin employs a kappa validation technique and compares actual and projected NDVI and LST images. Following model validation, data from 2002 and 2018, including auxiliary variables and transition matrices, were utilized to forecast NDVI and LST for the year 2033.

3.4.3 Determining the Effects of Plant Species on Thermal Comfort in an Urban Environment

The means of the collected microclimate data (relative humidity, wind speed, air and surface temperatures) for Day 1, 2 and 3 ($n=3$), were calculated and the results used to show the continuous distribution from 8 am to 6 pm (10 hours) for both sites. (Loughner *et al.*, 2012; Shahidan, 2015; Sodoudi *et al.*, 2018) data for three specific hours; 8am, 1pm and 6pm were extracted from the entire 20-minute interval data set and were used for analysis. This is because, at 8am the air is still chilled, at 1pm the air is quite heated up by the scorching sun and at 6pm the sun is down, and the heat islands knock-on-effect is felt.

The data in this study was assumed not to follow a normal distribution, as the population was not homogenous. Statistical Package for Social Sciences (SPSS) software was used to statistically analyze the measured microclimatic parameters. To reduce possibilities of skewed data distribution, Kruskal-Wallis non-parametric analysis of variance (ANOVA) was used for statistical evaluation of the significant difference among the means of microclimate variables measured (McKight & Najab, 2010; Miari *et al.*, 2022). Mann-Whitney's U Test was then used to investigate the significant distinction between the two independent study sample sites (inter-sites) (Zhang & Zhang, 2009).

Whenever p was < 0.05 the mean difference was deemed as a statistical significance. Values of SVF and PET obtained from the Rayman model were used to assess the

human thermal comfort under the trees along with the control areas (Fang *et al.*, 2018; Ji *et al.*, 2022). (Figure 3.10). Simple correlation analysis was performed between LAI and PET. Results were presented in graphs and tables.

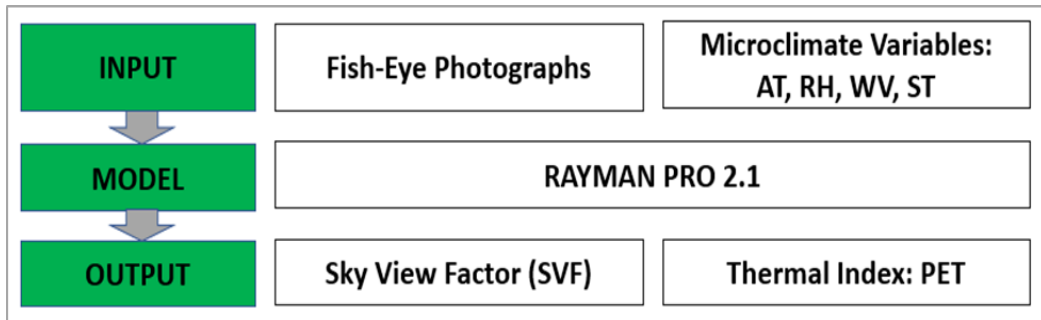


Figure 3.10: Overview of the PET Analysis Process

CHAPTER FOUR

RESULTS AND DISCUSSION

4.1 Introduction

This chapter encompasses the research outcomes for each of the three specific objectives. The results and discussion for evaluated vegetation changes of LULCs in LCZ of Nairobi at a macro-scale are presented in sub-section 4.2. The changes in LST along the urban gradient are highlighted in sub-section 4.3, and the micro-scale of specific tree species effects on microclimate in an urban park and street are underscored in sub-section 4.4.

4.2 Spatial and Temporal Changes of Vegetation Cover In Local Climate Zones of Nairobi from 1988 - 2018

4.2.1 LULC Images' Accuracy

The overall accuracy generated were 90%, 86.7% and 93.3% for 1988, 2002 and 2018 respectively. In the same manner, the kappa coefficients obtained were 0.87, 0.83 and 0.91 (Table 4.1), an indication of a strong to almost accurate level of agreement.

Table 4.1: The LULC Accuracy Assessment Report for 1988, 2002 and 2018

Class Name	1988 (TM)		2002 (ETM+)		2018 (OLI)	
	Producers (%)	Users (%)	Producers (%)	Users (%)	Producers (%)	Users (%)
Forests	100.0	87.5	100.0	100.0	100.0	83.3
Built-Up Areas	85.7	85.7	85.7	85.7	100.0	100.0
Agriculture	83.3	100.0	83.3	83.3	100.0	85.7
Rangelands	85.7	85.7	71.4	100.0	88.9	100.0
Water	100.0	100.0	100.0	71.4	80.0	100.0
Overall Accuracy	90%		86.67%		93.33%	
Kappa coefficient	0.8727		0.8333		0.9156	

4.2.2 Changes in LULC within LCZs of Nairobi (1988-2018)

a) Overall LULC Changes 1988, 2002, and 2018

The LULC distribution maps for the study period are presented in Figure 4.1. The results depicted an escalation in the intensity of built-up areas around Nairobi central, extending towards the eastern side from 1988 to 2018. Urban agriculture's magnitude slightly increased on the western side of Nairobi, around the Ngong forest areas. On the contrary, forests' spatial extents declined and were predominantly replaced by urban agriculture and built-up areas through the thirty-year duration. The same was the case for the rangeland areas.

The outcome demonstrated a notable decrease in forests and rangelands by 47% and 24%, respectively for the thirty-year period (Figure 4.2b). Between 1988 and 2002, forests reduced by 33 Km², and progressively by 47Km² between 2002 and 2018, a cumulative detriment of approximately 80 Km² area coverage. In a similar manner, the rangelands declined gradually by 96Km² between 1988 and 2018. A higher reduction in forests and rangelands occurred between 2002 and 2018 (Table 4.2; Figure 4.1).

Table 4.2: Areal Extent of the LULC Types of Nairobi County (1988, 2002 and 2018)

Land Use & Land Cover Classes	Years					
	1988		2002		2018	
	Area (Km ²)	Percentage (%)	Area (Km ²)	Percentage (%)	Area (Km ²)	Percentage (%)
i. Forests	125	17.73	92	-13.05	45	-6.38
ii. Built-up Areas	70	9.93	106	15.04	234	33.19
ii Urban i. Agriculture	209	29.65	208	-29.50	218	30.92
iv Rangelands	299	42.41	295	-41.84	203	-28.79
V Water Bodies	2	0.28	4	0.57	5	0.71
Total	705	100.00	705	100.00	705	100.00

Dissimilarly, built-up areas, urban agriculture and water bodies signified a substantial rise by 71%, 4% and 40%, sequentially, for the study period (Figure 4.2b). Between 1988 and 2002, the built-up area increased by 67 Km². The spatial extent increased further by 128 Km² between 2002 and 2018, totaling to 195 Km² increment. Urban

agriculture reduced by 1 Km² from 1988 to 2002, it then increased by 10 Km² from 2002 to 2018, making it 11 Km² rise in area expanse. Comparably, a surge in the geographical size of water bodies increased by 2 Km² and 1 Km² from 1988 to 2002 and from 2002 to 2018 in that order, with the construction of wastewater treatment facilities such as the Ruai treatment plant. Figure 4.2 (A) showing the LULC change trends, while (B) illustrating the LULCs percentage change from 1988 to 2018.

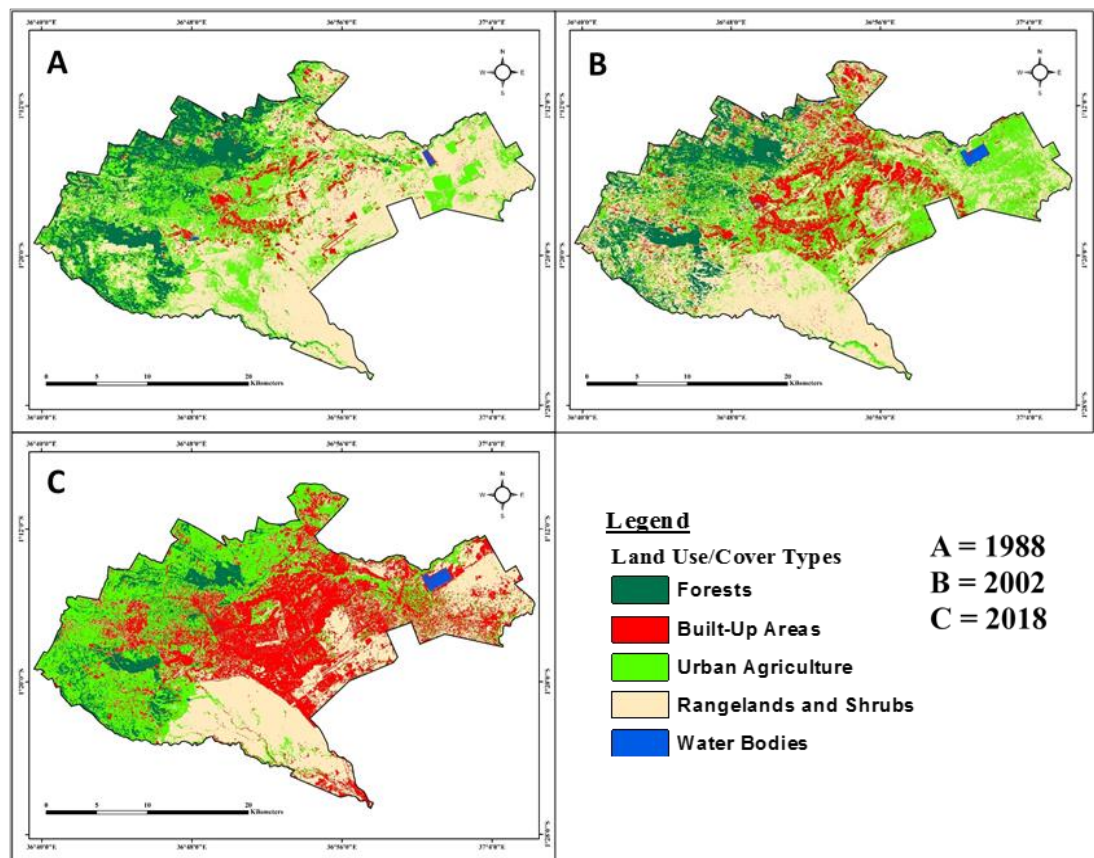


Figure 4.1: Land Use Land Cover (LULC) Distribution Maps of Nairobi for the Years 1988, 2002, and 2018

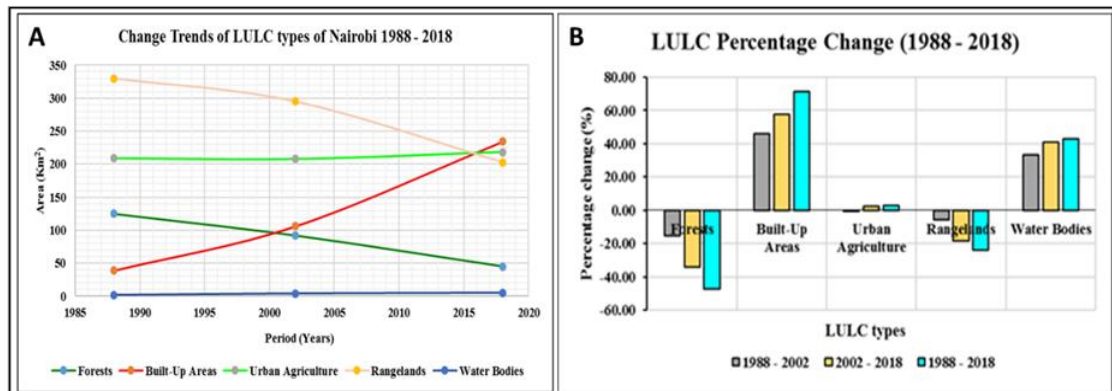


Figure 4.2: LULC Change Trends (A) and Percentage Change (B) between 1988 and 2018

b) LULC Changes within LCZs of Nairobi (1988 – 2018)

The spatial changes in area for LULC types in each of the 17 LCZs were computed in ArcMap 10.8.2. The outputs are illustrated in (Table 4.3) for the built-type, LCZs (1-10), and (Table 4.4) for the vegetated land cover (LC)-type, LCZs (A-G). Within the study period, forests were absent in LCZ 1, 2, 3, 8, 10, E, F, and G, which are representatives of compact high, mid and low-rise, large low-rise, heavy industry, bare rocks and soils, and water, sequentially, with the most forested areas decline by 45 Km² in LCZ 9 (Table 4.3). However, they were greatly present in LCZ A and B depicting dense and scattered trees, and sparsely built areas (Table 4.3). They all marked a declining trend in the area from 1988 to 2018.

Built-up areas were predominantly present in LCZs 1 to 10 (Table 4.3), with a scanty area extent in the LC-type LCZs, especially LCZ A and B (Table 4.4). There was a notable increase in built-up areas by 29Km² and 21 Km² in LCZ 5 and LCZ 10 respectively. Urban agriculture was mainly appearing in LCZ B, C, D, 5, 6 and 9, while lowest in LCZ 7-10, E, F and G. Rangelands were highest in LCZ F, recorded in 1988 and declined by 16Km² in 2018 (Table 4.4). Water was dominant in LCZ G and rose by 2.3Km² by 2018.

Table 4.3: Transition of LULC Composition within the Built-type LCZs 1-10 in 1988, 2002 and 2018

Local Climate Zones (LCZs)	Year	Land Use Land Cover Area Changes (Km ²)					Total Area (Km ²)
		Forests	Built-Up Areas	Urban Agriculture	Rangelands	Water Bodies	
LCZ 1	1988	0	0.8	0.2	0.1	0	1.1
	2002	0	0.8	0.1	0.1	0.1	1.1
	2018	0	1	0	0	0.1	1.1
LCZ 2	1988	0.3	4.4	5.2	4.7	0	14.6
	2002	0.3	9.5	3.3	-1.6	0.1	14.8
	2018	0	13.2	-0.7	-0.8	0	14.7
LCZ 3	1988	0.2	2.3	6.7	13.3	0	22.5
	2002	0.1	7.4	9.7	-5.2	0	22.4
	2018	0	16.2	-1.1	-5.2	0	22.5
LCZ 4	1988	6.3	0.8	14.3	2	0	23.4
	2002	-4.8	1.8	10.2	6.4	0.2	23.4
	2018	-1.1	10.4	-9.8	-2	0.1	23.4
LCZ 5	1988	5.1	5.2	29.8	21.4	0.2	61.7
	2002	-2.7	13.8	23.4	21.6	0.3	61.8
	2018	-0.5	34.1	-18.8	-8.3	0	61.7
LCZ 6	1988	1.1	1	10.8	22.1	-0.1	35.1
	2002	-0.5	3.3	9.7	21.7	0	35.2
	2018	-0.1	9.4	-8.4	-17.3	0	35.2
LCZ 7	1988	0.5	2.3	4.2	4.3	0	11.3
	2002	0.4	5.2	3.7	-1.9	0	11.2
	2018	0	9.1	-1	-1.1	0	11.2
LCZ 8	1988	0.4	1.4	4.9	15.1	0	21.8
	2002	0.3	7	10.1	-4.4	0.1	21.9
	2018	0	19.2	-1.2	-1.4	0	21.8
LCZ 9	1988	67.4	2.5	40.5	12.8	0.1	123.3
	2002	-51	8.1	58.6	35.4	0.3	153.4
	2018	-22	9.5	89.4	-2.4	0.2	123.5
LCZ10	1988	0.3	7.8	16.4	21.6	0	46.1
	2002	-0.1	12.9	17.5	15.5	0.2	46.2
	2018	0	28.8	-2.8	-14.6	0	46.2

Table 4.4: Transition of LULC composition within the Land Cover-Type LCZs A-G in 1988, 2002 and 2018)

Local Climate Zones (LCZs)	Year	Land Use Land Cover Area Changes (Km ²)					Total Area (Km ²)
		Fores ts	Built-Up Areas	Urban Agriculture	Rangela nds	Water Bodies	
LCZ A	1988	13.8	0.1	0.4	0.2	0	14.5
	2002	-13.4	0.1	-0.3	0.7	0	14.5
	2018	-12.4	0.3	1.8	0.1	0	14.6
LCZ B	1988	12.1	0.1	3.6	1.2	0	17
	2002	-9.2	0.2	1	6.5	0	16.9
	2018	-6.9	1.3	8.6	-0.2	0	17
LCZ C	1988	14.7	4	32.9	43.1	0.1	94.8
	2002	-7.8	17	-22.3	47.4	0.3	94.8
	2018	-2.1	21.8	56.8	-13.7	0.3	94.7
LCZ D	1988	1.2	0.2	1.6	1.4	0	4.4
	2002	-0.6	0.8	-1.4	1.5	0	4.3
	2018	-0.2	0.9	3	-0.3	0	4.4
LCZ E	1988	0	0.7	1.2	3.1	0	5
	2002	0	1.4	2.3	-1.1	0.1	4.9
	2018	0	4.5	-0.1	0.4	0	5
LCZ F	1988	1.2	4.8	35	161	0	202
	2002	-0.5	16.2	62.7	-122.4	0.2	202
	2018	0	43.5	-13.6	144.7	0.1	201.9
LCZ G	1988	0	0.3	0.3	2.6	0.8	4
	2002	0	0.2	0.6	-0.2	3.1	4.1
	2018	0	0.7	-0.1	0.2	3.1	4.1

The spatial rate of change of LULC within the LCZs is illustrated in Figure 4.3. Between 1988 and 2002, there was a high change rate of LULC in the LC-type LCZs (A-G). Moderate and minimal changes occurred in the built-type LCZs (1-10) for that same period. Despite that, an increase in the change rate of LULC in LCZ 1 to 10 escalated substantially between 2002 and 2018, and cumulatively for the entire study duration.

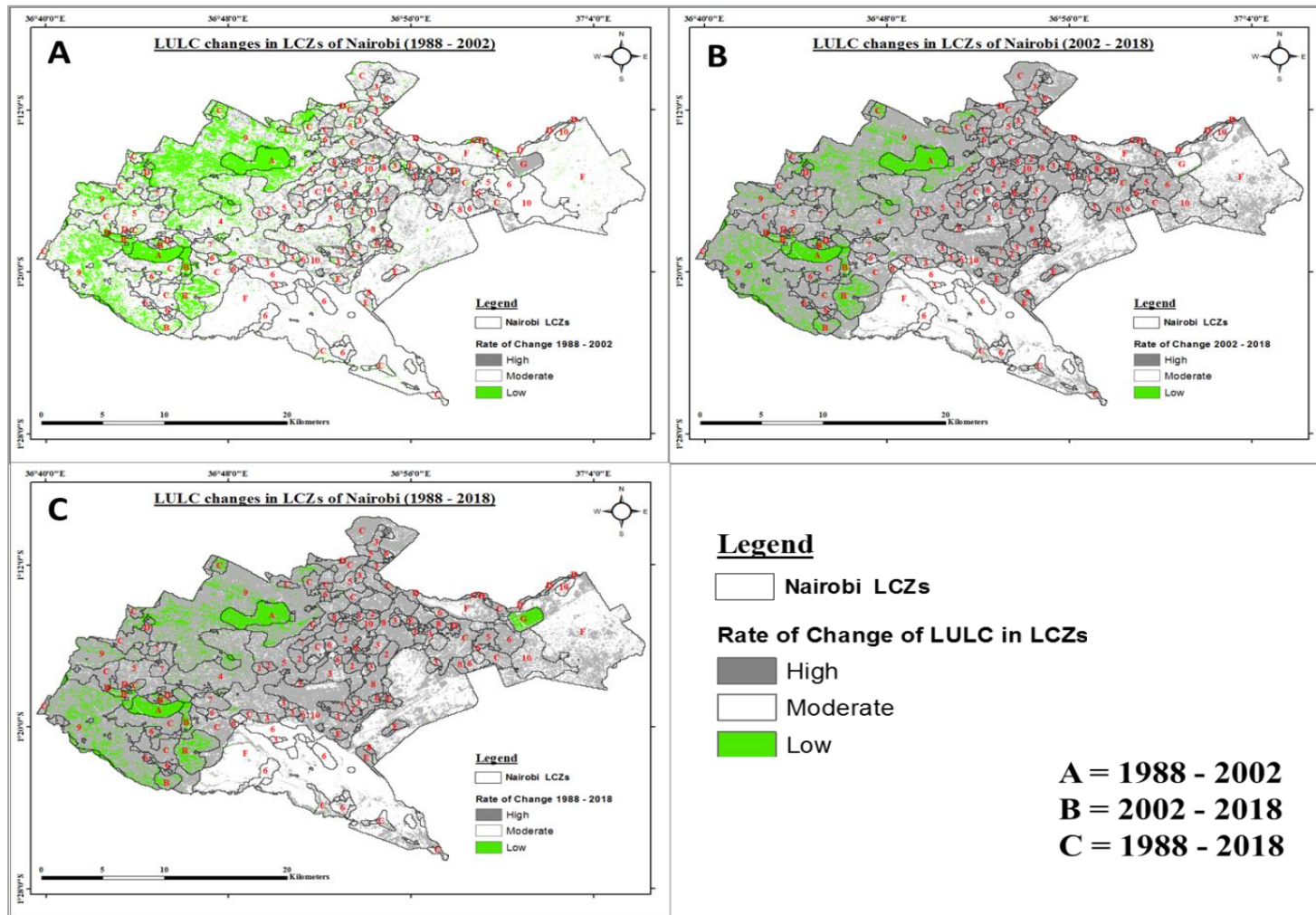


Figure 4.3: Spatial Changes of LULC within LCZs of Nairobi for 1988 to 2018

4.2.3 Conversions of LULC and within LCZs of Nairobi (1988-2018)

The conversions of LULC in each of the LCZs of Nairobi and their areas were calculated and presented in descriptive tables. The conversions were established between 1988-2002, 2002-2018 and 1988-2018.

a) Overall LULC Conversions 1988-2018

During the thirty-year duration, conversions of one LULC to another had been encountered from time to time. The research revealed that the highest rate of LULC conversions occurred between 2002 and 2018 (Table 4.5, Figure 4.3). The maximum conversion was from rangelands to built-up areas by 110Km² between 1988 and 2018, in the areas around Nairobi national park, Langata, Dagoretti south and in Embakasi east parts of Ruai. Secondly, built-up to more built-up conversions recorded an increase by 88Km², commonly within the CBD, Starehe, Westlands, Makadara, Embakasi south and Kamukunji sub-counties (Table 4.5, Figure 4.3).

Forests conversion to built-up areas was third highest by 87Km² for the research period, mostly around the major Nairobi forests including Karura, Ngong, Arboretum, and City park (Table 4.5, Figure 4.3), with urban agriculture changing to built-up by 73Km². Equally, forests to agriculture changed by 69Km², generally in the outskirts around Dagoretti south in Ngong. Rangelands to urban agriculture followed by 55Km². Lastly, conversion of urban agriculture to rangelands was 44Km². The other conversions were minimal and close to none, particularly in the water LULC (Table 4.5, Figure 4.3).

b) LULC Conversions within LCZs of Nairobi

The conversions of LULC are shown in each LCZ. Thereafter, they were presented in Table 4.6 (1988 – 2002), Table 4.7 (2002 – 2018) and Table 4.8 (1988 - 2018). The highest rate of conversions within the LCZs occurred from 2002 to 2018, as compared to the period between 1988 and 2002 (Table 4.6, Table 4.7). Between 1988 and 2002, LCZ 9 (sparsely built) experienced the most LULC conversions with forests to agriculture, forests to built-up, forests to rangelands, and forests to built-up covering 9Km², 3.3Km², 13.8Km², and 41Km² respectively (Table 4.6). Likewise, the leading LULC conversion was from rangeland to agriculture by 47Km² and rangeland to rangeland by 32Km² within

LCZ F (Bare soil/sand), as well as LCZ C (Bush/Shrubs) by 25Km² for the same period (Table 4.6), signifying a potential drought experienced from 1988-2002.

The LULC conversion from built-up to built-up was most significant within LCZ 2 (compact mid-rise), 4 (open high-rise), 5 (open mid-rise), 7 (lightweight low-rise), 8 (large low-rise) and E by 4.06Km², 8.43Km², 7.5 Km², 5.01Km², 7.9 Km², 6.24Km² and 5.5Km² respectively, underscoring the evidence of Nairobi's urban development. The LCZs that experienced minimal LULC conversions from 1988-2002 were LCZ D (low plants) and G (water) with <2Km² changes in area (Table 4.6). Between 2002 and 2018 (Table 4.7), LCZ 5, 9, 10, C and F experienced the highest LULC conversions such as agriculture to built-up, rangelands to built-up, forests to built-up and forests to agriculture. For the entire study period (Table 4.8), these same LCZs experienced the highest rate of LULC conversions.

The LULC conversions within Nairobi's LCZs from 1988 to 2018 hold significant implications. The primary conversion frontier involves the shift from vegetation to built-up areas due to urbanization. This alteration relates to increased LST within LCZs, contributing to urban heat island effects. Consequences include compromised local climate, reduced air quality, and escalated energy consumption. Informed by this data, urban planning interventions could prioritize green spaces, efficient building designs, and sustainable infrastructure to mitigate heat impacts, enhance urban resilience, and improve overall quality of life for residents

Table 4.5: LULC Conversion and Area of Change from 1988 to 2018

LULC Conversions		1988 - 2002		2002 - 2018		1988 -2018	
		Area (Km ²)	Change %	Area (Km ²)	Change %	Area (Km ²)	Change %
1.	Built-Up - Built - Up	98.62	13.99	88.47	12.55	87.93	12.33
2.	Built-Up - Forests	0.70	0.10	0.14	0.02	0.33	0.05
3.	Built-Up - Rangelands	6.38	0.91	4.57	0.65	4.81	0.68
4.	Built-Up - Urban Agriculture	5.64	0.80	11.30	1.60	5.18	0.74
5.	Built-Up - Water Bodies	1.03	0.15	0.23	0.03	0.58	0.08
6.	Forests - Built - Up	65.15	9.24	66.39	9.42	87.24	12.38
7.	Forests - Forests	75.30	10.68	40.18	5.70	40.70	5.78
8.	Forests - Rangelands	26.84	3.81	1.17	0.17	2.70	0.38
9.	Forests - Urban Agriculture	37.59	5.33	64.06	9.09	69.26	9.83
10.	Forests - Water Bodies	0.18	0.03	0.09	0.01	0.14	0.02
11.	Rangelands - Built - Up	68.88	9.77	92.56	13.13	110.89	15.73
12.	Rangelands - Forests	1.92	0.27	3.27	0.46	0.61	0.09
13.	Rangelands - Rangelands	25.10	3.56	39.47	5.60	27.95	3.97
14.	Rangelands - Urban Agriculture	79.23	11.24	80.10	11.37	55.39	7.86
15.	Rangelands - Water Bodies	2.23	0.32	0.16	0.02	2.07	0.29
16.	Urban Agriculture - Built - Up	26.51	3.76	84.34	11.97	72.83	10.33
17.	Urban Agriculture - Forests	13.69	1.94	1.76	0.25	3.63	0.52
18.	Urban Agriculture - Rangelands	82.65	11.73	58.87	8.35	43.74	6.21
19.	Urban Agriculture - Urban Agriculture	84.87	12.04	62.26	8.83	87.88	12.47
20.	Urban Agriculture - Water Bodies	0.75	0.11	0.20	0.03	0.40	0.06
21.	Water Bodies - Built - Up	0.04	0.01	1.35	0.19	0.20	0.03
22.	Water Bodies - Forests	0.30	0.04	0.05	0.01	0.11	0.02
23.	Water Bodies - Rangelands	0.06	0.01	0.10	0.01	0.01	0.00
24.	Water Bodies - Urban Agriculture	0.12	0.02	0.22	0.03	0.23	0.03
25.	Water Bodies - Water Bodies	0.98	0.14	3.45	0.49	0.95	0.13
Total		704.76	100.00	704.76	100.00	704.76	100.00

Table 4.6: LULC Conversion and Area of Change in Each LCZ from 1988 to 2002 (15 Yrs)

LULC Conversions		Local Climate Zone Area Change (Km ²)																
		1	2	3	4	5	6	7	8	9	10	A	B	C	D	E	F	G
1.	Agriculture - Agriculture	0.04	1.59	3.37	7.82	14.21	3.73	1.82	2.44	15.52	6.77	0.1	0.59	10.72	0.49	0.72	14.62	0.12
2.	Agriculture - Built - Up	0.07	2.72	1.62	0.93	4.65	0.64	1.31	1.32	3.03	3.14	0.02	0.1	4.23	0.38	0.23	2.06	0.01
3.	Agriculture - Rangelands	0.04	0.75	1.64	3.94	10.01	6.28	0.88	0.99	13.48	6.4	0.18	2.72	16.25	0.59	0.2	17.99	0.01
4.	Agriculture - Forests	0	0.1	0.03	1.5	0.81	0.15	0.18	0.14	8.44	0.04	0.12	0.23	1.62	0.09	0	0.19	0.02
5.	Agriculture - Water Bodies	0.01	0.03	0.01	0.1	0.11	0.01	0.01	0.02	0.05	0.06	0	0.01	0.06	0.01	0.01	0.09	0.16
6.	Rangelands - Agriculture	0.02	1.23	5.68	0.64	6.93	5.42	1.47	7	3.22	9.71	0.02	0.08	8.45	0.45	1.48	46.73	0.42
7.	Rangelands - Built - Up	0.05	2.68	4.35	0.21	5.23	2.1	1.88	4.77	1.45	3.43	0.01	0.06	9.78	0.32	0.72	11.63	0.15
8.	Rangelands - Rangelands	0.01	0.71	3.3	1.09	9.05	14.61	0.86	3.16	7.1	8.41	0.13	1.06	24.54	0.61	0.87	32.42	0.16
9.	Rangelands - Forests	0	0.03	0.01	0.04	0.19	0.01	0.03	0.09	1.06	0.01	0.05	0.01	0.3	0.02	0	0.04	0
10.	Rangelands - Water Bodies	0.01	0.01	0.01	0.02	0.04	0.01	0.01	0.04	0.02	0.06	0	0	0.01	0	0.02	0.08	1.89
11.	Forests - Agriculture	0	0.2	0.07	1.6	1.47	0.28	0.21	0.26	9.23	0.16	0.15	0.36	2.68	0.41	0	0.44	0
12.	Forests - Built - Up	0	0.01	0	0.22	0.38	0.06	0.03	0.04	3.26	0.04	0.04	0.03	0.91	0.06	0	0.04	0
13.	Forests - Rangelands	0	0.03	0.03	1.17	1.84	0.43	0.1	0.08	13.81	0.09	0.42	2.73	5.25	0.31	0	0.44	0
14.	Forests - Forests	0	0.1	0.07	3.26	1.37	0.37	0.13	0.02	41.05	0.03	13.17	8.96	5.78	0.46	0	0.26	0.01
15.	Forests - Water Bodies	0	0	0	0.02	0.01	0	0	0	0.07	0	0.02	0	0.02	0	0	0.02	0
16.	Built-Up - Agriculture	0.02	0.24	0.59	0.16	0.8	0.21	0.21	0.33	0.64	0.82	0.01	0.01	0.45	0.1	0.13	0.87	0.03
17.	Built-Up - Built - Up	0.66	4.06	1.42	8.43	7.5	0.47	5.01	7.9	0.37	6.24	0.01	0.02	2.01	0.05	5.47	2.44	0.02
18.	Built-Up - Rangelands	0.01	0.12	0.25	0.19	0.75	0.33	0.05	0.17	1	0.59	0.01	0.02	1.33	0.02	0.04	1.46	0.01
19.	Built-Up - Forests	0	0.01	0.01	0	0.07	0.01	0.01	0	0.39	0	0.09	0.02	0.06	0	0	0.03	0
20.	Built-Up - Water Bodies	0.12	0.01	0	0.06	0.11	0	0	0.04	0.08	0.12	0	0	0.13	0.01	0.02	0.05	0.28
21.	Water Bodies - Agriculture	0	0	0.02	0	0.01	0.03	0	0.03	0.01	0	0.01	0	0	0	0	0	0
22.	Water Bodies - Built - Up	0	0	0	0	0	0	0	0.01	0	0	0	0.01	0	0	0	0.01	0
23.	Water Bodies - Rangelands	0	0	0	0	0	0.03	0	0.01	0.01	0	0	0	0	0	0	0.01	0
24.	Water Bodies - Forests	0	0.02	0.01	0	0.23	0	0.01	0	0.01	0	0	0	0	0	0	0.02	0
25.	Water Bodies - Water Bodies	0	0.01	0	0	0	0	0	0	0.07	0	0	0.09	0.01	0	0	0	0.8

Table 4.7: LULC Conversion and Area of Change in Each LCZ from 2002 to 2018 (15 Yrs)

LULC Conversions		Local Climate Zone Area Change (Km ²)																
		1	2	3	4	5	6	7	8	9	10	A	B	C	D	E	F	G
1.	Agriculture - Forests	0.0	0.0	0.0	0.1	0.1	0.0	0.0	0.0	1.2	0.0	0.0	0.1	0.2	0.0	0.0	0.0	0.0
2.	Agriculture - Built - Up	0.1	2.7	6.9	4.7	12.9	3.8	2.9	8.7	3.0	10.2	0.0	0.1	6.6	0.4	2.1	18.8	0.3
3.	Agriculture - Rangelands	0.0	0.3	2.3	0.8	2.9	3.1	0.4	0.7	0.6	5.9	0.0	0.0	2.4	0.1	0.2	39.1	0.1
4.	Agriculture - Agriculture	0.0	0.3	0.6	4.6	7.5	2.8	0.5	0.7	23.8	1.3	0.2	0.8	13.1	0.9	0.0	4.8	0.1
5.	Agriculture - Water Bodies	0.0	0.0	0.0	0.0	0.0	0.0	0.0	0.0	0.0	0.0	0.0	0.0	0.0	0.0	0.0	0.0	0.1
6.	Built - Up - Forests	0.0	0.0	0.0	0.0	0.0	0.0	0.0	0.0	0.1	0.0	0.0	0.0	0.0	0.0	0.0	0.0	0.0
7.	Built - Up - Built - Up	0.7	9.1	6.1	1.2	9.9	1.9	4.9	6.4	1.1	11.8	0.0	0.1	6.0	0.2	1.3	8.4	0.1
8.	Built - Up - Rangelands	0.0	0.2	1.1	0.2	1.7	0.7	0.2	0.4	0.3	0.9	0.0	0.0	2.5	0.0	0.1	2.2	0.0
9.	Built - Up - Agriculture	0.0	0.1	0.2	0.3	2.1	0.7	0.1	0.2	2.6	0.1	0.0	0.1	3.4	0.6	0.0	1.5	0.0
10.	Built - Up - Water Bodies	0.0	0.0	0.0	0.0	0.0	0.0	0.0	0.0	0.0	0.0	0.0	0.0	0.0	0.0	0.0	0.0	0.1
11.	Rangelands - Forests	0.0	0.0	0.0	0.1	0.1	0.0	0.0	0.0	2.0	0.0	0.2	0.6	0.4	0.0	0.0	0.0	0.0
12.	Rangelands - Built - Up	0.0	1.2	3.2	3.3	10.3	3.5	1.1	3.7	3.3	6.4	0.1	0.5	8.4	0.3	1.0	16.0	0.1
13.	Rangelands - Rangelands	0.0	0.2	1.7	0.8	3.6	13.5	0.5	0.4	1.1	7.8	0.0	0.1	8.7	0.1	0.1	99.4	0.1
14.	Rangelands - Agriculture	0.0	0.2	0.3	2.2	7.6	4.6	0.3	0.3	29.0	1.3	0.5	5.4	29.9	1.1	0.0	6.9	0.0
15.	Rangelands - Water Bodies	0.0	0.0	0.0	0.0	0.0	0.0	0.0	0.0	0.0	0.0	0.0	0.0	0.0	0.0	0.0	0.0	0.0
16.	Forests - Forests	0.0	0.0	0.0	0.9	0.3	0.1	0.0	0.0	8.7	0.0	12.3	6.2	1.5	0.1	0.0	0.0	0.0
17.	Forests - Built - Up	0.0	0.2	0.0	1.0	0.7	0.1	0.2	0.2	2.0	0.1	0.1	0.7	0.8	0.1	0.0	0.2	0.0
18.	Forests - Rangelands	0.0	0.0	0.0	0.2	0.1	0.0	0.0	0.0	0.4	0.0	0.0	0.1	0.2	0.0	0.0	0.0	0.0
19.	Forests - Agriculture	0.0	0.1	0.1	2.7	1.5	0.3	0.1	0.0	29.9	0.0	1.0	2.2	5.3	0.3	0.0	0.3	0.0
20.	Forests - Water Bodies	0.0	0.0	0.0	0.0	0.0	0.0	0.0	0.0	0.0	0.0	0.0	0.0	0.0	0.0	0.0	0.0	0.0
21.	Water Bodies - Forests	0.0	0.0	0.0	0.0	0.0	0.0	0.0	0.0	0.0	0.0	0.0	0.0	0.0	0.0	0.0	0.0	0.0
22.	Water Bodies - Built - Up	0.1	0.1	0.0	0.2	0.2	0.0	0.0	0.1	0.1	0.2	0.0	0.0	0.1	0.0	0.1	0.1	0.1
23.	Water Bodies - Rangelands	0.0	0.0	0.0	0.0	0.0	0.0	0.0	0.0	0.0	0.0	0.0	0.0	0.0	0.0	0.0	0.0	0.0
24.	Water Bodies - Agriculture	0.0	0.0	0.0	0.0	0.0	0.0	0.0	0.0	0.0	0.0	0.0	0.0	0.1	0.0	0.0	0.0	0.0
25.	Water Bodies - Water Bodies	0.0	0.0	0.0	0.0	0.0	0.0	0.0	0.0	0.1	0.0	0.0	0.0	0.2	0.0	0.0	0.1	3.0

Table 4.8: LULC Conversion and Area of Change in Each LCZ from 1988 to 2018 (30 Yrs)

LULC Conversions		LULC Changes Local Climate Zone Area Change (Km ²)																
		1	2	3	4	5	6	7	8	9	10	A	B	C	D	E	F	G
1.	Agriculture - Forests	0	0	0	0.3	0.1	0	0	0	2.6	0	0.1	0.2	0.3	0	0	0	0
2.	Agriculture - Built - Up	0.1	4.4	4.9	6.9	16.7	2.5	3.1	4.2	3.6	9.3	0	0.2	6.1	0.3	1	9.2	0.1
3.	Agriculture - Rangelands	0	0.3	1.3	1.2	3.6	5.4	0.5	0.2	0.9	5.7	0	0.1	3.1	0.1	0.1	21.1	0
4.	Agriculture - Agriculture	0	0.5	0.5	5.9	9.4	2.8	0.6	0.5	33.4	1.4	0.3	3.2	23.3	1.2	0	4.6	0
5.	Agriculture - Water Bodies	0	0	0	0.1	0	0	0	0	0	0	0	0	0	0	0	0	0.2
6.	Rangelands - Forests	0	0	0	0	0	0	0	0	0.4	0	0.1	0	0.1	0	0	0	0
7.	Rangelands - Built - Up	0.1	4.2	9.4	1.2	11.5	6	3.5	13.4	1.9	12.2	0	0.1	12.4	0.3	2.8	31.2	0.5
8.	Rangelands - Rangelands	0	0.3	3.5	0.3	3.6	11.6	0.5	1.1	0.5	8.3	0	0.1	9.7	0.2	0.2	121.5	0.2
9.	Rangelands - Agriculture	0	0.1	0.5	0.5	6.2	4.5	0.3	0.6	10	1.1	0.1	1	20.9	0.9	0	8.1	0
10.	Rangelands - Water Bodies	0	0	0	0	0	0	0	0	0	0	0	0	0	0	0	0.1	1.9
11.	Forests - Forests	0	0	0	0.8	0.2	0.1	0	0	18.8	0	12.2	6.7	1.6	0.1	0	0	0
12.	Forests - Built - Up	0	0.3	0.1	1.7	1.9	0.3	0.3	0.3	3.5	0.1	0.2	1	1.8	0.2	0	0.6	0
13.	Forests - Rangelands	0	0	0	0.4	0.5	0.1	0	0	0.8	0.1	0	0.1	0.4	0	0	0.1	0
14.	Forests - Agriculture	0	0.1	0.1	3.3	2.5	0.7	0.1	0.1	44.2	0.1	1.4	4.3	10.8	0.9	0	0.5	0
15.	Forests - Water Bodies	0	0	0	0	0	0	0	0	0.1	0	0	0	0	0	0	0	0
16.	Built-Up - Forests	0	0	0	0	0	0	0	0	0.2	0	0.1	0	0	0	0	0	0
17.	Built-Up - Built - Up	0.7	4.3	1.9	0.6	4	0.6	2.2	1.2	0.4	7.1	0	0	1.6	0.1	0.6	2.5	0.1
18.	Built-Up - Rangelands	0	0.1	0.4	0.1	0.7	0.2	0.1	0.1	0.1	0.5	0	0	0.5	0	0	2	0
19.	Built-Up - Agriculture	0	0	0.1	0.1	0.6	0.3	0	0.1	1.7	0.1	0	0	1.7	0.1	0	0.3	0
20.	Built-Up - Water Bodies	0	0	0	0	0	0	0	0	0.1	0	0	0	0.1	0	0	0	0.2
21.	Water Bodies - Forests	0	0	0	0	0.1	0	0	0	0	0	0	0	0	0	0	0	0
22.	Water Bodies - Built - Up	0	0	0	0	0	0	0	0	0	0	0	0	0	0	0	0	0
23.	Water Bodies - Rangelands	0	0	0	0	0	0	0	0	0	0	0	0	0	0	0	0	0
24.	Water Bodies - Agriculture	0	0	0	0	0.1	0.1	0	0	0	0	0	0	0	0	0	0	0
25.	Water Bodies - Water Bodies	0	0	0	0	0	0	0	0	0.1	0	0	0	0.1	0	0	0	3.8

4.2.4 Predicted Land Use/Cover for 2033

i. The Spatial Variables

Maps representing the three independent variables (DEM, Slope, and Distance from major roads) were presented in figure 4.4. Based on the transition matrix, there was a notable expansion in built-up areas, which may be associated with the fragmentation of vegetation and rangelands.

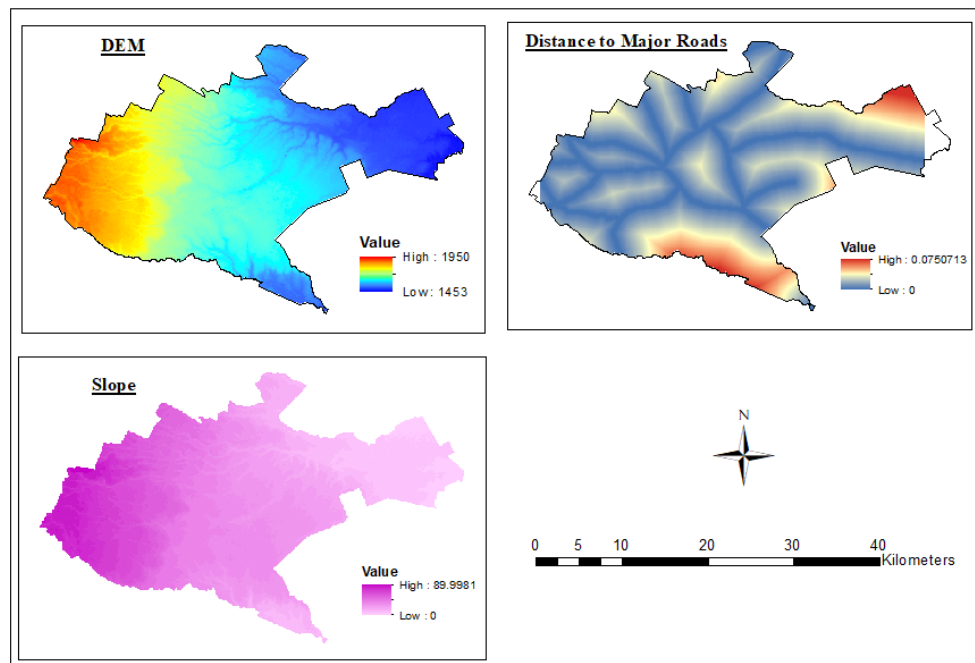


Figure 4.4: Spatial Variables Used in the Study

ii. Predicted LULC and LULC Changes between 2018 and 2033

Using LULC 2002 and 2018, a prediction for LULC in 2033 was obtained, with a kappa value of 0.82. The LULC map for 2033, as well as the LULC changes between 2018 and 2033 were presented in figure 4.5. Likewise, the predicted area statistics for (a) LULC for 2033 and (b) the Rate of Change between 2018 and 2033 were presented in table 4.9.

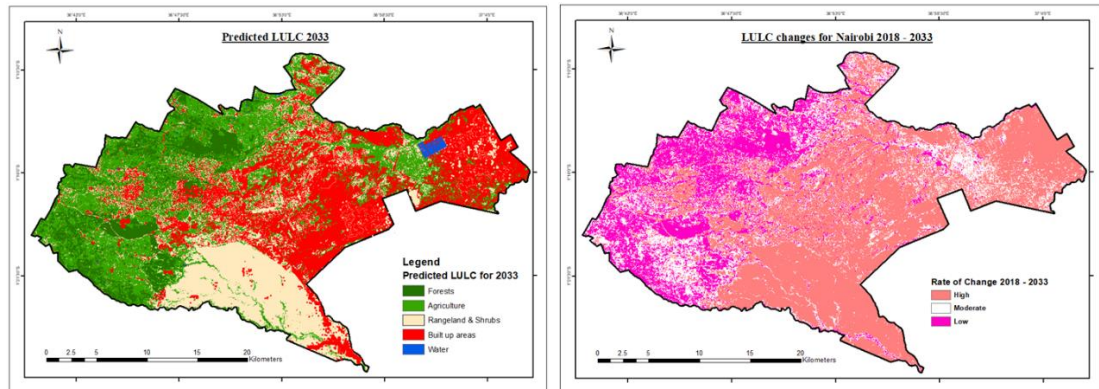


Figure 4.5: (a) Predicted LULC for 2033 and (b) the Rate of Change Maps (2018-2033)

Table 4.9: The Area of Predicted LULC for 2033 and the Rate of Change between 2018 and 2033

LULC Classes	(a) Area of Predicted LULC 2033			LULC Classes	(b) Rate of Change from 2018 to 2033	
	Area (Km ²)	Percentage (%)	Kappa		Percentage change (%)	Rate (Km ² /yr)
Forests	36	- 5.11	0.82	Forests	-20.2	- 0.6
Built-up Areas	303	42.98		Built-up Areas	29.5	4.6
Urban	196	- 27.80		Urban	-10.1	-1.5
Agriculture				Agriculture		
Rangelands	164	- 23.26		Rangelands	-19.2	-2.6
Waterbodies	6	0.85		Waterbodies	20.8	0.1
Total	705	100				

The predicted LULC 2033 statistics (Table 4.9) show a continuation of the trends observed from 1988 to 2018, indicating significant changes in Nairobi's landscape. There is a projected reduction in forests, urban agriculture, and rangelands by 9 Km², 22 Km², and 39 Km², respectively, which reflects ongoing deforestation and the loss of agricultural and rangeland areas. This reduction may be due to urban expansion and increased pressure on land resources. Conversely, built-up areas are expected to increase by 69 Km², suggesting rapid urbanization and infrastructure development. Additionally, the slight increase in water bodies by 1 Km² might indicate improved water management practices or natural changes. These shifts underscore the need for balanced land use planning to ensure sustainable urban growth while preserving natural and agricultural landscapes.

4.2.5 Discussion

Urban greenery actively enhances ecological soundness, along with enriching health for its inhabitants, by controlling air and urban hydrological qualities, and minimizing temperatures. In Nairobi, LULC changes have had adverse impacts on its vegetation status, mainly represented by forests in this study, in all the LCZs they were present in, for thirty years. Preceding research by (Mundia & Aniya, 2006; Bosco *et al.*, 2011) highlighted a similar forest cover degradation, however, this study registered a more decrease by 47 Km² between 2002 and 2018. The existing anthropogenic activities have compromised the air and water qualities, which would otherwise be naturally mitigated by more flora.

Built-up areas, urban agriculture and water bodies increased, each by 195 Km², 9 Km² and 3 Km², respectively. This rising trend was in conformity with a precedent study by Mundia & Aniya, (2006), even so, this research's findings showed a rise by 128 Km² between 2002 and 2018. Rangelands registered an overall decrease by 96 Km². The research findings substantiated its highest conversion to the built-up areas with moderate portions turned to urban agriculture. The utmost conversion rates of forests, rangelands, agriculture to built-up areas has influenced habitat traits, and biodiversity degradation in Nairobi's green spaces (Table 4.5) comparable to the studies by (Oloo *et al.*, 2020; Oyugi *et al.*, 2017). A case in point is the established transit corridors, where a railway line traversed through the national park, and currently the expressway, cutting partly into the main urban park. A habitual surveillance of these alterations using the concept of LCZs will ensure early detection appropriate for urban areas hence providing evidence-based urban planning frameworks.

Likewise, Nairobi City county's park managers should collaborate with local companies and organizations to conduct more environmental CSRs focusing on greening the Urban Green Spaces (UGS), as part of a collective community effort. Moreover, planting additional native tree species in the existing forests and riparian areas, with guidance of the conservators, will improve their long-term adaptability. Sustainable designing and development of Nairobi's LCZs, following set standards of

development, guarantees the vegetation cover improvement and attaining both SDG 11 (Sustainable Cities) and SDG 13 (Climate Action) by 2030.

4.3 Determining LST Changes in Nairobi along an Urban Gradient

The NDVI and LST distribution maps were generated together with the LST profiles for the specific years. The mean, range and standard deviations were calculated and presented in a descriptive table. A correlation analysis on NDVI and LST showed a strong negative trend ($r = -0.94$), ($r = -0.87$), ($r = -0.90$), for 1988, 2002 and 2018 respectively. This was evidence that for the study period, a decrease in NDVI increased LST in Nairobi, and vice versa.

4.3.1 NDVI Maps of Nairobi 1988 - 2018

The highest values of NDVI showed a decrease for the entire study period, and they were recorded as 0.86, 0.71 and 0.49 for 1988, 2002 and 2018 respectively (Table 4.10; Figure 4.6). Positive NDVI values represent vegetated features, such as forests and agriculture. The research's result is an indicator that both sparse and dense vegetation cover of Nairobi have decreased over the past thirty years. The highest decrease rate was experienced between 2002 and 2018. Contrastingly, the lowest NDVI values increased towards the negative scale, recorded as -0.46, -0.49 and -0.65 for 1988, 2002 and 2018 respectively (Table 4.10; Figure 4.6). Negative values represent non-vegetated features, in particular, built-up areas, water or bare surface. The study's result is a confirmation that these features have increased, with the lowest NDVI values shifting more towards the negative scale.

The NDVI distribution maps (Figure 4.6) showed the highest values present at the west and north-western sides of Nairobi. The predominant LULC types in these areas are urban agriculture and forests, precisely Karura and Ngong forests. However, the maximum NDVI spatial coverage for these features was reduced by 0.37, resulting in a 1.23% annual decrease from 1988 to 2018. The lowest NDVI values were present at the east and north-east and southern parts of Nairobi. The primary LULC types here are built-up areas, rangelands, and water, precisely Nairobi CBD, industrial area, Ruai sewage plant, national park rangelands among others. The minimum NDVI spatial

coverage for these features has increased by 0.19, resulting in 0.63% annual increase from 1988 to 2018.

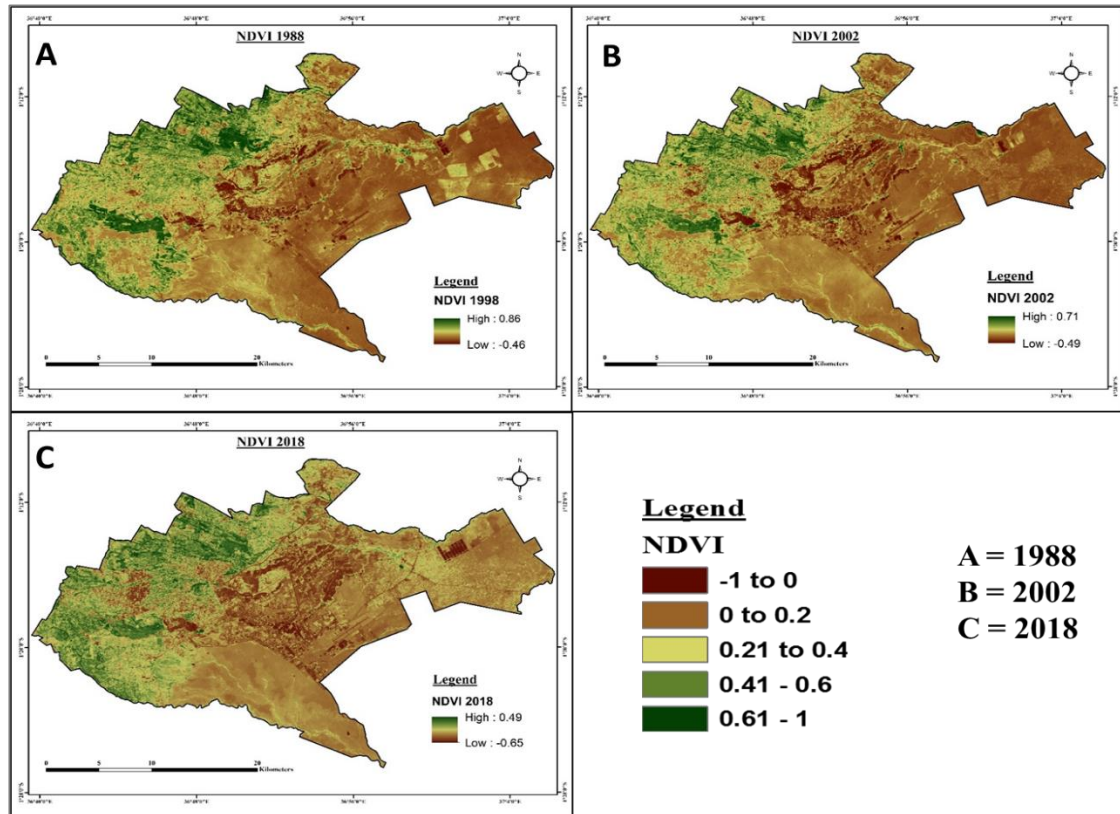


Figure 4.6: NDVI Distribution Maps of Nairobi for the Year 1988, 2002 and 2018

4.3.2 LST Maps of Nairobi 1988 - 2018

The maximum LST values for the study period indicated an increase from 30.7°C to 32°C and 40.1°C in 1988, 2002 and 2018 respectively. Similarly, the minimum LST values increased from 18.3°C to 20.11°C and 21.43°C for 1988, 2002 and 2018. The LST increase rate was lower between 1988 and 2002 with a mean difference of 0.5°C, and higher between 2002 and 2018 with a mean difference of 3.65°C. The general variations for the entire thirty-year period showed that LST mean increased by 4.15°C (Table 4.10; Figure 4.7). To determine the spatial LST characteristics in Nairobi, and visually interpret their variability for the selected years, distribution maps were generated and presented in Figure 4.7.

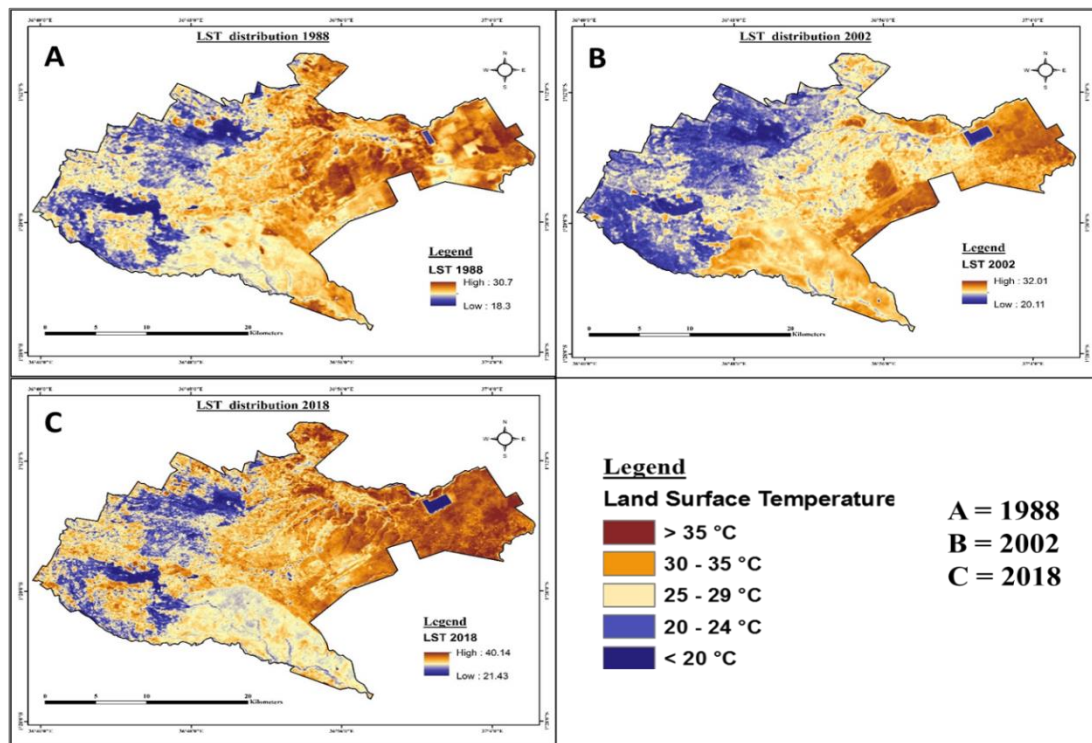


Figure 4.7: LST (°C) Distribution Maps of Nairobi for 1988, 2002 and 2018

Higher temperatures were present around the central, northeastern, eastern and southern parts of Nairobi for all the three selected years. These areas are characterized by construction, industries, and rangelands among other features. The intensity increased significantly from 1988 to 2018. On the other hand, lower temperatures were observed around the western and northwestern parts of Nairobi, which is characterized by agriculture and dense vegetation, such as forests. The intensity slightly increased between 1988 and 2002 but decreased significantly between 2002 and 2018.

Table 4.10: LST and NDVI Mean, Range and Standard Deviations (1988 – 2018)

Index	LST			NDVI		
	1988	2002	2018	1988	2002	2018
Max.	30.7	32	40	0.86	0.71	0.49
Min.	18.3	20	21.3	-0.46	-0.49	-0.65
Mean	26.5	27	30.65	0.2	0.11	-0.08
Range	12.4	12	18.7	1.32	1.2	1.14
Stdev	6.2	6	9.35	0.66	0.6	0.57

4.3.3 LST Gradient Trends

To ascertain the presence of UHI in Nairobi, two transects oriented in the four cardinal directions were established on the LST maps for 1988, 2002 and 2018. The LST profile trends for North-South (Transect 1) and West-East (Transect 2) were presented in Figure 4.8. Transect 1 was 25 Km, while Transect 2 was 35 Km in length, cutting across the existing LULC and passing through the Nairobi Central area. Both profiles showed lower temperatures in forested and agricultural areas and moderate temperatures around the rangeland and open areas. Higher surface temperatures were shown around the central parts of Nairobi, dominated by construction, a validation of UHI existence in Nairobi.

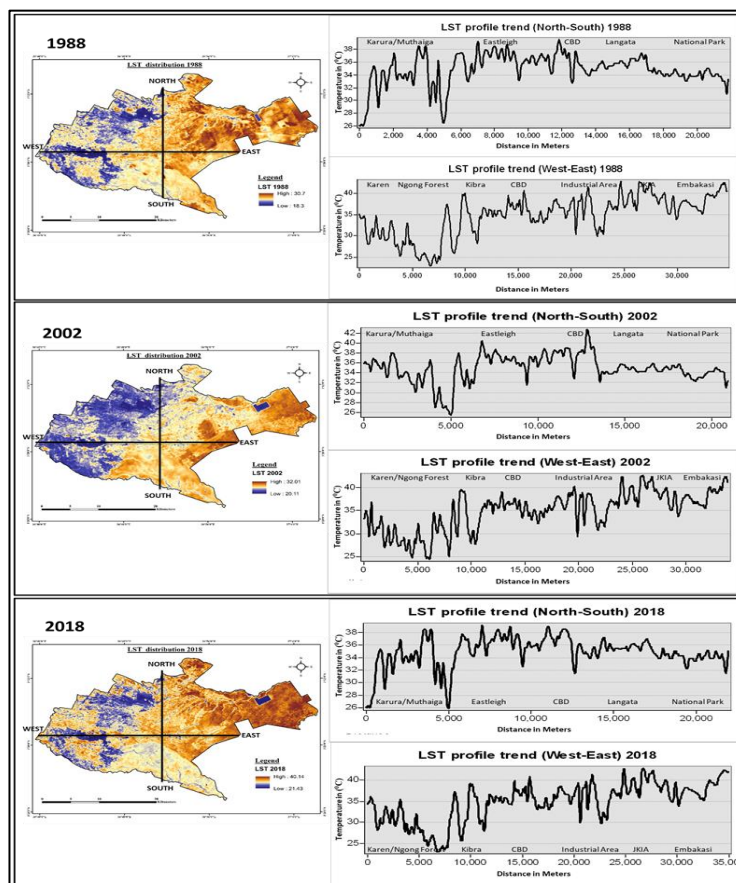


Figure 4.8: LST Profile Trends for Nairobi (North-South, West-East) in 1988, 2002 & 2018

4.3.4 Predicted Vegetation and Land Surface Temperature for 2033

The predicted NDVI and LST map for 2033 were obtained and presented in figure 4.9. The results for Nairobi's predicted NDVI and LST for 2033 indicate significant environmental changes of concern. The mean NDVI of 0.08 and the highest predicted NDVI showing a decrease by 0.28 from 2018 suggest a decline in vegetation cover, likely due to urban expansion and land degradation. Concurrently, the predicted mean LST of 33.05°C and an increase in the highest LST by 3.7°C highlight a substantial rise in surface temperatures. This increase can exacerbate UHI effects, negatively impacting thermal comfort and public health. These findings underscore the urgent need for sustainable urban planning and enhanced green infrastructure to mitigate adverse environmental impacts in Nairobi.

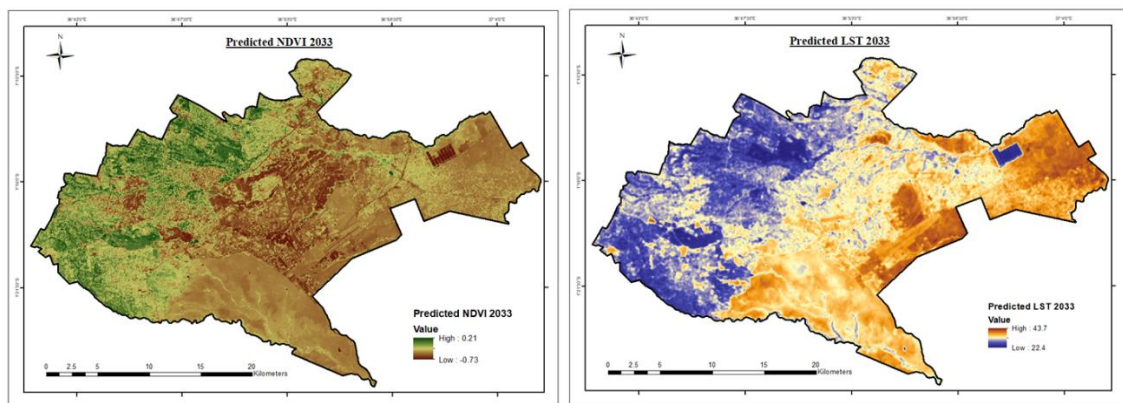


Figure 4.9: (a) Predicted NDVI Map and (b) LST Map for 2033

4.3.5 Discussion

Urban sprawl for Nairobi has largely contributed to the changes in microclimate, particularly the surface temperature over the past three decades. Construction materials, which are compact and have high albedo, have replaced both the natural and less compact surfaces that existed before. The low-reflectivity nature of these materials makes them absorb heat and release very little back, contributing to UHI build up. In addition, the research asserted that rangelands exhibited moderate surface temperatures. They have sparse vegetation and bare soils, which absorb and store some

heat thereby increasing their surface temperatures in contrast to entirely vegetated zones.

As a vegetation cover indicator, NDVI changes for the study period substantiated that vegetation cover for Nairobi has declined. The maximum NDVI spatial coverage reduced by 0.37, resulting in a 1.23% annual decrease (1988-2018), while minimum NDVI spatial coverage increased by 0.19, resulting in 0.63% annual increase for the same period. Nairobi's consistent NDVI downward trends (1988-2018), similar to patterns observed in other African cities such as Lagos and Johannesburg, and globally in São Paulo and Mumbai, suggest a widespread urbanization-induced decline in vegetation health. This potentially impacts local ecosystems and increases vulnerability to climate-related risks, underscoring the need for sustainable urban planning and conservation efforts in these regions.

Likewise, the surface temperatures have increased as more surfaces that are compact have been constructed within Nairobi. The study confirms that Nairobi is experiencing UHI illustrated by the temperature profiles, with a rise in the mean LST for the study period being 4.15°C. Comparably, the mean ambient temperature from the World Bank's Climate Change historical data for the same period showed a positive increase by 0.6°C, indicative of significant warming driven by urban development. Without intervention, this trend may lead to exacerbated heatwaves and heightened risks to human health and urban ecosystems, reduced water availability, and compromised urban livability over the next decade, emphasizing the urgency of climate mitigation measures.

Giguère, (2012) affirms that increasing albedo for building products used by engineers and construction project supervisors will be an asset in reflecting vast amounts of irradiation, contrary to absorbing it. This will be inclusive of the roofing products used for the constructions, brighter color codes will improve heat reflectivity, reducing UHI in Nairobi.

Reducing surface temperatures will ensure improved health as well as better well-being of Nairobi city dwellers. The UHI effects will be minimal, a win-win scenario for both humans and the environment (Giguère, 2012). Incorporating eco-friendly

infrastructure in the city’s spatial advancement plans is imperative, specifically the use of reflecting roofs and walls, UV-absorbent windows, and permeable pavements with high albedo. Additionally, installing water features, such as, pools, ponds or fountains, in landscape designs regulate LST through convectional heat exchange. Since rural-urban migration has been a major contributor to UHI, the national government should disburse resources equally to all the counties to avoid the migration.

4.4 The Effects of Plant Species on Microclimatic Parameters in the Sampled Sites

Plant canopy densities were determined, the mean microclimate distribution were equally presented, together with the species effects on microclimate within the park and street. Likewise, the human thermal comfort for the same sites was evaluated.

4.4.1 Plant Canopy Density and the Tree Allometric Properties

The measured LAI values were used to determine the sample plants’ canopy densities. *Terminalia mantaly* (P3) had the highest density in both two sites with the value of 4.03 and 4.08 in Site 1 (CP) and Site 2 (TR), respectively. *Tipuana tipu* (P4) was the second highest with 3.58 and 3.85, followed by *Cassia spectabilis* (P1) with 3.25 and 3.43, and finally *Podocarpus falcatus* (P2) with 3.02 and 3.21. The plant species in Site 2 (TR) had slightly higher densities than those in Site 1 (CP) with a difference of 0.18, 0.20, 0.04 and 0.27 for P1, P2, P3 and P4, respectively (Table 4.11). The tree allometric properties that were measured were the Diameter at Breast Height (DBH), tree height and the crown diameter.

Table 4.11: Selected Plants’ Allometric Properties; Site 1: CP - Central Park, Site 2: TR - Taifa Rd

Plant Species	LAI		DBH (m)		Crown Diameter (m)		Tree Height (m)	
	CP	TR	CP	TR	CP	TR	CP	TR
P1: <i>Cassia spectabilis</i>	3.25	3.43	0.83	0.80	8.00	8.20	7.90	7.60
P2: <i>Podocarpus falcatus</i>	3.02	3.21	0.80	0.76	7.60	7.00	8.90	8.50
P3: <i>Terminalia mantally</i>	4.03	4.08	0.95	0.93	10.80	10.40	8.50	8.30
P4: <i>Tipuana tipu</i>	3.58	3.85	0.89	0.87	10.10	10.00	8.20	7.70

4.4.2 Mean Microclimatic Variables Distribution at the Trunk, at 5 m and Control

The results of the calculated mean microclimate parameters are presented in graphs to show the continuous distribution for the ten hours measurement period. This was done for both site 1 (Figure 4.10) and site 2 (Figure 4.11), at the trunk and 5 m away from the trunk.

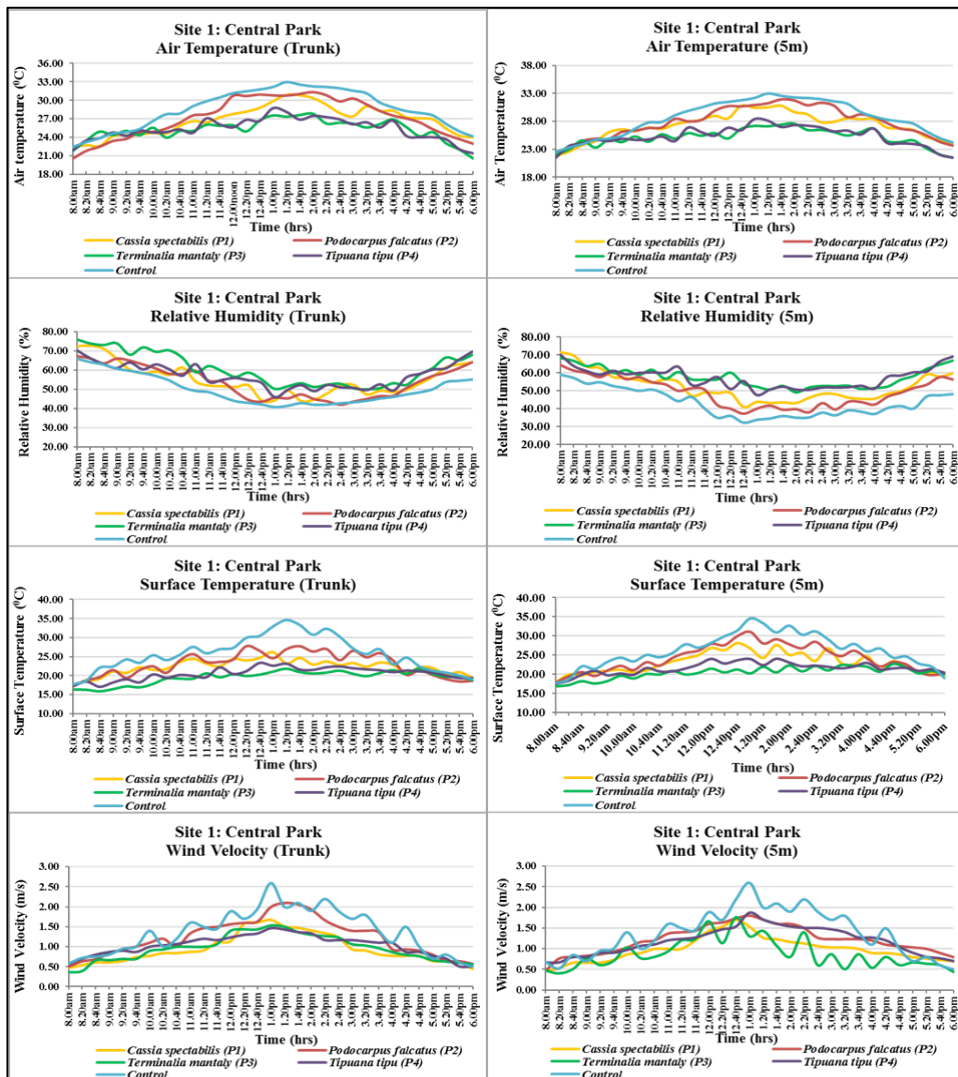


Figure 4.10: The Mean Values of Climatic Variables for Continuous 10-Hour Measurement for Site 1 (Central Park) (Trunk, 5 m)

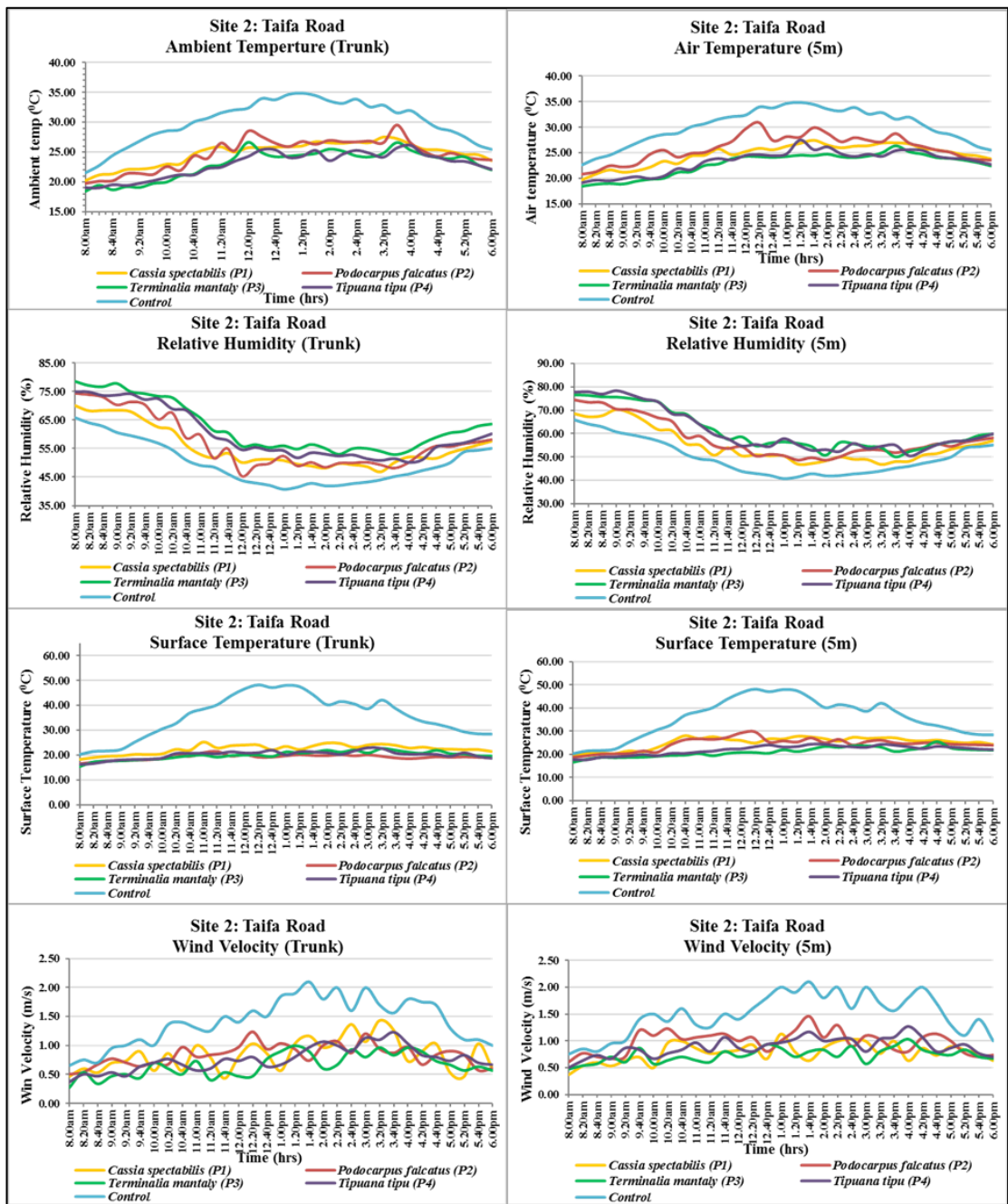


Figure 4.11: The Mean Values of Climatic Variables for Continuous 10-Hour Measurement for Site 2 (Taifa Road) (Trunk, 5 m)

4.4.3 Inter-Site / Inter-Species Effects on Microclimatic Parameters

4.4.3.1 Air Temperature (AT)

Mean ambient temperatures ($n=3$) in the park (Site 1) were 2.1% (1.0°C), 3.3% (2.3°C) and 2.6% (1.3°C) lower than the AT along the street (Site 2) at 8am, 1pm and 6pm, respectively. The highest temperatures were recorded at 1pm, followed by 6pm and the lowest at 8am for all the plant species, at the trunk, 5 m away and at the control points (Table 4.12). At the trunk, AT was lower compared to the AT 5 m away from the trunk and the highest recorded being at the control point with no trees. In both sites, the lowest AT was recorded under *Terminalia mantaly* (P3) with 20.4°C and 20.7°C, respectively, followed by *Tipuana tipu* (P4) with 20.7°C and 20.8°C.

Thirdly *Cassia spectabilis* (P1) followed with 20.9°C and 21.0°C, *Podocarpus falcatus* (P2) followed with 21.2°C and 21.3°C and finally at the control with 23.3°C and 23.5°C correspondingly (Table 4.12). The highest AT were recorded at the control at 1pm-5 m away from the trunk with 33.9°C and 36.2°C for both Site 1 and Site 2, respectively. A significant variation in AT was achieved between the plant species, the time and levels of measurement for each independent site ($p<0.05$) and no significant differences between both sites at 8am ($p = 0.880$) (Table 4.12).

4.4.3.2 Relative Humidity (RH)

The mean RH ($n=3$) was 1.4%, 8.2% and 9.3% higher in Site 1 compared to Site 2 at 8am, 6pm and 1pm respectively. It showed a general trend with highest values recorded at the trunk level, followed by the 5 m and lastly at the control (Table 4.12). A significant change in RH was noted between the plant species, the timing and levels of measurement for both independent sites ($p<0.05$).

In the two sites, the highest RH was recorded under P3 (*Terminalia mantaly*) with 74.6% and 71.7% in Site 1 and 2, respectively. Second was P4 with 71.3% and 68.2%, followed by P1 with 70.1% and 67.6%, and lastly P2 with 64% and 63.4%. All of these were recorded at 8am. Control had the lowest RH with 38.2% and 30% both recorded at 1pm-5 m in the respective sites. (Table 4.12).

4.4.3.3 Surface Temperature (ST)

The mean ST ($n=3$) in Site 2 were 8.2% (3.5°C), 9.1% (6.4°C) and 10.6% (5°C) warmer compared to Site 1 at 8am, 1pm and 6pm respectively. A general trend of cooler surfaces was shown at 8am, slightly warmer at 6pm and warmest at 1pm (Table 4.12). A significant distinction in ST was achieved between the plant species, the time and levels of measurement for both independent sites ($p<0.05$). The lowest ST were measured under P3 with 16.5°C and 17.5°C in Site 1 and Site 2, correspondingly (Table 4.12). This was followed closely by P4 with 16.9°C and 18.4°C, thirdly by P1 with 17.1°C and 19.2°C and lastly P2 with 17.5°C and 19.5°C. All of the lowest temperatures were recorded at 8am. The highest ST recorded were at the control with 31.8°C and 43.2°C measured 5 m away at 1pm both sites (Table 4.12).

4.4.3.4 Wind Velocity (WV)

The mean WV ($n=3$) in Site 2 was 8.7% (0.2m/s), 11% (0.3m/s) and 4.9% (0.1m/s) higher compared to Site 1 at 8am, 1pm and 6pm, respectively (Table 4.12). It showed no general trend in either site but the highest wind velocity trends were recorded in the afternoon and slightly towards the evening at 6pm in both sites. A significant change in WV was observed between the plant species, time and levels of measurement for both independent sites at 8am and 1pm ($p<0.05$) with no significant differences at 6pm ($p = 0.143$).

Significant change between the two sites was noted at 1pm and 6pm ($p<0.05$) with no significant differences at 8am ($p = 0.820$) (Table 4.12). In Site 1, the lowest WV was 0.5 m/s recorded under P1-8am and P4-6pm both at the trunk. The highest WV was 1.2m/s recorded at the control, both at the tree trunk and 5 m away at 1pm. In Site 2, the lowest WV was recorded under P3 and P4 both with 0.53 m/s at 8am. P1 followed with 0.63m/s and P2 with 0.65 m/s. The highest WV was 1.8m/s recorded at 1pm, 5 m away from the trunk in site 2 (Table 4.12).

Table 4.12: Mean Microclimatic Variable Measurements under the Tree for the Study Sites

Climatic variables	Plant	SITE 1 (CENTRAL PARK)						SITE 2 (TAIFA ROAD)					
		8am		1pm		6pm		8am		1pm		6pm	
		Trunk	5 m	Trunk	5 m	Trunk	5 m	Trunk	5 m	Trunk	5 m	Trunk	5 m
Air Temp. (°C)	P1	20.9	22.8	25.9	26.2	23.0	23.1	21.0	21.4	31.2	31.2	23.6	23.8
	P2	21.2	22.6	25.9	25.9	23.4	23.7	21.3	21.4	29.9	33.4	23.6	23.6
	P3	20.5	20.9	24.3	24.3	20.9	21.5	20.8	20.8	27.5	27.2	22.0	22.4
	P4	20.7	21.5	24.1	23.5	21.4	21.5	20.8	21.1	28.8	28.9	22.1	22.7
	Control	23.3	24.5	33.3	33.9	24.0	24.2	23.5	25.5	35.4	36.2	25.2	25.5
		CP: <i>K.W 8am</i> ($p = 0.003^{**}$)		<i>K.W 1pm</i> ($p = 0.012^*$)		<i>K.W 6pm</i> ($p = 0.02^*$)		<i>K.W Overall</i> ($p = 0.03^*$)					
		TR: <i>K.W 8am</i> ($p = 0.007^*$)		<i>K.W 1pm</i> ($p = 0.032^*$)		<i>K.W 6pm</i> ($p = 0.002^*$)		<i>K.W Overall</i> ($p = 0.007^*$)					
		<i>M.W 8am</i> ($p = 0.880$)		<i>M.W 1pm</i> ($p = 0.008^*$)		<i>M.W 6pm</i> ($p = 0.025^*$)		<i>M.W Overall</i> ($p = 0.035^*$)					
Relative Humidity (%)	P1	70.2	69.5	50.9	48.6	63.7	59.8	67.2	67.6	44.8	43.7	57.3	57.0
	P2	63.9	64.4	48.4	47.3	59.8	57.6	63.4	62.9	41.2	39.0	56.1	55.2
	P3	74.6	73.6	57.7	57.4	68.7	67.1	71.7	70.0	53.2	52.1	61.4	59.8
	P4	71.3	70.0	55.6	55.5	67.9	66.9	68.2	67.8	48.8	47.6	60.2	60.0
	Control	64.9	64.3	38.7	38.2	65.4	64.4	63.9	62.9	32.2	30.0	55.4	55.1
		CP: <i>K.W 8am</i> ($p = 0.006^*$)		<i>K.W 1pm</i> ($p = 0.002^{**}$)		<i>K.W 6pm</i> ($p = 0.02^*$)		<i>K.W Overall</i> ($p = 0.04^*$)					
		TR: <i>K.W 8am</i> ($p = 0.003^{**}$)		<i>K.W 1pm</i> ($p = 0.004^{**}$)		<i>K.W 6pm</i> ($p = 0.007^*$)		<i>K.W Overall</i> ($p = 0.007^*$)					
		<i>M.W 8am</i> ($p = 0.012^*$)		<i>M.W 1pm</i> ($p = 0.009^*$)		<i>M.W 6pm</i> ($p = 0.004^{**}$)		<i>M.W Overall</i> ($p = 0.049^*$)					
Surface Temp. (°C)	P1	17.1	17.4	23.2	25.7	19.2	19.4	19.2	19.2	33.5	34.5	21.4	23.1
	P2	17.5	18.5	26.2	28.0	19.6	19.9	19.5	19.8	35.7	36.9	23.9	25.0
	P3	16.5	17.1	21.1	22.2	18.2	18.9	17.5	17.8	28.2	29.0	19.6	21.9
	P4	16.9	17.5	22.6	24.0	19.2	19.4	18.4	18.6	30.2	31.2	20.8	22.0
	Control	19.6	19.7	31.6	31.8	20.8	21.0	22.2	23.2	37.4	38.2	28.4	29.4
		CP: <i>K.W 8am</i> ($p = 0.01^*$)		<i>K.W 1pm</i> ($p = 0.02^*$)		<i>K.W 6pm</i> ($p = 0.03^*$)		<i>K.W Overall</i> ($p = 0.01^*$)					
		TR: <i>K.W 8am</i> ($p = 0.02^*$)		<i>K.W 1pm</i> ($p = 0.008^*$)		<i>K.W 6pm</i> ($p = 0.029^*$)		<i>K.W Overall</i> ($p = 0.026^*$)					
		<i>M.W 8am</i> ($p = 0.015^*$)		<i>M.W 1pm</i> ($p = 0.001^{**}$)		<i>M.W 6pm</i> ($p = 0.001^{**}$)		<i>M.W Overall</i> ($p = 0.005^*$)					
Wind Velocity (m/s)	P1	0.5	0.6	0.5	0.7	0.6	0.7	0.6	0.6	0.8	0.9	0.8	0.9
	P2	0.6	0.7	0.8	0.9	0.5	0.9	0.7	0.6	1.2	1.3	1.0	1.1
	P3	0.7	0.6	0.7	0.8	0.6	0.6	0.6	0.5	0.9	0.8	0.6	0.8
	P4	0.5	0.8	0.6	0.8	0.5	0.7	0.6	0.5	0.9	1.1	0.7	0.8
	Control	0.8	0.8	1.2	1.2	0.8	0.9	0.9	1.0	1.4	1.8	0.9	0.9
		CP: <i>K.W 8am</i> ($p = 0.03^*$)		<i>K.W 1pm</i> ($p = 0.023^*$)		<i>K.W 6pm</i> ($p = 0.024^*$)		<i>K.W Overall</i> ($p = 0.02^*$)					
		TR: <i>K.W 8am</i> ($p = 0.028^*$)		<i>K.W 1pm</i> ($p = 0.042^*$)		<i>K.W 6pm</i> ($p = 0.143$)		<i>K.W Overall</i> ($p = 0.001^{**}$)					
		<i>M.W 8am</i> ($p = 0.820$)		<i>M.W 1pm</i> ($p = 0.010^{**}$)		<i>M.W 6pm</i> ($p = 0.011^*$)		<i>M.W Overall</i> ($p = 0.006^*$)					

K.W: Kruskal Wallis Test, **M.W:** Mann Whitney U Test, **CP:** Central Park, **TR:** Taifa Road
Significance level: (*) when $P < 0.05$, and (**) when $P < 0.01$

4.4.4 Human Thermal Comfort (TC) Evaluation

The standard comfort index of PET formulated for specific thermal conditions as described by (Matzarakis & Amelung, 2008) was presented in Table 4.13. Plants in Site 2 had relatively higher values for both SVF and PET compared to plants in Site 1 (Table 4.14; Figure 4.12). The PET range for Site 1, for all the species, was between 22°C and 23.7°C (Table 4.14; Figure 4.12) which implies a neutral to slightly warm thermal perception for the users under the trees (Table 4.13). In Site 2, the PET range was between 25.5°C and 28°C (Table 4.14; Figure 4.12) implying a slight heat stress for the users under the trees (Table 4.13). This shows that Site 2 was warmer than Site 1 by a range of 3.5°C to 4.3°C. The sections with no trees (control) in both sites exhibited warm thermal perception with that of Site 2 being 3.2°C warmer than Site 1 (Table 4.14; Figure 4.12). Users of these spaces with no trees are likely to suffer moderate heat stress (Table 4.13).

Table 4.13: The Comfort Index of PET Formulated for Specific Thermal Conditions

PET (°c)	Thermal Impression	Degree of physiological stress
<4.0	Very cold	Extreme cold stress
4.1 - 8.0	Cold	Strong cold stress
8.1 – 13.0	Cool	Moderate cold stress
13.1 – 18.0	Slightly cool	Slightly cold stress
18.1 – 23.0	Neutral (comfortable)	No thermal stress
23.1 – 29.0	Slightly warm	Slightly heat stress
29.1 – 35.0	Warm	Moderate heat stress
35.1 – 41.0	Hot	Strong heat stress
41>	Very hot	Extreme heat stress

Source: (Matzarakis & Amelung, 2008)

P3 had the lowest PET in both sites with 22°C and 25.5°C, exhibiting a percentage temperature reduction of 18% (9.6°C) and 15% (9.3°C) in Site 1 and 2 respectively (Table 4.14; Figure 4.12). People under this tree experience neutral thermal perception and are comfortable with no thermal stress in Site 1 while being under the same tree in Site 2, they experience a slight heat stress (Table 4.13). P4 had the second lowest with 22.4°C and 26.6°C, a temperature reduction of 17% (9.2°C) and 13% (8.2°C) (Table 4.14; Figure 4.12). The same thermal perception as that of P3 is experienced by

the users under this plant but with slightly higher temperature differences of 0.4°C and 1.1°C than those under P3 in both sites respectively. P1 had the third-lowest PET with 23.1°C and 27.2°C, a reduction of 16% (8.5°C) and 12% (7.6°C) respectively (Table 4.14; Figure 4.12). The people under this tree experience a slight heat stress in both sites (Table 4.13).

Table 4.14: Computed PET and SVF Values for Each Tree Species and the Control Points in Central Park (CP) and Taifa Road (TR)

Tree Species	PET (°C)				SVF			
	Site 1: CP		Site 2: TR		Site 1: CP		Site 2: TR	
	PET 1	Percentage (%)	PET 2	Percentage (%)	SVF 1	Percentage (%)	SVF 2	Percentage (%)
P1 <i>Cassia spectabilis</i>	23.10	16	27.20	12	0.19	60	0.22	64
P2 <i>Podocarpus falcatus</i>	23.70	14	28.40	10	0.24	51	0.29	54
P3 <i>Terminalia mantaly</i>	22.00	18	25.50	15	0.08	80	0.18	70
P4 <i>Tipuana tipu</i>	22.40	17	26.60	13	0.13	71	0.20	67
C Control	31.60	0.00	34.80	0.00	0.74	0.00	0.99	0.00

P2 had the highest PET among all the four species with 23.7°C and 28.4°C, a reduction of 14% (7.9°C) and 10% (6.4°C) in both sites. People are likely to experience a slight heat stress under this tree in both sites similar to P1 but with temperature differences of 0.6°C and 1.2°C higher than those under P1 in both sites (Table 4.14; Figure 4.12). A strong negative correlation between the LAI and PET was obtained from both sites (S1; $r = -0.96$, S2; $r = -0.8$). This implies that an increase in LAI reduces PET and a decrease in LAI would most likely cause a higher PET under the plants' shade.

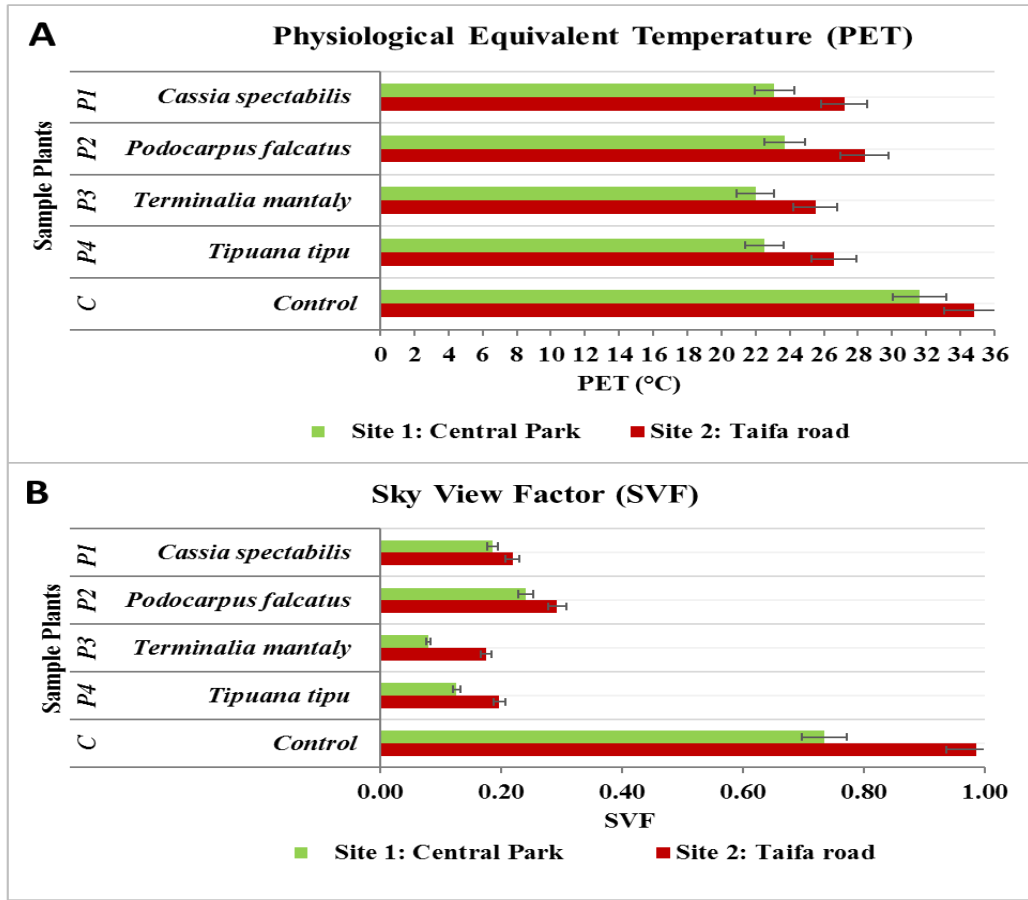


Figure 4.12: Derived PET (A) and SVF (B) for the Sampled Tree Species for the Two Study Sites (Central Park and Taifa Road)

4.4.5 Discussion

AT is much higher in urban regions resulting from human activities which include construction, burning of fossil fuels and use of motor vehicles (Morris, 2010; Geddes & Murphy, 2012) that highly contribute to production of anthropogenic heat causing the buildup of UHI (Voogt, 2020). UHI alters human thermal comfort and poses adverse environmental and health implications to the urban residents (Santamouris *et al.*, 2017; Voogt, 2020). In this study, the plant species in both the park and the street were able to regulate microclimate regardless of their external environments.

Notably, the temperatures in the park were lower compared to the temperatures at the street and this cut across all the species. The park was able to reduce the AT by 3.3% (2.3°C) than the street at 1pm when it is mostly hot and by 2.6% (1.3°C) in the evening

at 6pm when the effect of UHI is felt. The park was also able to increase the RH by 8.2% and 9.3% than the street both at 1pm and at 6pm, respectively. This shows that improving tree cover within urban open spaces will help reduce AT and increase RH making the out-of-door spaces comfortable for the urban dwellers (Narita *et al.*, 2008; Loughner *et al.*, 2012; Feyisa, 2014).

When urban greenery is lost, the lesser its surface area will be, the lesser the rate of evapotranspiration (Leuzinger *et al.*, 2010; Lin *et al.*, 2017) and the lesser the cooling effect of the vegetation will be felt. This poses a lot of environmental and health risks to the city dwellers. Urban planners, policy makers and ecologists should create numerous patches of green spaces (Giguère, 2012; Anjos & Lopes, 2017) and not single-big greenery patches. Likewise, habitual street tree maintenance will provide an economical approach for urban landscape improvement (Jim, 2013).

From the study, there were significant differences among the species' performances because of their canopy densities shown by LAI (Table 4.8). Plants species with higher canopy densities have larger surface areas for evapotranspiration (Loughner *et al.*, 2012; Shahidan, 2015; Sodoudi *et al.*, 2018) and providing shade which in turn reduces temperatures to a greater extent compared to trees with less canopy densities. The results also showed a surface temperature difference of 9.1% (6.4°C) in the street warmer than the park at 1pm (Table 4.12). This shows that materials used to make the surfaces in streets have low albedo and tend to absorb more heat (Anjos & Lopes, 2017; Voogt, 2020), compared to the natural surfaces in parks (Govindarajulu, 2014) which are also permeable. Narita *et al.*, (2008) proposes parking lots should at least be 35% paved and 65% vegetated.

Minimizing trees-construction and pavements damages is achievable through development of a proper planting design. Some factors to be considered during installation include the crown height and width, the utility clearance as well as the size of the planting pit. Besides the aesthetics and functionality of the plants, considering the urban trees' architectural aspect is essential in regulating microclimate in Nairobi. Avoiding tree species having drooping branches, weak trunks or having thorns is imperative for safety purposes. To avoid damaging the roads or surrounding

pavements, the use of root barriers and root trainers is essential. Moreover, the trees should be planted approximately six meters away from any building. Generally, a habitual maintenance of the existing urban trees is vital in reducing structural failures and their potential hazardous risks.

CHAPTER FIVE

SUMMARY, CONCLUSION AND RECOMMENDATION

5.1 Summary

- In the entire study period, vegetation cover of Nairobi declined in the different LCZs, besides the rangeland areas. The decrease was evident and attested to be driven by the growth of additional built surfaces. Conversion of rangelands to built-up areas was highest by 110 Km², followed by built-up to built-up (88 Km²), forests to built-up (87 Km²), urban agriculture to built-up (73 Km²), forest to urban agriculture (69 Km²), and rangelands to urban agriculture (44 Km²) in all the LCZs respectively.
- A rise in the mean LST for the study period was 4.15°C, comparable to the World Bank's Climate Change historical data, which indicated an increase in the mean ambient temperature (AT) by 0.6°C for the same period, indicative of significant warming driven by urban development. The highest values noted at the central, the east and northeastern sides of Nairobi, while the lowest LST were spatially distributed on the western side. LST gradient trends showed evidence of UHI in Nairobi.
- Plant species effect on microclimatic parameters differed both intra and inter site. Their architectural properties, particularly the canopy densities played a key role in regulation of microclimate and improving thermal comfort in Nairobi. They modified microclimate greatly within the park compared to the street. Their characteristics and quantified abilities to improve thermal comfort is a great blueprint for the plant selection process in urban greening projects for Nairobi.

5.2 Conclusion

5.2.1 Spatial and Temporal Changes of Vegetation Cover in LCZ of Nairobi from 1988 to 2018

The research focused more on vegetation cover change besides the other existing LULC types in the respective LCZs. It was more dominant in LCZ A (dense trees) and B (scattered trees), with sparse distribution in LCZ 4, 5, 6 (open high, mid and low-rise), and 9 (sparsely built). Even so, the high rate of increase in the built-type LCZs has posed extreme downward effects on vegetation's spatial extent of Nairobi. From the study, vegetation has decreased by 80 Km², with respect to Forests, and the declining trend is likely to continue if there are no proper conservational efforts in place. Therefore, the first null hypothesis was rejected, as there were significant changes in LULC within the LCZs of Nairobi over the past three decades.

Further, the study affirms that the LCZ approach to management of LULC in Nairobi is effective, as it specifically highlights the precise areas in urgent need for greening. Managing these urban landscapes at a local scale is therefore attainable, focusing on the specified LCZs, eventually contributing to change in the wider Nairobi landscape extent. In this case, according to the results, vegetation improvement and maintenance efforts should be strongly prioritized on LCZ A, B, 4, 5, 6 and 9 of Nairobi, which were highly transformed during the three-decade study period. These underscore the pressing need for sustainable urban planning and conservation efforts to mitigate further vegetation loss and its potential ecological and environmental repercussions in Nairobi's rapidly growing urban landscape.

5.2.2 LST Changes in Nairobi along an Urban Gradient

The study confirms that Nairobi's spatial growth is evident, extending from the city center towards the outskirts, especially on the eastern parts of Embakasi east and Kasarani sub-counties. The growth is exhibited by increase in constructed surfaces causing a steady rise in the LST over the past three decades by 4.15⁰C. Thereby, rejecting the research's second null hypothesis, as LST has changed for Nairobi since

2018. On the other hand, existence of vegetation in westerns side of Nairobi, have shown that they have a potential in LST reduction

Further, the research confirmed a notable strong relation between NDVI and LST, substantive evidence that a loss in urban flora increases the surface temperatures and vice versa. Besides, the LST profiles pinpointed the areas that need more focus and effort on UHI mitigation within Nairobi, particularly the central and the eastern sides. For sustainable urbanization in a city like Nairobi, maintaining a balanced NDVI value through greening is essential in ensuring sufficient vegetation cover, while limiting LST increases to avoid significant UHI effects. The knowledge from the study is therefore constructive to Nairobi city planners, health experts, engineers and other decision makers.

5.2.3 Effects of Plant Species on Microclimatic Parameters in the Study Area

The results of this study showed that plants with dense canopies and low SVF reduce temperatures more than plants with less dense canopies, hence, the third null hypothesis of this study was rejected. Temperatures in open built and paved areas within Nairobi city are higher than the temperatures in green spaces and they highly contribute to the UHI effects felt by the city dwellers. Nairobi city residents are more likely to suffer no thermal stress in parks but will experience warm moderate heat stress in built areas during hot seasons.

There is therefore a need to increase greenery especially native evergreen tree species with dense foliage crowns, together with spreading, rounded and vase canopy forms within the urban open spaces such as *Olea africana*, *Calodendrum capense* among others. This will help regulate climatic factors and enhance the thermal comfort of the city's inhabitants. Additionally, during plant selection, Nairobi's landscape planners should consider native tree species that are resistant to the unfavorable urban environmental conditions. Such measures should be used to influence relevant policies within the local government and to sensitize other stakeholders with interests in the urban environment and greening of Nairobi city.

5.3 Recommendations

Objective 1:

Nairobi's urban development strategies should prioritize ecosystem conservation to safeguard existing vegetation within the different local climate zones. Integrating sustainable greening methods for urban open spaces by Nairobi city planners and green space managers is essential, while adopting environmentally friendly construction technologies. In addition, continually monitoring vegetation changes using satellite-derived data, detailed land use monitoring, socioeconomic trends, and urban climate monitoring is recommended for a holistic evidence-based decision-making for urban planning, sustainable development, and ecosystem management strategies towards mitigating further vegetation loss and enhancing the city's resilience to environmental changes.

Objective 2:

As a focus of capacity, urban landscape planners and architects should focus on cutting down anthropogenic heat sources, while integrating green infrastructure in open spaces of Nairobi. For instance, incorporation of green roofs and walls, trees on parking lots, along the roads, and potted plants along streets. Similarly, promoting high albedo surfaces, using perforated pavements and strategically designing urban layouts that encourage natural cooling and minimize heat-absorbing materials is recommended to mitigate LST rise and UHI formation. Additionally, mixed land use, efficient transportation systems, and energy-efficient building designs should be prioritized to counter the heat impact of urban expansion. Collaboration between both the construction and environment sectors such as National Construction Authority and NEMA supported by research is equally essential for sustainability of green infrastructural developments in Nairobi city.

Objective 3:

Urban landscape planners and designers in Nairobi should take into consideration tree species' allometric properties characterized by sturdy trunks, spreading canopies, and

well-rounded forms, such as *Tipuana tipu*. Similarly, evergreen trees displaying greater foliage density akin to *Terminalia mantaly*, yet featuring elevated crowns, offer a suitable option for regulating microclimates. Notably absent from the study's recommendations for Nairobi's streetscapes is the *Ficus benjamina* species. This is attributed to its invasive tendencies, manifesting in both canopy and root expansion, which are deemed unfavorable in proximity to construction. Nonetheless, such trees could find a fitting placement within urban parks and verdant spaces, well removed from any infrastructure. More research on screening for adaptable and matching tree architectures suitable for different urban setting is recommended. Additionally, incorporating direct human physiological and psychological measurements such as heart rate variability, and mental stress, based on different demographics such as age and gender of the city dwellers who commonly use these spaces is encouraged for future studies.

REFERENCES

- Aabeyir, R., Peprah, K., & Hackman, K. O. (2022). Spatio-temporal pattern of urban vegetation in the central business district of the Wa municipality of Ghana. *Trees, Forests and People*, 8.
- Abbas, Z., Yang, G., Zhong, Y., & Zhao, Y. (2021). Spatiotemporal change analysis and future scenario of lulc using the CA-ANN approach: A case study of the greater bay area, China. *Land*, 10(6).
- Abdel-Ghany, A. M., I. M. Al-Helal, I. M., & Shady, M. R. (2013). Human Thermal Comfort and Heat Stress in an Outdoor Urban Arid Environment : A Case Study. *Advances in Meteorology*, 2013.
- Akın, A., Sunar, F., & Berberoğlu, S. (2015). Urban change analysis and future growth of Istanbul. *Environmental Monitoring and Assessment*, 187(8).
- Alqurashi, A. F., & Kumar, L. (2019). An assessment of the impact of urbanization and land use changes in the fast-growing cities of Saudi Arabia. *Geocarto International*, 34(1), 78–97.
- Amegah, A. K., Rezza, G., & Jaakkola, J. J. K. (2016). Temperature-related morbidity and mortality in Sub-Saharan Africa: A systematic review of the empirical evidence. *Environment International*, 91, 133–149.
- Amiri, R., Weng, Q., Alimohammadi, A., & Alavipanah, S. K. (2009). Spatial-temporal dynamics of land surface temperature in relation to fractional vegetation cover and land use/cover in the Tabriz urban area, Iran. *Remote Sensing of Environment*, 113(12), 2606–2617.
- Anbazhagan, S., & Paramasivam, C. R. (2016). Statistical Correlation between Land Surface Temperature (LST) and Vegetation Index (NDVI) using Multi-Temporal Landsat TM Data. *International Journal of Advanced Earth Science and Engineering*, 5(1), 333–346.

- Anjos, M., & Lopes, A. (2017). Urban Heat Island and Park Cool Island intensities in the coastal city of Aracaju, North-Eastern Brazil. *Sustainability (Switzerland); MDPI*, 9(8), 1379.
- Armson, D. (2012). *The Effect of Trees and Grass on the Thermal and Hydrological Performance of an Urban Area*.
- Aslam, A., Rana, I. A., & Bhatti, S. S. (2021). The spatiotemporal dynamics of urbanisation and local climate: A case study of Islamabad, Pakistan. *Environmental Impact Assessment Review*, 91, 106666.
- Bechtel, B., Alexander, P. J., Böhner, J., Ching, J., Conrad, O., Feddema, J., Mills, G., See, L., & Stewart, I. (2015). Mapping local climate zones for a worldwide database of the form and function of cities. *ISPRS International Journal of Geo-Information*, 4(1), 199–219.
- Bechtel, B., & Daneke, C. (2012). Classification of local climate zones based on multiple earth observation data. *IEEE Journal of Selected Topics in Applied Earth Observations and Remote Sensing*, 5(4), 1191–1202.
- Bellard, C. (2012). Impact of climate change on biodiversity. In *Ecol. Lett.* (Issue 15, pp. 365–377).
- Bigsby, K. M., McHale, M. R., & Hess, G. R. (2014). Urban morphology drives the homogenization of tree cover in Baltimore, MD, and Raleigh, NC. *Ecosystems*, 17(2), 212–227.
- Billah, M., & Haque, A. (2021). Dynamics Of Landuse Pattern & Land Surface Temperature Dynamics Of Landuse Pattern & Land Surface Temperature Changes In Dhaka City. *5th International Conference on Advances in Civil Engineering (ICACE-2020)*, April.
- Binyanya, M. R., Mugwima, N. B., Karanja, D., Mbiti, S., Binyanya, M. R., Mugwima, N. B., Karanja, D., & Mbiti, S. (2022). Sustainable Urban Forest Conservation: Assessing Public Attitudes towards Urban Forests in Nairobi City. *Current Urban*

Studies, 10(4), 655–672.

- Bosco, N. J., Geoffrey, M. M., & Kariuki, N. N. (2011). Assessment of landscape change and occurrence at watershed level in city of Nairobi. *African Journal of Environmental Science and Technology*, 5(10), 873–883.
- Boukhabla, M., & Alkama, D. (2012). Impact of Vegetation on Thermal Conditions Outside, Thermal Modeling of Urban Microclimate, Case Study: The Street of the Republic, Biskra. *Energy Procedia*, 18, 73–84.
- Brousse, O., Georganos, S., Demuzere, M., Vanhuysse, S., Wouters, H., Wolff, E., Linard, C., van Lipzig, N. P. M., & Dujardin, S. (2019). Using Local Climate Zones in Sub-Saharan Africa to tackle urban health issues. *Urban Climate*, 27, 227–242.
- Brousse, O., Martilli, A., Foley, M., Mills, G., & Bechtel, B. (2016). WUDAPT, an efficient land use producing data tool for mesoscale models? Integration of urban LCZ in WRF over Madrid. *Urban Climate*, 17, 116–134.
- Brudler, S., Arnbjerg-Nielsen, K., Hauschild, M. Z., & Rygaard, M. (2016). Life cycle assessment of stormwater management in the context of climate change adaptation. *Water Research*, 106, 394–404.
- Cater, M., Dammann, I., Derome, J., Greve, M., & Leuchner, M. (2009). Leaf Area Index (LAI). In *Field protocol on Radiation measurements and Leaf Area Index (LAI)* (Vol. 3, Issue May, pp. 1–14).
- CCN. (2007). “*City of Nairobi Environment Outlook*”. *City Council of Nairobi, United Nations Environment Programme and the United Nations Centre for Human Settlement*.
- Chapman, L., & Thrones, J. E. (2004). Real-Time Sky-View Factor Calculation and Approximation. *Atmospheric and Oceanic Technology*, 21(5), 730–741.
- Chen, G., Chen, Y., He, H., Wang, J., Zhao, L., & Cai, Y. (2023). Assessing the

synergies between heat waves and urban heat islands of different local climate zones in Guangzhou, China. *Building and Environment*, 240.

Chen, L., Ng, E., An, X., Ren, C., Lee, M., Wang, U., & He, Z. (2012). Sky view factor analysis of street canyons and its implications for daytime intra-urban air temperature differentials in high-rise , high-density urban areas of Hong Kong : a GIS-based simulation approach. *International Journal of Climatology*, 32(1), 121–136.

Cheng, X., & Su, H. (2010). Effects of climatic temperature stress on cardiovascular diseases. *European Journal of Internal Medicine*, 21(3), 164–167.

Chiesura, A. (2004). The role of urban parks for the sustainable city. *Landscape and Urban Planning*, 68(1), 129–138.

Ching, J., Mills, G., Bechtel, B., See, L., Feddema, J., Wang, X., Ren, C., Brorousse, O., Martilli, A., Neophytou, M., Mouzourides, P., Stewart, I., Hanna, A., Ng, E., Foley, M., Alexander, P., Aliaga, D., Niyogi, D., Shreevastava, A., ... Theeuwesits, N. (2018). WUDAPT: An Urban Weather, Climate, and Environmental Modeling Infrastructure for the Anthropocene. *Bulletin of the American Meteorological Society*, 99(9), 1907–1924.

Cilek, U. M., & Cilek, A. (2021). Analyses of land surface temperature (LST) variability among local climate zones (LCZs) comparing Landsat-8 and ENVI-met model data. *Sustainable Cities and Society*, 69, 102877.

Corine, T., & Cover, L. (2012). *CORINE Land Cover nomenclature conversion to Land Cover Classification system*. Clc. <https://land.copernicus.eu/eagle/files/eagle-related->

Deb, C., & Alur, R. (2010). The significance of Physiological Equivalent Temperature (PET) in outdoor thermal comfort studies. *International Journal of Engineering Sciences and Technology*.

Demuzere, M., Kittner, J., & Bechtel, B. (2021). LCZ Generator: A Web Application

- to Create Local Climate Zone Maps. *Frontiers in Environmental Science*, 9(April).
- Di-Leo, N., Escobedo, F. J., & Dubbeling, M. (2016). The role of urban green infrastructure in mitigating land surface temperature in Bobo-Dioulasso, Burkina Faso. *Environment, Development and Sustainability*, 18(2), 373–392.
- Dissanayake, D. M., Morimoto, T., Murayama, Y., & Ranagalage, M. (2019). Impact of Landscape Structure on the Variation of Land Surface Temperature in Sub-Saharan Region: A Case Study of Addis Ababa using Landsat Data (1986–2016). *Sustainability*, 11(8), 2257.
- Dissanayake, D., Morimoto, T., Murayama, Y., Ranagalage, M., & Handayani, H. H. (2019). Impact of urban surface characteristics and socio-economic variables on the spatial variation of land surface temperature in Lagos City, Nigeria. *Sustainability*, 11(1).
- El-Tantawi, A. M., Bao, A., Chang, C., & Liu, Y. (2019). Monitoring and predicting land use/cover changes in the Aksu-Tarim River Basin, Xinjiang-China (1990–2030). *Environmental Monitoring and Assessment*, 191(8).
- Elnabawi, M. H., & Hamza, N. (2019). Behavioural Perspectives of Outdoor Thermal Comfort in Urban Areas : A Critical Review. *Atmosphere*.
- Estoque, R. C., Murayama, Y., & Myint, S. W. (2017). Effects of landscape composition and pattern on land surface temperature: An urban heat island study in the megacities of Southeast Asia. *Science of The Total Environment*, 577, 349–359.
- Fahmy, M., Sharples, S., & Yahiya, M. (2010). LAI based trees selection for mid-latitude urban developments: A microclimatic study in Cairo, Egypt. *Building and Environment*, 45(2), 345–357.
- Fang, Z., Lin, Z., Mak, C. M., Niu, J., & Tse, K. T. (2018). Investigation into sensitivities of factors in outdoor thermal comfort indices. *Building and*

Environment, 128, 129–142.

- Fenta, A. A., Yasuda, H., Haregeweyn, N., Belay, A. S., Hadush, Z., Gebremedhin, M. A., & Mekonnen, G. (2017). The dynamics of urban expansion and land use/land cover changes using remote sensing and spatial metrics: The case of Mekelle city of northern Ethiopia. *International Journal of Remote Sensing*, 38(14), 4107–4129.
- Ferreira, L. S., & Duarte, D. H. S. (2019). Exploring the relationship between urban form, land surface temperature and vegetation indices in a subtropical megacity. *Urban Climate*, 27, 105–123.
- Feyisa, G. L. (2014). Efficiency of parks in mitigating urban heat island effects; example of Addis Ababa. *Landscape and Urban Planning*, 123; 87–95.
- Forman, R. T. T. (2013). Infrastructure and Nature: Reciprocal Effects and Patterns for Our Future. In *Infrastructure Sustainability and Design* (pp. 35–49). Taylor and Francis.
- Friends of Nairobi Arboretum (FONA). (2020). *Trees – The Nairobi Arboretum*.
- Furukawa, T., Kiboi, S. K., Mutiso, P. B. C., & Fujiwara, K. (2016). Multiple use patterns of medicinal trees in an urban forest in Nairobi, Kenya. *Urban Forestry & Urban Greening*, 18, 34–40.
- Gayathri, R., Mahboob, S., Govindarajan, M., Al-Ghanim, K. A., Ahmed, Z., Al-Mulhm, N., Vodovnik, M., & Vijayalakshmi, S. (2021). A review on biological carbon sequestration: A sustainable solution for a cleaner air environment, less pollution and lower health risks. *Journal of King Saud University - Science*, 33(2), 101282.
- Geddes, J. A., & Murphy, J. G. (2012). The science of smog: a chemical understanding of ground level ozone and fine particulate matter. *Metropolitan Sustainability: Understanding and Improving the Urban Environment*, 205–230.

- Geletič, J., Lehnert, M., Savić, S., & Milošević, D. (2019). Inter-/intra-zonal seasonal variability of the surface urban heat island based on local climate zones in three central European cities. *Building and Environment*, *156*, 21–32.
- Georgi, N. J., & Zafiriadis, K. (2006). The impact of park trees on microclimate in urban areas. *Urban Ecosystems*, *9*(3), 195–209.
- Giguère, M. (2012). *Urban Heat Island Mitigation Strategies*.
- GIZ. (2018). Climate Risk Profile: Kenya. In *Federal Ministry for Economic Cooperation and Development* (Issue July).
- Govindarajulu, D. (2014). Urban green space planning for climate adaptation in Indian cities. *Urban Climate*, *10*, 2006–2008.
- Grime, J. P., Crick, J. C., & Rincon, E. (2007). The ecological significance of plasticity. In D. H. Jennings (Ed.), *Plasticity in Plants* (pp. 5–12). Company of Biologists, Cambridge.
- Halmy, M. W. A., Gessler, P. E., Hicke, J. A., & Salem, B. B. (2015). Land use/land cover change detection and prediction in the north-western coastal desert of Egypt using Markov-CA. *Applied Geography*, *63*, 101–112.
- Hang, J., Li, Y., Sandberg, M., Buccolieri, R., & Di Sabatino, S. (2012). The influence of building height variability on pollutant dispersion and pedestrian ventilation in idealized high-rise urban areas. *Building and Environment*, *56*, 346–360.
- Heaviside, C., Macintyre, H., & Vardoulakis, S. (2017). The Urban Heat Island: Implications for Health in a Changing Environment. *Current Environmental Health Reports*, *4*(3), 296–305.
- Huang, F., Jiang, S., Zhan, W., Bechtel, B., Liu, Z., Demuzere, M., Huang, Y., Xu, Y., Ma, L., Xia, W., Quan, J., Jiang, L., Lai, J., Wang, C., Kong, F., Du, H., Miao, S., Chen, Y., & Chen, J. (2023). Mapping local climate zones for cities: A large review. *Remote Sensing of Environment*, *292*.

- Huang, K., Li, X., Liu, X., & Seto, K. C. (2019). Projecting global urban land expansion and heat island intensification through 2050. *Environmental Research Letters*, *14*(11).
- Ji, Y., Song, J., & Shen, P. (2022). A review of studies and modelling of solar radiation on human thermal comfort in outdoor environment. *Building and Environment*, *214*, 108891.
- Jiang, Y., & Lin, W. (2021). A Comparative Analysis of Retrieval Algorithms of Land Surface Temperature from Landsat-8 Data : A Case Study of Shanghai , China. *International Journal of Environmental Research and Public Health*, *18*(5659).
- Jim, C. Y. (2013). Sustainable urban greening strategies for compact cities in developing and developed economies. *Urban Ecosystem*, *16*, 741–761.
- Karanja, P. W., & Kamau, F. N. (2018). Analysis of the Relationship between Land Surface Temperature and Vegetation and Built-Up Indices in Upper-Hill, Nairobi. *Journal of Geoscience and Environment Protection*, *6*, 1–16.
- Karatasou, S., Santamouris, M., & Geros, V. (2006). Prediction of energy consumption in buildings with artificial intelligent techniques and Chaos time series analysis. *International Workshop on Energy Performance and Environmental Quality of Buildings.*, July, 1–5.
- Kenya Meteorological Department (KMD). (2020). *State of the Climate Kenya*.
- Kenya National Bureau of Statistics (KNBS). (2019). *National Census: Population by County and Sub-County*.
- Kim, M., Jeong, D., & Kim, Y. (2021). Local climate zone classification using a multi-scale, multi-level attention network. *ISPRS Journal of Photogrammetry and Remote Sensing*, *181*, 345–366.
- Klingberg, J., Konarska, J., Lindberg, F., Thorsson, S., & Klingberg, J. (2015). Measured and modelled leaf area of urban woodlands , parks and trees in

Gothenburg , Sweden. *9th International Conference on Urban Climate Jointly with 12th Symposium on the Urban Environment*, 1–6.

Kumar, D., & Shekhar, S. (2016). Linear gradient analysis of kinetic temperature through geostatistical approach Linear gradient analysis of kinetic temperature through geostatistical approach. *Modeling Earth Systems and Environment*, 2(145).

Kwong, I. H. Y. (2022). Physical environment, species choice and spatio-temporal patterns of urban roadside trees in Hong Kong. *Trees, Forests and People*, 10.

Leal, W., Echevarria, L., Neht, A., Klavins, M., & Morgan, E. A. (2018). Coping with the impacts of urban heat islands. A literature based study on understanding urban heat vulnerability and the need for resilience in cities in a global climate change context. *Journal of Cleaner Production*, 171, 1140–1149.

Leuzinger, S., Vogt, R., & Körner, C. (2010). Tree surface temperature in an urban environment. *Agricultural and Forest Meteorology*, 150(1), 56–62.

Li, C., Ju, T., Li, B., Zhang, J., Wang, J., Xia, X., & Lei, S. (2023). Spatial and temporal distribution of absorbing aerosols in sub-Saharan Africa and GTWR model analysis. *Air Quality, Atmosphere and Health*, 1–14.

Li, X., Stringer, L. C., & Dallimer, M. (2021). The Spatial and Temporal Characteristics of Urban Heat Island Intensity: Implications for East Africa's Urban Development. *Climate 2021, Vol. 9, Page 51*, 9(4), 51.

Lin, H., Chen, Y., Zhang, H., Fu, P., Fan, Z., & Lin, H. (2017). Stronger cooling effects of transpiration and leaf physical traits of plants from a hot dry habitat than from a hot wet habitat. *Functional Ecology, British Ecological Society*, 31(12), 2202–2211.

Liu, X., Sun, R., Yang, Q., Su, G., & Qi, W. (2012). Simulating urban expansion using an improved SLEUTH model. *Journal of Applied Remote Sensing*, 6(1), 061709.

- Liu, Y., Wang, X., Guo, M., Tani, H., Matsuoka, N., & Matsumura, S. (2013). Spatial and Temporal Relationships among NDVI, Climate Factors, and Land Cover Changes in Northeast Asia from 1982 to 2009. *GIScience & Remote Sensing*, 48(3), 371–393.
- Lorenz, K., & Lal, R. (2010). The Importance of Carbon Sequestration in Forest Ecosystems. *Carbon Sequestration in Forest Ecosystems*, 241–270.
- Loughner, C. P., Zhang, D. J. A. and D.-L., Pickering, K. E., Dickerson, R. R., & Landry, L. (2012). Roles of Urban Tree Canopy and Buildings in Urban Heat Island Effects : Parameterization and Preliminary Results. *Applied Meteorology and Climatology*, 1775–1793.
- Makokha, G. L., & Shisanya, C. A. (2010). Trends in Mean Annual Minimum and Maximum Near Surface Temperature in Nairobi City, Kenya. *Advances in Meteorology*, 2010, 1–6.
- Makworo, M., & Mireri, C. (2011). Public open spaces in Nairobi City, Kenya, under threat. *Journal of Environmental Planning and Management*, 54(8), 1107–1123.
- Matzarakis, A., & Amelung, B. (2008). Physiological Equivalent Temperature as Indicator for Impacts of Climate Change on Thermal Comfort of Humans. *Seasonal Forecasts, Climate Change and Human Health*, 30(01), 161–172.
- Matzarakis, A., Rutz, F., & Mayer, H. (2009). Modelling radiation fluxes in simple and complex environments : basics of the RayMan model. *International Journal of Biometeorology*, 54(2), 131–139.
- Maundu, P., Tengnas, B., Muema, N., & Birnie, A. (2005). *Useful Trees and Shrub for Kenya*.
- McKight, P. E., & Najab, J. (2010). Kruskal-Wallis Test. *The Corsini Encyclopedia of Psychology*, 1–1.
- Miari, M., Taher Anan, M., Bisher Zeina, M., Valued Neutrosophic Kruskal-Wallis,

- S., & Whitney Tests, M. (2022). Single Valued Neutrosophic Kruskal-Wallis and Mann Whitney Tests. *Neutrosophic Sets and Systems*, 51, 948–957.
- Middel, A., Lukasczyk, J., Maciejewski, R., Demuzere, M., & Roth, M. (2018). Sky View Factor footprints for urban climate modeling. *Urban Climate*, 25(May), 120–134.
- Mondal, M. S., Sharma, N., Garg, P. K., & Kappas, M. (2016). Statistical independence test and validation of CA Markov land use land cover (LULC) prediction results. *Egyptian Journal of Remote Sensing and Space Science*, 19(2), 259–272.
- Morakinyo, T. E., Ouyang, W., Lau, K. K. L., Ren, C., & Ng, E. (2020). Right tree, right place (urban canyon): Tree species selection approach for optimum urban heat mitigation - development and evaluation. *Science of the Total Environment*, 719.
- Morris, R. J. (2010). Anthropogenic impacts on tropical forest biodiversity: a network structure and ecosystem functioning perspective. In *Philosophical Transactions of the Royal Society* (pp. 3709–3718).
- Muhammad, R., Zhang, W., Abbas, Z., Guo, F., & Gwiazdzinski, L. (2022). Spatiotemporal Change Analysis and Prediction of Future Land Use and Land Cover Changes Using QGIS MOLUSCE Plugin and Remote Sensing Big Data: A Case Study of Linyi, China. *Land 2022*, Vol. 11, Page 419, 11(3), 419.
- Müller, A., Österlund, H., Marsalek, J., & Viklander, M. (2020). The pollution conveyed by urban runoff: A review of sources. *Science of The Total Environment*, 709(136125).
- Mundia, C. N., & Aniya, M. (2006). Dynamics of Land Use/Cover Changes and Degradation of Nairobi City, Kenya. *Land Degradation and Development*, 17, 97–108.
- Mundia, C. N., & Murayama, Y. (2013). Modeling Spatial Processes of Urban Growth

in African Cities: A Case Study of Nairobi City. *Urban Geography*, 31(2), 259–272.

Nagendra, H., Lucas, R., Honrado, J. P., Jongman, R. H. G., Tarantino, C., Adamo, M., & Mairota, P. (2013). Remote sensing for conservation monitoring: Assessing protected areas, habitat extent, habitat condition, species diversity, and threats. *Ecological Indicators*, 33, 45–59.

Naikoo, M. W., Rihan, M., Ishtiaque, M., & Shahfahad. (2020). Analyses of land use land cover (LULC) change and built-up expansion in the suburb of a metropolitan city: Spatio-temporal analysis of Delhi NCR using landsat datasets. *Journal of Urban Management*, 9(3), 347–359.

Narita, K., Sugawara, H., & Honjo, T. (2008). Effects Of Roadside Trees On The Thermal Environment Within A Street Canyon. *Geographical Reports Of Tokyo Metropolitan University*, 43, 41–48.

Okech, E. A., & Nyadera, I. N. (2022). Urban green spaces in the wake of Covid-19 pandemic: reflections from Nairobi, Kenya. *GeoJournal*, 87(6), 4931–4945.

Oloo, F., Murithi, G., & Jepkosgei, C. (2020). Quantifying Tree Cover Loss in Urban Forests within Nairobi City Metropolitan Area from Earth Observation Data. *Environmental Sciences Proceedings*, 3(1), 78.

Onyango, S. A. (2022). *Urban Heat and Air Pollution: Resilience Planning in Africa*. URBANET.

Onyango, S. A., Mukundi, J. B., Adimo, A. O., Wesonga, J. M., & Sodoudi, S. (2021). Variability of In-Situ Plant Species Effects on Microclimatic Modification in Urban Open Spaces of Nairobi, Kenya. *Current Urban Studies*, 09(01), 126–143.

Orimoloye, I. R., Mazinyo, S. P., Nel, W., & Kalumba, A. M. (2018). Spatiotemporal monitoring of land surface temperature and estimated radiation using remote sensing: human health implications for East London, South Africa. *Environmental Earth Sciences*, 77(3), 1–10.

- Ouyang, Z., Sciusco, P., Jiao, T., Feron, S., Lei, C., Li, F., John, R., Fan, P., Li, X., Williams, C. A., Chen, G., Wang, C., & Chen, J. (2022). Albedo changes caused by future urbanization contribute to global warming. *Nature Communications*, *13*(1), 1–9.
- Oyugi, M. O., Odenyo, V. A. O., & Karanja, F. N. (2017). The Implications of Land Use and Land Cover Dynamics on the Environmental Quality of Nairobi City, Kenya. *American Journal of Geographic Information System*, *6*(3), 111–127.
- Pal, S., & Ziaul, S. (2017). Detection of land use and land cover change and land surface temperature in English Bazar urban centre. *Egyptian Journal of Remote Sensing and Space Science*, *20*(1), 125–145.
- Park, M., Hagishima, A., Tanimoto, J., Narita, K. I. (2012). Effect of urban vegetation on outdoor thermal environment: field measurement at a scale model site. *Building and Environment*, *56*, 38–46.
- Pauleit, S. (2003). Urban street tree plantings: identifying the key requirements. *Proceedings of the Institution of Civil Engineers-Municipal Engineer*, *156*, 43–50.
- Pauleit, S., Zölch, T., Hansen, R., Randrup, T. B., & Konijnendijk van den Bosch, C. (2017). Nature-Based Solutions and Climate Change – Four Shades of Green. *Theory and Practice of Urban Sustainability Transitions*, 29–49.
- Peng, J., Ma, J., Liu, Q., Liu, Y., Hu, Y., Li, Y., & Yue, Y. (2018). Spatial-temporal change of land surface temperature across 285 cities in China: An urban-rural contrast perspective. *Science of The Total Environment*, *635*, 487–497.
- Perović, V., Jakšić, D., Jaramaz, D., Koković, N., Čakmak, D., Mitrović, M., & Pavlović, P. (2018). Spatio-temporal analysis of land use/land cover change and its effects on soil erosion (Case study in the Oplenac wine-producing area, Serbia). *Environmental Monitoring and Assessment*, *190*(11).
- Pollalis, S., Georgoulas, A., Ramos, S., & Schodek, D. (2013). Infrastructure

Sustainability and Design. In *Infrastructure Sustainability and Design*. Taylor and Francis.

Poorter, H., Van de Vijver, C. A. D. M., Boot, R. G. A., & Lambers, H. (2009). Growth and carbon economy of a fast-growing and a slow-growing grass species as dependent on nitrate supply. In *Plant Soil* (Issue 171, p. 217—227).

Priya, U. K., & Senthil, R. (2021). A review of the impact of the green landscape interventions on the urban microclimate of tropical areas. *Building and Environment*, 205, 108190.

Rahman, M. A., Moser, A., Rötzer, T., & Pauleit, S. (2019). Comparing the transpirational and shading effects of two contrasting urban tree species. *Urban Ecosyst.*, 22(4), 683–697.

Rahman, M. T. U., Tabassum, F., Rasheduzzaman, M., Saba, H., Sarkar, L., Ferdous, J., Uddin, S. Z., & Zahedul Islam, A. Z. M. (2017). Temporal dynamics of land use/land cover change and its prediction using CA-ANN model for southwestern coastal Bangladesh. *Environmental Monitoring and Assessment*, 189(11).

Ren, Y. (2011). Relationship between vegetation carbon storage and urbanization; case study of Xiamen China. *Forest Ecology and Management*, 261(7), 1214–1223.

Robinson, N. (2004). Spatial Characteristics of Plants. In *The Planting Design Handbook*.

Rossi, F., Castellani, B., Presciutti, A., Morini, E., Filipponi, M., Nicolini, A., & Santamouris, M. (2015). Retroreflective façades for urban heat island mitigation : Experimental investigation and energy evaluations. *Applied Energy*, 145, 8–20.

Ryff, C. D. (2014). Psychological Well-Being Revisited: Advances in Science and Practice. *Psychotherapy and Psychosomatics*, 83(1), 10.

Santamouris, M., Haddad, S., Fiorito, F., Osmond, P., Ding, L., Prasad, D., Zhai, X., & Wang, R. (2017). Urban Heat Island and Overheating Characteristics in

- Sydney, Australia. An Analysis of Multiyear Measurements. *Sustainability*, 9(12), 712.
- Sanusi, R., & Bidin, S. (2020). Re-naturing Cities: Impact of Microclimate, Human Thermal Comfort and Recreational Participation. *Climate Change Management*, 545–562.
- Saxe, H., R., C. M. G., O., J., Ryan, M. G., & Vourlitis G. (2001). Tree and forest functioning in response to global warming. *New Phycologist*, 149, 369–400.
- Scott, A. A., Misiani, H., Okoth, J., Jordan, A., Gohlke, J., Ouma, G., Arrighi, J., Zaitchik, B. F., Jjemba, E., Verjee, S., & Waugh, D. W. (2017). Temperature and heat in informal settlements in Nairobi. *PLOS ONE*, 12(11).
- Shahidan, M. F. (2015). Potential of Individual and Cluster Tree Cooling Effect Performances through Tree Canopy Density Model Evaluation in Improving Urban Microclimate. *Current World Environment*, 10(2), 398–413.
- Sidiqui, P., Huete, A., & Devadas, R. (2016). Spatio-temporal mapping and monitoring of Urban Heat Island patterns over Sydney, Australia using MODIS and Landsat-8. *4th International Workshop on Earth Observation and Remote Sensing Applications, EORSA 2016 - Proceedings*, 217–221.
- Silva, J. S., Silva, R. M. da, & Santos, C. A. G. (2018). Spatiotemporal impact of land use/land cover changes on urban heat islands: a case study of Paço do Lumiar, Brazil. *Building and Environment*, 136, 279–292.
- Simwanda, M., Ranagalage, M., Estoque, R. C., & Murayama, Y. (2019). Spatial Analysis of Surface Urban Heat Islands in Four Rapidly Growing African Cities. *Remote Sensing 2019, Vol. 11, Page 1645, 11(14)*, 1645.
- Singh, N., Singh, S., & Mall, R. K. (2020). Urban ecology and human health: implications of urban heat island, air pollution and climate change nexus. *Urban Ecology: Emerging Patterns and Social-Ecological Systems*, 317–334.

- Sodoudi, S., Zhang, H., Chi, X., Müller, F., & Li, H. (2018). The influence of spatial configuration of green areas on microclimate and thermal comfort. *Urban Forestry and Urban Greening*, 34(June), 85–96.
- Soltani, A., & Sharifi, E. (2017). Daily variation of urban heat island effect and its correlations to urban greenery: A case study of Adelaide. *Frontiers of Architectural Research*, 6(4), 529–538.
- Statista. (2021). *Urbanization in Kenya*.
- Stewart, I. D., & Oke, T. R. (2012). Local Climate Zones for Urban Temperature Studies. In *Bulletin of the American Meteorological Society* · (Issue April).
- Stoewen, D. L. (2017). Dimensions of wellness: Change your habits, change your life. *The Canadian Veterinary Journal*, 58(8), 861.
- Tang, W., Hu, J., Zhang, H., Wu, P., & He, H. (2015). Kappa coefficient: a popular measure of rater agreement. *Shanghai Archives of Psychiatry*, 27(1), 62.
- Tarawally, M., Xu, W., Hou, W., & Mushore, T. D. (2018). Comparative analysis of responses of land surface temperature to long-term land use/cover changes between a coastal and Inland City: A case of Freetown and Bo Town in Sierra Leone. *Remote Sensing*, 10(1).
- Tesfamariam, S., Govindu, V., & Uncha, A. (2023). Spatio-temporal analysis of urban heat island (UHI) and its effect on urban ecology: The case of Mekelle city, Northern Ethiopia. *Heliyon*, 9(2), e13098.
- Teshnehdel, S., Gatto, E., Li, D., & Brown, R. D. (2022). Improving Outdoor Thermal Comfort in a Steppe Climate: Effect of Water and Trees in an Urban Park. *Land*, 11(3).
- Tibajuka, A. (2007). Nairobi and its Environment. In *Kenya Atlas* (pp. 145–161).
- Turner-Skoff, J. B., & Cavender, N. (2019). The benefits of trees for livable and sustainable communities. *Plants, People, Planet*, 1(4), 323–335.

- Ulpiani, G. (2021). On the linkage between urban heat island and urban pollution island: Three-decade literature review towards a conceptual framework. *Science of The Total Environment*, 751(141727).
- UN-Habitat. (2020). Nairobi City County: Public Space Inventory and Assessment. In *UN-Habitat*.
- United Nations Human Settlements Programme (UN-Habitat). (2020). *Public Space Inventory and Assessment: Nairobi City County, Reclaiming the Green City in the Sun*.
- University of Capetown. (2017). Nairobi Climate Profile. In *Urban Africa Risk Knowledge* (Issue November).
- USEPA. (2015). *A Report of United States Environmental Protection Agency (USEPA) on Reducing Urban Heat Island Impacts*.
- Van Hoof, J., Mazej, M., & Hensen, J. (2010). Thermal comfort: Research and practice. *Frontiers in Bioscience*, 15, 765–788.
- Vang, D. H., City, D., Tran Thi An, V., Raghavan, V., Vinh Long, N., -, A., Thi Mai Hoa, L., Tai Chi, N., Minh Triet, N., Nguyen-Van-Anh, V., Hoang-Phi, P., Nguyen-Kim, T., Lam-Dao, N., & Vu, T. (2021). The influence of satellite image spatial resolution on mapping land use/land cover: a case study of Ho Chi Minh City, Vietnam. *IOP Conference Series: Earth and Environmental Science*, 652(1), 012002.
- Voogt, J. A. (2020). Urban Heat Islands. In *Atmosphere and Climate* (2nd ed.). Taylor & Francis Group.
- Wang, C., Wang, Z. H., & Yang, J. (2018). Cooling effect of urban trees on the built environment of contiguous United States. *Earth Future*, 6(8), 1066–1081.
- Welles, J. M., & Norman, J. M. (2001). Instrument for indirect measurement of canopy architecture. *Agronomy*, 83, 818–825.

- WHO. (2017). *Urban Green Space Interventions and Health: A Review of Impacts and Effectiveness*.
- Xu, M., Hong, B., Mi, J., & Yan, S. (2018). Outdoor thermal comfort in an urban park during winter in cold regions of China. *Sustainable Cities and Society*, 43, 208–220.
- Yahia, M. W., Johansson, E., Thorsson, S., Lindberg, F., & Rasmussen, M. I. (2018). Effect of urban design on microclimate and thermal comfort outdoors in warm-humid Dar es Salaam, Tanzania. *International Journal of Biometeorology*, 62(3), 373–385.
- Yin, C., Yuan, M., Lu, Y., Huang, Y., & Liu, Y. (2018). Effects of urban form on the urban heat island effect based on spatial regression model. *Science of The Total Environment*, 634, 696–704.
- Zafiriadis, N. J. G. K. (2014). *The impact of park trees on microclimate in urban areas*. September 2006.
- Zhang, B., & Zhang, Y. (2009). Mann-Whitney U test and Kruskal-Wallis test should be used for comparisons of differences in medians, not means: comment on the article by van der Helm-van Mil *et al.* *Arthritis and Rheumatism*, 60(5), 1565.
- Zhang, L., Zhan, Q., & Lan, Y. (2018). Effects of the tree distribution and species on outdoor environment conditions in a hot summer and cold winter zone: A case study in Wuhan residential quarters. *Building and Environment*, 130, 27–39.
- Zhao, C., Weng, Q., Wang, Y., Hu, Z., & Wu, C. (2022). Use of local climate zones to assess the spatiotemporal variations of urban vegetation phenology in Austin, Texas, USA. *GIS & Remote Sensing*, 59(1), 393–409.